

**UNCLASSIFIED**

---

**AD 288 576**

*Reproduced  
by the*

**ARMED SERVICES TECHNICAL INFORMATION AGENCY  
ARLINGTON HALL STATION  
ARLINGTON 12, VIRGINIA**



---

**UNCLASSIFIED**

NOTICE: When government or other drawings, specifications or other data are used for any purpose other than in connection with a definitely related government procurement operation, the U. S. Government thereby incurs no responsibility, nor any obligation whatsoever; and the fact that the Government may have formulated, furnished, or in any way supplied the said drawings, specifications, or other data is not to be regarded by implication or otherwise as in any manner licensing the holder or any other person or corporation, or conveying any rights or permission to manufacture, use or sell any patented invention that may in any way be related thereto.

63-1-4

ASD TDR-62-763

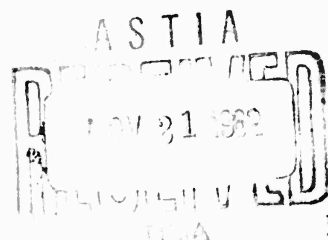
CATALOGED BY ASTIA  
AS AD No. 288576

THE MINIMUM WEIGHT DESIGN OF STRUCTURES  
OPERATING IN AN AEROSPACE ENVIRONMENT

TECHNICAL DOCUMENTARY REPORT NO. ASD-TDR-62-763

October 1962

288 576



Flight Dynamics Laboratory  
Aeronautical Systems Division  
Air Force Systems Command  
Wright-Patterson Air Force Base, Ohio

Project No. 1467, Task No. 146701

(Prepared under Contract No. AF33(657)-7872 by Republic Aviation Corporation,  
Farmingdale, L. I., N. Y. Author: H. Switzky.)

## NOTICES

When Government drawings, specifications, or other data are used for any purpose other than in connection with a definitely related Government procurement operation, the United States Government thereby incurs no responsibility nor any obligation whatsoever; and the fact that the Government may have formulated, furnished, or in any way supplied the said drawings, specifications, or other data, is not to be regarded by implication or otherwise as in any manner licensing the holder, or any other person or corporation, or conveying any rights or permission to manufacture, use, or sell any patented invention that may in any way be related thereto.

Qualified requesters may obtain copies of this report from the Armed Services Technical Information Agency (ASTIA), Arlington Hall Station, Arlington 12, Virginia.

Copies of this report should not be returned to the Aeronautical Systems Division unless return is required by security considerations, contractual obligations, or notice on a specific document.



## FOREWORD

This report was prepared by Mr. H. Switzky of the Structures Department, Applied Research and Development, Republic Aviation Corporation, Farmingdale, New York, under Contract No. AF 33(657)-7872.

The contract was sponsored by the Flight Dynamics Laboratory under Technical Area 750A, "Mechanics of Flight." It was initiated under Project 1367, "Structural Design Criteria" and was completed under Project 1467, "Structural Analysis Methods," Task 146701, "Stress-Strain Analysis for Structures Exposed to Creep Environment."

The work was administered under the direction of the Structures Branch by Mr. J.R. Johnson, Project Engineer. He was assisted by Mr. W.L. Fourney. The time period covered by the contract was January 15, 1962 to November 15, 1962.

The author wishes to acknowledge the efforts of Mr. A. Hamilton for his assistance in obtaining typical aerospace environmental conditions for the design examples, Mr. E. Reitz and Mr. N. Kozyreff for their assistance in the calculations and plotting of the data, and Mr. S. Serben and Miss L. Callejo for the necessary digital programming. The author also wishes to acknowledge the engineering and administration assistance secured from Dr. R. Levy, Mr. C. Rosenkranz, and Mr. A. Alberi.

This report was issued by Republic Aviation Corporation as Report RAC 442-1 (ARD-823-2).

## ABSTRACT

A nondimensional design technique is developed to obtain the minimum weight of structural components (columns, plates, and beams) subjected to an aerospace environment. Design curves are developed and presented for various structural configurations in terms of the applied loads and geometric and material parameters which can be readily evaluated. The design technique can be employed to obtain, in a relatively simple and rapid manner, preliminary estimates of the structural design weight as well as a good approximation to the final design. The design procedure for minimum weight is illustrated for a truss-like spar and a wing section which are typical of aerospace structures.

## PUBLICATION REVIEW

This technical documentary report has been reviewed and is approved.



RICHARD F. HOENER  
Chief, Structures Branch  
Flight Dynamics Laboratory

## TABLE OF CONTENTS

<u>Section</u>	<u>Title</u>	<u>Page</u>
I	INTRODUCTION AND SUMMARY	1
II	ANALYTICAL STUDIES	3
A.	Techniques	3
1.	Approach	3
a.	Load Equation ( $P = \sigma A$ )	3
b.	Stability Equation	3
c.	Maximum Over-all Stability	4
d.	Maximum Local Stability	4
2.	Geometry Factors	7
3.	Material Factors	8
B.	Columns	14
1.	One Unknown Dimension	14
2.	Two Unknown Dimensions	16
3.	Three Unknown Dimensions	22
4.	Four or More Unknown Dimensions	24
C.	Plates	26
1.	Unreinforced Plate	27
2.	Corrugated Plate	30
a.	Double Faced Corrugations in Compression	31
b.	No Faces or Single Face Corrugations in Compression	34
c.	Corrugation Panels in Shear	35
3.	Reinforced Plate	43
4.	Sandwich Plates	50
D.	Tubes in Torsion	59
1.	Long Tube	59
2.	Cylindrical Tube	62
E.	Bending of Beams and Beam-Like Plates	62
1.	Beams	67
2.	Corrugation Plate Beams	70
F.	Combined Loading Conditions	71
1.	Interaction Equations	71
2.	Combined Axial Load and Bending of Beams	75
G.	Design Hints	76

## TABLE OF CONTENTS (Cont'd)

<u>Section</u>	<u>Title</u>	<u>Page</u>
III	ILLUSTRATIVE EXAMPLES	81
A.	Beam Truss	81
	1. Load Temperature Time History	83
	2. Design Stresses	83
	3. Design of Members	84
	a. Tension Members	84
	b. Compression Members	86
B.	Wing Portion	95
	1. Structure	95
	2. Unit Solutions	95
	a. Bending Moment in Covers	95
	b. Spar No. 1	95
	c. Rib Truss	95
	3. Environmental History	97
	4. Material Selection	98
	5. Design of Structural Components for Mission 1	105
	a. Lower Cover	105
	b. Corrugated Spar Web	108
	c. Vertical Truss Member ( $U_4 - L_4$ )	111
	d. Spar Cap	113
	6. Design of Structural Components for Mission 2	116
	a. Lower Cover in TZM	116
	b. Corrugation Web in TZM	117
	c. Vertical Truss Member ( $U_4 - L_4$ ) in TZM	118
	d. Spar Cap	119
	REFERENCES	122
	APPENDIX	124

## LIST OF ILLUSTRATIONS

<u>Figure No.</u>	<u>Title</u>	<u>Page</u>
1a	Strain Deviation vs. Stress	9
1b	Material Constants $E_A$ , $\sigma_o$ , and $\log \beta$ vs. Temperature	11
2	Parametric Creep Rate Plots of TZM and FS-85	12
3	Parametric Plots for Rene' 41 a. Yield Strength Deterioration vs. Exposure b. Creep Rate vs. Stress	13
4	Stress Ratio vs. Column Stability Parameter	15
5	Stress Ratio vs. Plate Stability Parameter	19
6	Stress Ratio vs. Load Index for a Column with Rectangular Plates	20
7	Stress Ratio vs. Load Index for a Tubular Column	21
8	Stress Ratio vs. Load Index for an Unreinforced Plate	29
9	Stress Ratio vs. Load Index for a Corrugated Sandwich Plate	33
10	Stress Ratio vs. Load Index for an Orthotropic Plate	36
11	Stress Ratio vs. Load Index for a Corrugated Plate in Shear	39
12	Nondimensional Stress-Strain Curves	40
13a	Stress Ratio vs. Load Index for an Integrally Stiffened Plate	46
13b	Stress Ratio vs. Load Index for an Integrally Stiffened Plate	47
14a	Design Curves for Honeycomb Sandwich ( $t/s = 0.004$ )	52
14b	Design Curves for Honeycomb Sandwich ( $t/s = 0.006$ )	53
14c	Design Curves for Honeycomb Sandwich ( $t/s = 0.008$ )	54
14d	Design Curves for Honeycomb Sandwich ( $t/s = 0.012$ )	55

# LIST OF ILLUSTRATIONS (Ccnt'd)

<u>Figure No.</u>	<u>Title</u>	<u>Page</u>
15	Core Size Required to Stabilize the Faces	56
16	Stress Ratio vs. Load Index for Tube in Torsion	61
17	Stress Ratio vs. Load Index for Cylinder in Torsion	63
18	Typical Plot of Area Index vs. Stress Ratio	66
19	Optimum Stress, Depth, and Area Indices of a Beam	68
20	Optimum Stress, Depth, and Area Indices of a Corrugated Plate	72
21	Depth Ratio of a Beam Subjected to Bending and Axial Loads	77
22	Depth Ratio of a Corrugated Plate Subjected to Bending and Axial Loads	78
23	Creep Strain vs. Reference Stress	82
24	Wing Structure	96
25a	Pressure - Temperature History - Mission 1 Exit	99
25b	Pressure - Temperature History - Mission 1 Reentry	100
26	Ultimate Strength vs. Temperature	103
27	Creep of Upper Cap of Rene' 41	104
A-1a	Optimum Fabrication Angle for Corrugation Panels in Compression ( $\sqrt{C_t/C_f} = 1$ )	A-3
A-1b	Optimum Fabrication Angle for Corrugation Panels in Compression ( $\sqrt{C_t/C_f} = 1.14$ )	A-4
A-2a	Optimum Fabrication Angle for Corrugation Panels in Shear ( $\sqrt{C_t/C_f} = 1$ )	A-5
A-2b	Optimum Fabrication Angle for Corrugation Panels in Shear ( $\sqrt{C_t/C_f} = 1.14$ )	A-6

## LIST OF SYMBOLS

a	Length of panel; Axial load index for beam [ Eq. (84) ]
b	Characteristic buckling dimension (width of panel, length of column) ; Moment index for beam [Eq. (84)]
c	Distance from neutral axis to extreme compression fiber
d	Characteristic dimension of cross section
f	Face thickness
h	Thickness of flange; Depth of truss or box beam
k	Stability constant employed in referenced texts
l	Length of tube, cylinder, or horizontal truss member
n	Exponent of thickness ratio in stability Eq(10a); Exponent of stress ratio in interaction Eq. (80b); Number of stiffeners; Ratio of flat to depth of corruga- tions
p	Pitch of the corrugations
r	Load ratio
s	Honeycomb cell spacing
t	Characteristic thickness of cross section; Thickness of honeycomb core cell
w	Width of flange
x	Stress ratio [ Eqs. (80) and (89) ]
y	Critical stress ratio [Eq. (80)] ; Flange width to depth ratio (w/d)
z	Flange to web area ratio $\left( \frac{hw}{dt} \right)$
A	Area of cross section; Average area per inch of cross section
A <sub>o</sub>	Area enclosed by median curve of tubular section
C	Stability coefficient defined by the boundary conditions [ obtained from k, e. g. , $C_t = \pi^2 k / 12(1 - \nu^2)$ ]  $C_h = \sigma / E_R (h/w)^2 = .388$ for a simple-free <u>flange</u>

# LIST OF SYMBOLS (Cont'd)

$C_t$	$= \sigma/E_R (t/d)^2 = 3.62$ for a simple-simple <u>web</u>
$C_d$	$= \sigma/E_T (d/b)^2 = 1.23$ for a pin ended tubular <u>column</u>
	$= C_c (I/Ad^2) = C_c (\alpha_3/\alpha_1)$
$C_c$	$= \sigma/E_T (I/Ab^2) = \pi^2$ for a pin ended <u>column</u>
$C_\tau$	$= \tau/E_R (t/b)^2 = 4.84$ for a simply supported <u>plate in shear</u>
$C_f$	$= \sigma/E_R (f/p)^2 = 3.62$ for a simple supported <u>face</u>
D	Bending stiffness of plate
$E_A$	Young's modulus
$E_R$	Effective stability modulus
$E_S$	Secant modulus
$E_T$	Tangent modulus
F.S.	Factor of safety
F	Correlation factor between experiments and theory
$G_R$	Effective shear modulus
I	Inertia of cross section
$I_{xx}$	Inertia per inch of width of a reinforced plate
K	Stability constant [obtained from k, e.g., Eq. (60c), $K = \pi^2 k / (1 - \nu^2)$ ]
$K_G$	Geometry parameter in load index $[C_d C_t^{1/2} / \alpha_1 = \bar{P} / (P/b^2 \sigma_o) (E_A / \sigma_o)^{3/2}]$
M	Moment
P	Axial load
$\bar{P}$	Load index (nondimensional load-material-geometry parameter that can be equated to a function of the stress ratio)
Q	Shear load
T	Torque
W	Weight per inch of cross section
X	Limit load; Bending index [Eq. (75b)]



# LIST OF SYMBOLS (Cont'd)

$\alpha$	Ratio defining geometry of cross section
$\alpha_1$	$= A/dt$ (beam) $= A/t$ (corrugation)
$\alpha_3$	$= I/d^3t$
$\alpha_4$	$= I_{xx}/d^2t$
$\alpha_5$	$= I_{yy}/d^2t$ or $I_{yy}/t^3$
$\alpha_6$	$= c/d$
$\alpha_7$	$= f/t$ or $n \alpha_1 + z$
$\alpha_8$	$= Q/bt \tau_t$
$\alpha_9$	$= (t/b) / (t/d)^{7/4}$
$\beta$	Material parameter indicative of the nonlinearity of the stress-strain relationship [Eq. (1d)]
$\gamma$	Shear strain
$\delta$	Operator indicating an incremental change; Nonlinear strain ( $\epsilon - \sigma/E$ )
$\epsilon$	Strain
$\bar{\epsilon}$	Stability strain $= \sigma_{cr}/E_R$
$\theta$	Corrugation angle
$\nu$	Poisson's ratio
$\xi$	Stability index (nondimensional material-geometry parameter that can be equated to a function of the stress ratio)
$\xi_c$	Column stability index $= (\sigma/\sigma_o) / (E_T/E_A)$
$\xi_p$	Compression plate stability index $= (\sigma/\sigma_o) / (E_R/E_A)$
$\xi_s$	Shear plate stability index or strain index $= (\sigma/\sigma_o) / (E_S/E_A) = \frac{E_A \epsilon}{\sigma_o}$
$\rho$	Density
$\sigma$	Axial stress
$\sigma_o$	Reference stress (material parameter indicating plasticity [Eq. (1c)])
$\tau$	Shear stress

## LIST OF SYMBOLS (Cont'd)

### Subscripts

a	allowable
am	minimum allowable
c	Column; core; creep; compression
cr	critical
d	depth
f	face
h	flange; corrugation flat
m	bending
p	plate
s	secant; shear
t	web; tension
u	ultimate
xx	x-axis
yy	y-axis
0	no faces
1	one face
2	two faces
$\tau$	shear plate

## SECTION I - INTRODUCTION AND SUMMARY

The prime objective of a structural designer is to distribute structural material in such a manner that it can satisfactorily perform its assigned tasks for the life of the vehicle with minimum weight and reasonable cost. His job has become more complex as the high performance characteristics required for aerospace vehicles have exposed the structures to loads at high temperatures for extended periods of time.

At the inception of the design, the designer must make preliminary estimates of the structural design of the vehicle in order to estimate its weight and its effect upon the performance. Methods of estimating the minimum weight must be employed before the design is finalized. The designer must use his ingenuity and imagination to supplement the present state of the art in order to obtain preliminary designs of "optimum" structure for the contemplated load and environment history. This must be done in a relatively rapid and simple manner, considering all logical types of constructions and configurations.

The design of a minimum weight structure is more complicated than its analysis. An analysis of the strength of a structure can be readily performed when given the applicable equations, the geometry, and the material properties. Given, however, the applied loads and material, it is a much more difficult task to determine a structure which would withstand the applied load and be of minimum weight.

A nondimensional approach has been employed in this report in order to make the design techniques applicable to the infinite possible variations in the material properties and geometric configurations. The various possible environments and load histories make it mandatory to consider all materials with modifications due to the effects of temperature, time, and load since each environment is equivalent to creating a different stress-strain relationship. The choice of the geometric configuration (area distribution) is also arbitrary and is usually determined by the designer after considering the applied loads and temperatures and the available materials. In addition, many analyses are encumbered with empirical constants which may change with the material, temperatures, etc. These considerations would make it impractical to develop design curves or to obtain adequate experimental data for each possible combination of environment, material, and geometry. The nondimensional technique presented in this report permits the designer to readily evaluate the effects of various modifications upon the minimum weight design. Such modifications as different materials, different environments, load magnitudes, changing empirical analysis constants or edge fixities can be considered utilizing the same design graph. Design graphs will usually be required for each type of construction.

---

Manuscript released by the author July 1962 for publication as an ASD Technical Documentary Report.

Nondimensional equations and graphs are developed to obtain the weight and cross-sectional description of minimum weight structures for a given load-temperature history. The solutions are expressed in terms of geometric and material parameters which are readily determined from the known boundary conditions, type of construction, and the stress-strain curve of the material after the contemplated exposure. Various criteria of structural adequacy or material behavior can be employed to supplement the design procedure by modifying allowables or material parameters.

The design procedure for minimum weight is illustrated for a truss-like spar and a wing section such as may be employed in an aerospace vehicle. The tension members are designed by an allowable stress which can be determined from such criteria as the short time static strength or the maximum creep strain. The design of compression members must also consider optimum distribution of materials for stability. The unspecified dimensions of a cross section of a compression member are determined by solving a set of equations defining the load, the stability, and the minimum weight in terms of these dimensions.

A compression structure can be visualized as a set of deformation springs in parallel and series. The springs are in parallel if they have the same deformation pattern (e.g., bending and transverse shear). The springs are in series if the deformation pattern can occur independently of each other (e.g., bending and local "wrinkling"). If the springs are in series then the structure becomes unstable when the applied load becomes equal to the critical load for the weakest spring. This critical load can be increased by a redistribution of the area of the cross section so as to increase the stiffness of the weakest spring. This is usually done at the expense of reducing the critical loads of the stiffer springs. The optimum distribution of the area of the cross section occurs when the weakest springs are made equally stiff by a judicious selection of the unspecified dimensions. This technique is sometimes described as the "one horse shay" approach.

Various types of structures designed to withstand compression, shear, or bending loads are considered. Columns with various types of cross sections (I-beam, channel, tee, angle, rectangular and circular tubes) are investigated in detail, although the technique is applicable to many more cross sections. Design considerations for plate constructions such as solid plate, corrugations, stiffened plate, and honeycomb sandwich are also analyzed. Bending of corrugation plate and beams is also investigated. In addition, the effects of combined loadings upon the design are reviewed.

This report is intended to provide a procedure for the preliminary design and weight estimation for a minimum weight structure. The final weight will include construction details and design modifications for additional problems which are not considered here. It is considered beyond the scope of this report to take into account the effects of fatigue and thermal stresses upon the minimum weight design. The failure of the structure due to fatigue or thermal stresses is not sufficiently defined for design purposes. In addition, the thermal stresses cannot be defined until the detail design is fixed.

## SECTION II - ANALYTICAL STUDIES

### A. TECHNIQUES

The procedure to obtain a minimum weight design is fairly straightforward. There exist a number of equations which must be satisfied by the geometry. In addition, there are subsidiary conditions which indicate the distribution of the cross-sectional area required to minimize the weight. The design technique for structures in compression or shear is described below for columns in compression in order to aid in the visualization of the procedure. This technique is equally applicable to plates and tubes in compression or shear. The design technique for structures in bending is only slightly different and is best described in Part E of this section (Bending Members).

#### 1. APPROACH

The selection of a type of construction results in a number of unknown dimensions of the structural cross section that must be specified by the designer. As an example, the diameter (d) and wall thickness (t) of a minimum weight cylindrical column of a prescribed length (b) and end fixity (Cc) must be determined.

The determination of these unknown dimensions requires the solution of an equal number of equations defining the geometry. These equations can be characterized in the following manner.

##### a. Load Equation ( $P = \sigma A$ )

The applied load is equal to the product of the allowable stress and the area of the cross section. This basic equation is employed in designing all types of minimum weight cross sections and is sufficient to determine the cross section with one unknown dimension (e.g., solid plate, solid circular tube). The buckling stress is employed as the allowable compressive stress since buckling and failure usually occur simultaneously in a minimum weight structure.

##### b. Stability Equation

The local stability stress of the cross section is made equal to the over-all stability stress of the structure. This is the "one horse shay" design philosophy described previously. Increasing the diameter of a circular tube, while maintaining a constant cross-sectional area, increases the column stability by increasing the inertia but reduces the local (wrinkling) stability by reducing the "t/d" ratio. The minimum weight design occurs when the ratio of diameter to column length "d/b" is a prescribed proportion of the thickness to diameter ratio "t/d". This relationship and the applied load equation are sufficient to determine cross sections with two unknowns. The value of the "t/d" ratio in terms of the "d/b" ratio is substituted into the load equation to obtain the load as a function of the "d/b" ratio. Cross sections of more than two unknown dimensions are designed in a similar manner by employing subsidiary conditions c. and d. described below, to represent the area and inertia of the cross section in terms of two characteristic dimensions.

### c. Maximum Over-all Stability

The relative distribution of the area in the flanges and webs of the cross section can be specified by considering the modes of over-all failure. If the column can only buckle about one axis because of boundary restraints (e.g., skins, webs, etc.), the minimum weight is assumed to be obtained when the inertia of the cross section about this axis is maximum, subject to the constraint that the area and the thickness ratios are stationary. If, however, over-all buckling is possible about both bending axes, then the equality of the buckling stabilities about each axis can be employed. This would require that the inertias about each axis be proportional to the end fixities associated with the buckling about that axis. Equations of these types can be employed to determine the ratio of areas ( $z = wh/dt$ ) of the cross-sectional elements. Cross sections of three unknowns ( $d, t, w$ ), as exemplified by bent-up sheets where the ratio of the thicknesses ( $h/t$ ) is known, can be designed with the above equations. Caution, however, must be exercised, for cross sections in which the ratio of the thicknesses is specified, to select the proper characteristic dimensions of the cross section. The characteristic dimensions must belong to the least stable of the elements of the cross section. This would ensure that the failing stress would occur when the maximum over-all stability would equal the lowest of the local stability stresses. For most cases investigated (summarized in Table 1) the "t" and "d" of the web are the characteristic dimensions of the cross section, since it satisfies the following inequality.

$$(h/t)^2 (C_h/C_t)^{1/2} \geq z$$

### d. Maximum Local Stability

When the cross section is defined by four or more unknown dimensions, then the equality of the local stability of each of the elements of the cross section must be employed. In addition, symmetry conditions which will maximize the inertia and equalize local stabilities are utilized.

Equations of the types described above are employed to obtain a relationship between the applied load and a characteristic dimension. The solution of this relationship for the geometry of the minimum weight structure would be quite simple if the material were linear. Unfortunately, the minimum weight design almost always occurs at stress levels which are beyond the proportional limit of the material and thus a direct closed form solution is not possible.

An inverse solution is employed in which a nondimensional load index ( $\bar{P}$ ) and a nondimensional stability index ( $\xi$ ) are equated to functions of the stress ratio

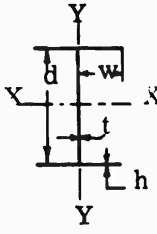
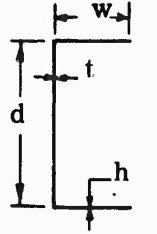
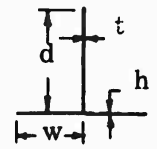
( $\sigma/\sigma_0$ ). The load index (e.g.,  $\bar{P} = (P) \left( \frac{\alpha_3 C_c \sqrt{C_t}}{b^2 \alpha_1^2} \right) \left( \frac{E_A^{3/2}}{\sigma_0^{5/2}} \right)$  for a flanged column) is

expressed in terms of the applied load ( $P$ ), the known boundary conditions ( $C_c, C_t$ ) and geometry ( $b, \alpha_1, \alpha_3$ ), and the material constants ( $E_A, \sigma_0$ ). The stability index

(e.g.,  $\xi_p = C_t \frac{E_A}{\sigma_0} \left( \frac{t}{d} \right)^2$  for a web) is expressed in terms of the material constants,

the known boundary conditions, and the unknown dimensions of the cross section. The procedure is to assume a stress ratio, compute the stability and load indices for a given type of construction which correspond to the minimum weight design, and to

TABLE 1 - GEOMETRIC FACTORS FOR COLUMNS

Section	Defining Condition	z	$\alpha_1$		$\alpha_3$		Thick. Ratio
		wh/dt	A/dt	A/wt	I/d <sup>3</sup> t	I/w <sup>3</sup> t	h/t <sup>(1)</sup>
<b>I-Beam</b> 	Max I <sub>xx</sub>	.083	1.333	-	.167	-	-
	I <sub>xx</sub> =I <sub>yy</sub> (3)	2.370 .470	10.480 -	- 6.124	2.450 -	- .667	- .500
	I <sub>xx</sub> =4I <sub>yy</sub> (4)	.643 .250	3.584 -	- 8.000	.729 -	- .667	- .500
			$\frac{1+4z}{2}$	$\frac{4+1/z}{2}$	$\frac{.083+z}{2}$	$\frac{1.333 h/t}{2}$	
<b>Channel</b> 	Max I <sub>xx</sub>	.167	1.333	-	.167	-	-
	I <sub>xx</sub> =I <sub>yy</sub> (3)	7.90 1.366	16.80 -	- 2.732	4.033 -	- .301	- 1.000
	I <sub>xx</sub> =4I <sub>yy</sub> (4)	1.72 .639	4.44 -	- 3.565	.943 -	- .386	- 1.000
			$\frac{1+2z}{2}$	$\frac{2+1/z}{2}$	$\frac{.083+.5z}{2}$	$\frac{.667-\frac{1}{2+1/z}}{2}$	
<b>Tee</b> 	Max I <sub>xx</sub>	.063	1.125	-	.111	-	-
	I <sub>xx</sub> =I <sub>yy</sub> (3)	.570 .553	2.140 -	- 3.81	.216 -	- .333	- .500
	I <sub>xx</sub> =4I <sub>yy</sub> (4)	.250 .356	1.500 -	- 4.81	.167 -	- .333	- .500
			$\frac{1+2z}{2}$	$\frac{2+1/z}{2}$	$\frac{.333-\frac{.25}{1+2z}}{2}$	$\frac{.667 h/t}{2}$	

(1) Unspecified h/t is defined by  $\frac{h}{t} = (z)^{1/2} (C_t/C_h)^{1/4}$

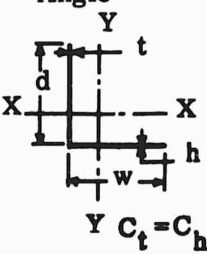
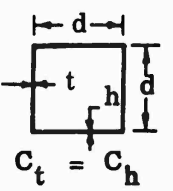

Specified h/t is defined by sheet metal construction

(2) X-axis and Y-axis are horizontal and vertical references axes, respectively, for all sections

(3)  $\frac{C_{cy}}{C_{cx}} = 1$  (Eq. 13c)

(4)  $\frac{C_{cy}}{C_{cx}} = 4$  (Eq. 13c)

TABLE 1 - GEOMETRIC FACTORS FOR COLUMNS (Cont'd)

Section	Defining Condition	z	$\alpha_1$		$\alpha_3$		Thick. Ratio
		wh/dt	A/dt	A/wt	$I/d^3t$	$I/w^3t$	$h/t^{(1)}$
Angle (5)  $C_t = C_h$	Max $I_{xx}$	.125	$\frac{1+z}{1.125}$	$\frac{1+1/z}{-}$	$\frac{.333-.25}{1+z}$	.111	.354
An angle free to bend about any axis would not buckle about x or y axes.							
Square Tube  $C_t = C_h$	Max $I_{xx}$ $I_{xx} = I_{yy}^{(3)}$ $I_{xx} = 4I_{yy}^{(4)}$	.167 1.000 .090	$\frac{2+2z}{2.333}$ 4.000 2.180	- - -	$\frac{.167+.5z}{.250}$ .667 .212	- - -	.409 1.000 .300
Circular Tube 	-	-	3.142	-	.393	-	-

(1) Specified  $h/t$  is defined by  $\frac{h}{t} = (z)^{1/2} (C_t/C_h)^{1/4}$

(2) X-axis and Y-axis are horizontal and vertical references axes, respectively, for all sections

(3)  $\frac{C_{cy}}{C_{cx}} = 1$  (Eq. 13c)

(4)  $\frac{C_{cy}}{C_{cx}} = 4$  (Eq. 13c)

(5) Angle assumed to bend about x axis only



plot these relationships. The design can then be determined by reversing the process. For a given type of construction, load, and material, a load index can be computed. The stress ratio can then be obtained from the  $\bar{P}$  vs.  $\sigma/\sigma_0$  plot and the detail design and minimum weight can then be determined with this stress ratio. The use of these nondimensional design curves results in a relatively simple and rapid method of designing a minimum weight structure and in a radical reduction in the amount of design data and aids required. The effects of modifying end fixity, introducing empirical constants, and considering materials with various thermal exposures and loading temperatures, can be rapidly evaluated with the same graph.

In addition, the detail design of a portion of a structure can sometimes be utilized to design other areas. If the structural arrangement is maintained over an area of the structure in which the temperatures and airload intensity are similar, then the detail design of one portion of the area will be a scale model of all the other portions. This is because the load index for a given material and temperature will be the same in all portions and will result in the same design stress and thickness ratios.

The design technique is illustrated in the examples which follow (Section III). The methods of obtaining the load and stability indices for various types of constructions are illustrated for the columns and summarized for plates, tubes, and bending members. The evaluation of the geometry and material parameters is discussed in the remaining parts of this section.

## 2. GEOMETRY FACTORS

The stability of a structure depends upon the type of construction, the detail geometry, the over-all geometry, and the edge fixity conditions. The type of construction, the over-all geometry, and the edge fixity conditions are known to the designer, and must be employed to obtain the detail geometry. The type of construction determines the form of the stability equation

(e.g.,  $\sigma = C_t E_R (t/b)^2$  for a plate), and coupled with the internal edge fixities, determines the relative distribution of the thickness ratios of the cross-sectional elements. The over-all geometry (e.g., aspect ratio) and the edge fixity de-

termine stability constants (e.g.,  $C_t = \frac{4\pi^2}{12(1-\nu^2)} = 3.62$  for an infinitely long simply supported plate). The effect of the nonlinearity of the material is reflected in an effective stability modulus  $E_R$  which is assumed to be defined knowing the end fixities. The end fixities determine the ratio of bending and twisting energies of the structure and result in an expression for the effective modulus in terms of the secant ( $E_S$ ) and tangent ( $E_T$ ) moduli.

Values of stability constants (or constants from which they can be derived) as well as expressions for the effective stability moduli in terms of the edge fixities and aspect ratios are readily available in the literature (e.g., References 1 through 9). A summary of such values can be found in References 2 and 4.

### 3. MATERIAL FACTORS

The stability of a structure is dependent upon the stress-strain relationship of the material. When the material is linear then only the modulus ( $E_A$ ) is required to determine the stability stress (up to the allowable stress at which time the allowable stress governs). In general, however, the design stress for minimum weight occurs above the proportional limit and recourse must be taken to employ the actual stress-strain relationship.

The nondimensional approach recommends the use of a mathematical expression of the stress-strain relationship with three arbitrary constants ( $E_A$ ,  $\sigma_0$ ,  $\beta$ ). This offers the widest latitude in matching the actual stress-strain curve while still being able to present single design graphs for each type of construction. The nondimensional form of the stress-strain law is

$$\frac{E_A \epsilon}{\sigma_0} = \frac{\sigma}{\sigma_0} (1 - \beta) + \beta \sinh \sigma / \sigma_0 \quad (1a)$$

The formulation is based upon representing the nonlinear material deformations as an exponential function employing a rate diffusion model of deformations (Reference 7). The formulation is in good agreement with experimental data and has been employed to approximate creep as well as instantaneous strains. It can be readily adapted to computation techniques since the nonlinear component is a simple product of  $\sinh \sigma / \sigma_0$  (which need be tabulated only once) and  $\beta$ , rather than an odd power function, (which would require many tabulations) as is exemplified by the Ramberg-Osgood representation

$$\frac{E_A \epsilon}{\sigma_{.7}} = \frac{\sigma}{\sigma_{.7}} + \frac{3}{7} \left( \frac{\sigma}{\sigma_{.7}} \right)^n \quad (1b)$$

The material constants are selected so as to match the initial portion of the stress-strain curve up to the area of interest in the design. This would require matching the linear and nonlinear portions of the curve up to the vicinity of the yield stress. Selecting  $E_A$  equal to the initial slope of the curve matches the initial portion of the curve. The remaining constants  $\sigma_0$  and  $\beta$  are selected to match the nonlinear portion of the curve. One procedure is to plot the strain deviation ( $\delta = \epsilon - \sigma / E_A$ ) on a log scale versus values of the stress ( $\sigma$ ) on a linear scale (Figure 1a). This plot would result in a straight line for the plastic portion of the stress-strain curve if the formulation was exact. Selecting values of  $\sigma_0$  and  $\beta$  which depend upon the best straight line would result in a good approximation to the actual curve with the error in the stress represented by the horizontal distance between an actual point and the straight line in the referenced plot. The material constants  $\sigma_0$  and  $\beta$  are determined, after two points ( $\sigma_1, \delta_1$ ) and ( $\sigma_2, \delta_2$ ) on the best straight line are selected, in the following manner:

$$\sigma_0 = \frac{\sigma_2 - \sigma_1}{2.3 \log(\delta_2 / \delta_1)} \quad (1c)$$

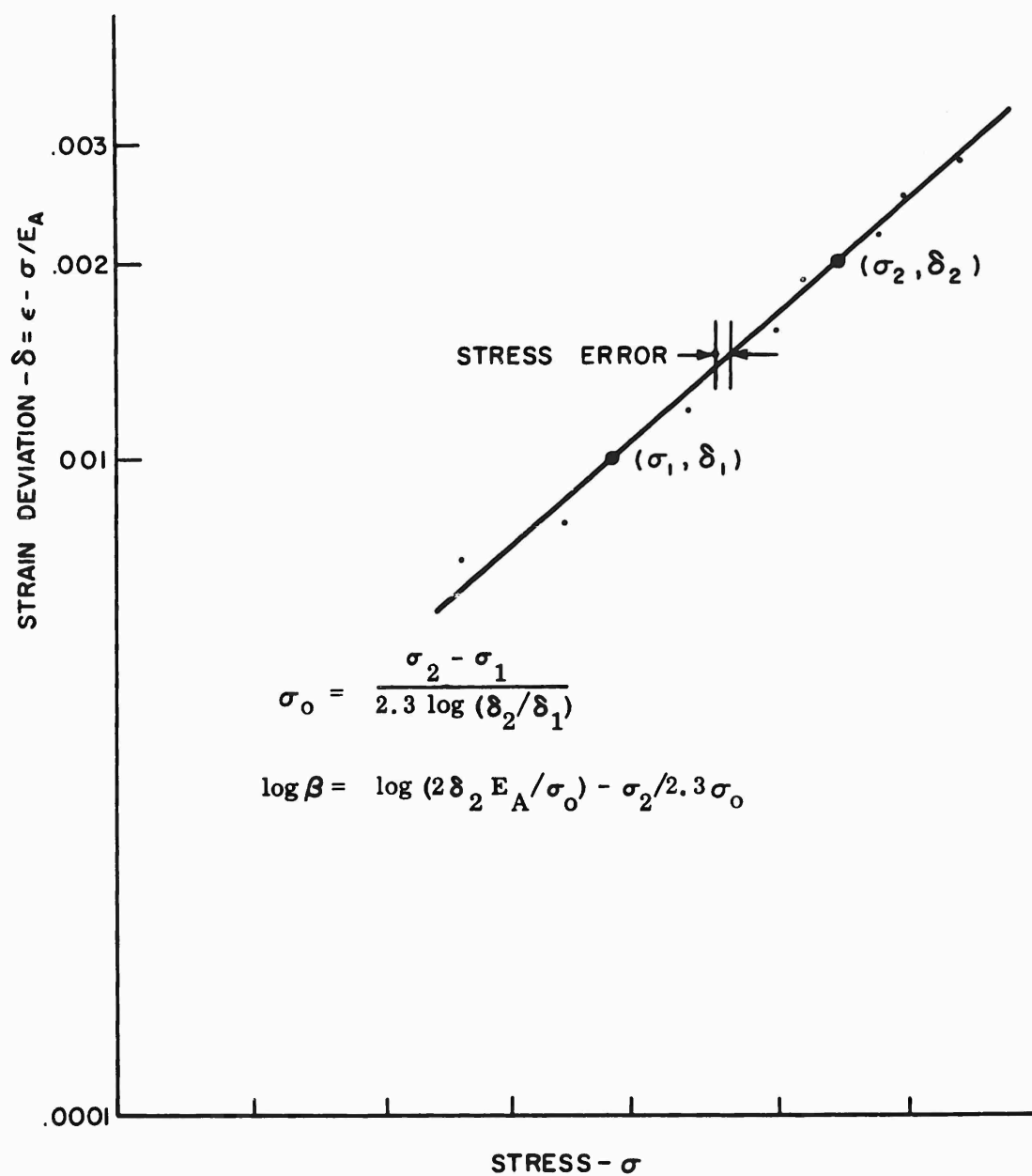


Figure 1a. Strain Deviation vs. Stress

$$\begin{aligned} \text{and } \log \beta &= \log \left( \frac{2\delta_2 E_A}{\sigma_0} \right) - \frac{\sigma_2}{2.3 \sigma_0} \\ &= \log \left( \frac{E_A}{\sigma_2 - \sigma_1} \right) + \log \left( 4.6 \delta_2 \log \frac{\delta_2}{\delta_1} \right) - \frac{\left[ \log \left( \frac{\delta_2}{\delta_1} \right) \right] \sigma_2}{\sigma_2 - \sigma_1} \end{aligned} \quad (1d)$$

Requiring the approximation of the stress-strain curve to pass through two nonlinear points on the actual curve is equivalent to selecting the stress and deviation of these two points to establish the straight line. As an example, if the .001 and .002 offset stresses are employed, then

$$\sigma_0 = 1.442 (\sigma_2 - \sigma_1) \quad (1e)$$

$$\text{and} \quad \log \beta = \log \left( \frac{E_A}{\sigma_2 - \sigma_1} \right) - 2.558 - \left[ \frac{.301 \sigma_2}{\sigma_2 - \sigma_1} \right] \quad (1f)$$

results in a computed stress-strain curve [Eq.(1a)] which passes through the yield stress ( $\sigma_2$ ) and the .001 offset stress ( $\sigma_1$ ) and which has an initial modulus equal to  $E_A$ .

The Ramberg-Osgood Parameters ( $E_A$ ,  $\sigma_{.7}$ ,  $n$ ) can be transformed to the above parameters ( $E_A$ ,  $\sigma_0$ ,  $\beta$ ) by making the curve pass through the same control points ( $\sigma_{.7}$  and  $\sigma_{.85}$ ). This results in the following formulae:

$$\sigma_0 = \left[ \frac{1 - (\sigma_{.85}/\sigma_{.7})}{\frac{n}{n-1} (.8878)} \right] \sigma_{.7} \quad (1g)$$

$$\text{and} \quad \beta = \frac{(3/7) (\sigma_{.7}/\sigma_0)}{\sinh \frac{\sigma_{.7}}{\sigma_0} - \frac{\sigma_{.7}}{\sigma_0}} \quad (1h)$$

where  $\sigma_{.85}/\sigma_{.7}$  is known or obtained from Figure 3b of Reference 4.

Data available in various texts (References 10 through 19) were analyzed to obtain the material constants and creep properties employed in the illustrative examples. These constants (Figures 1b, 2 and 3) should not be viewed as the best values for the materials investigated but rather as values to be employed in illustrating the design technique. Variations in the material constants, obtained from different tests, occurred because of variations in the stress-strain curves for the same material and temperature. The scatter was more severe with the higher temperatures and newer materials which are now being developed. Fortunately, the design stress and minimum weight are not too sensitive to variations of the nonlinear material constants ( $\sigma_0$  and  $\beta$ ). Engineering judgement was employed in obtaining the material constants for the illustrative examples.

A statistical analysis of all available data is recommended to obtain the most probable values of the material constants and to estimate the effects the variations have on the design stresses and weights in an actual design.

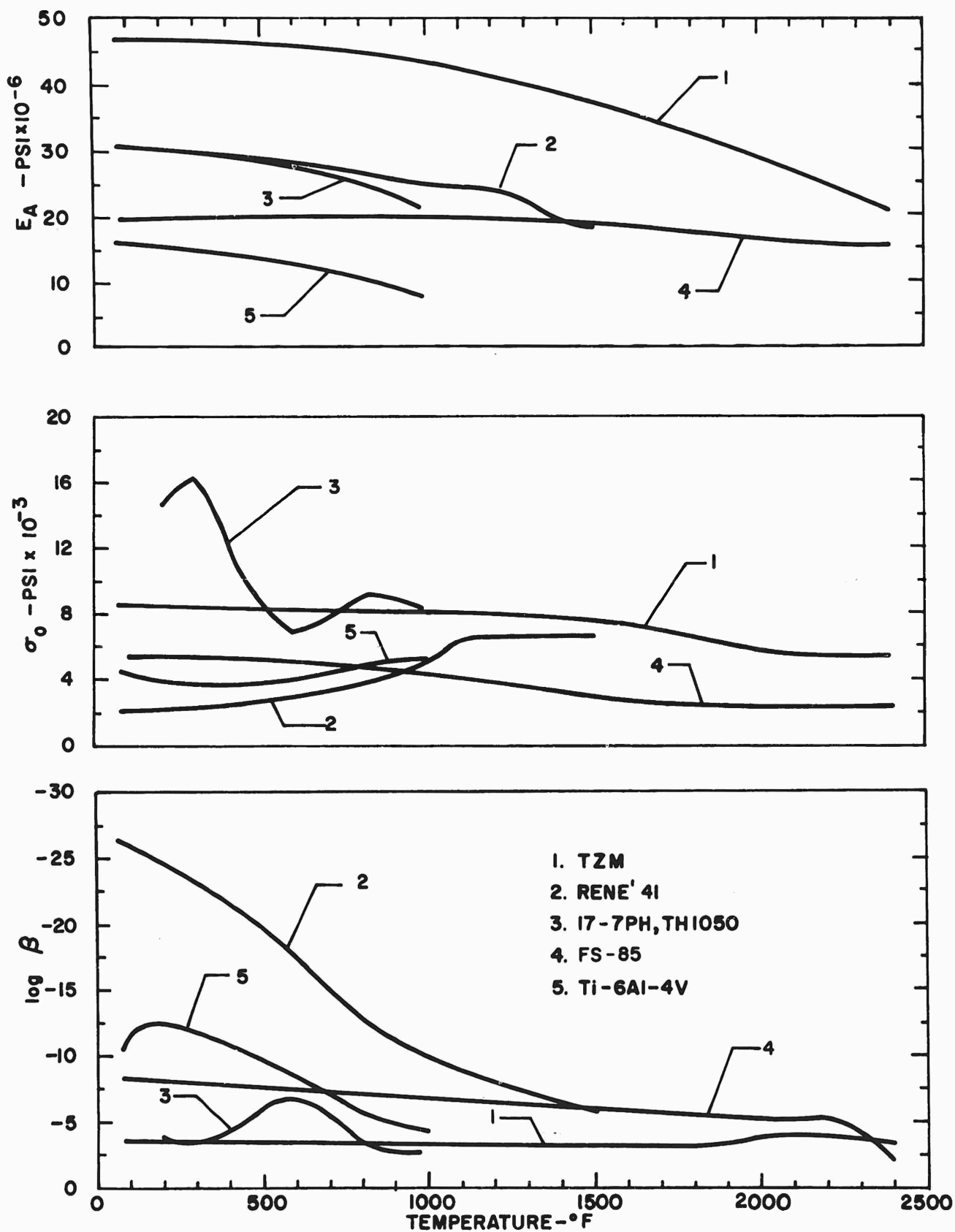


Figure 1b. Material Constants  $E_A$ ,  $\sigma_0$ , and  $\log \beta$  vs. Temperature

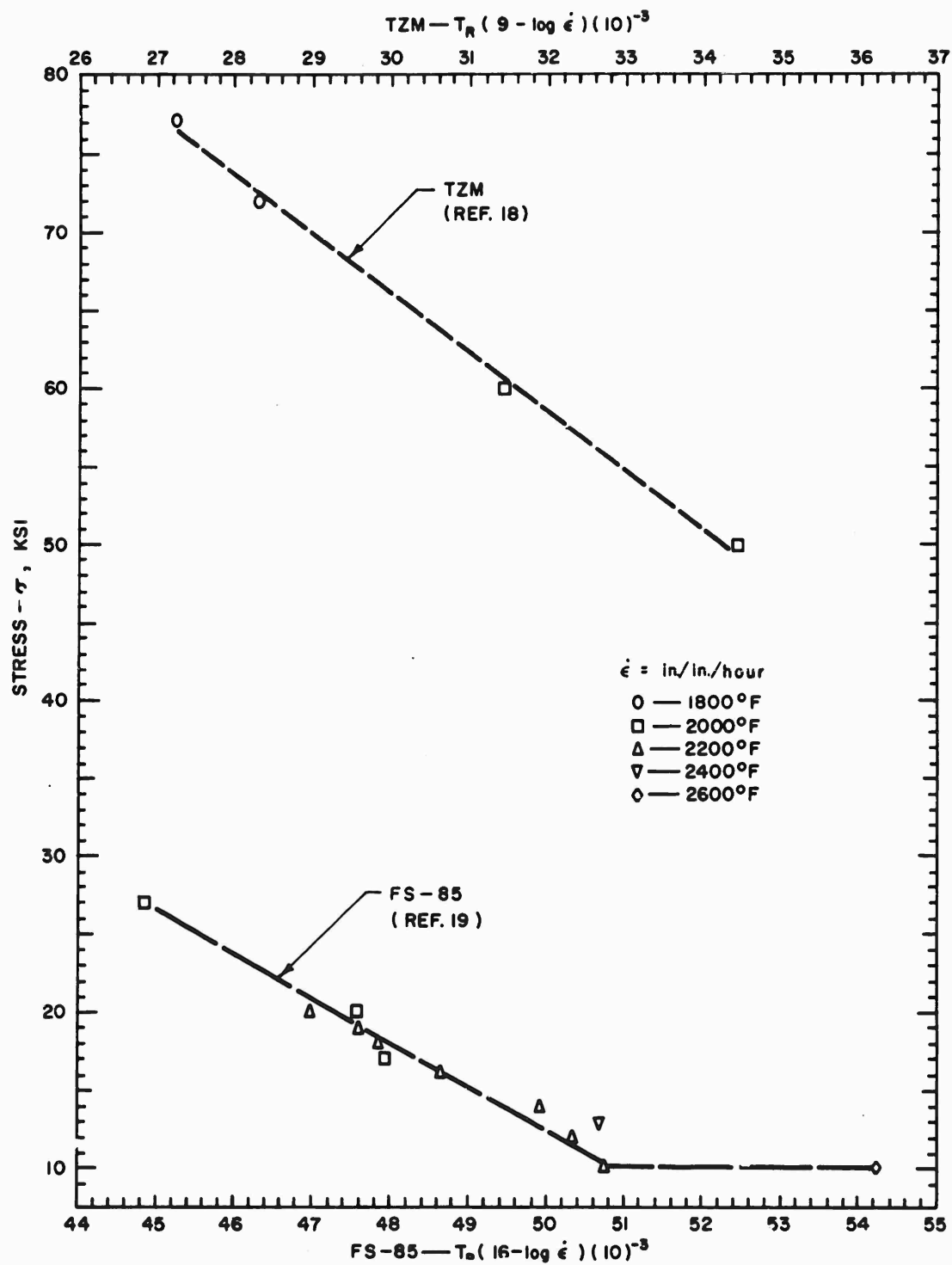
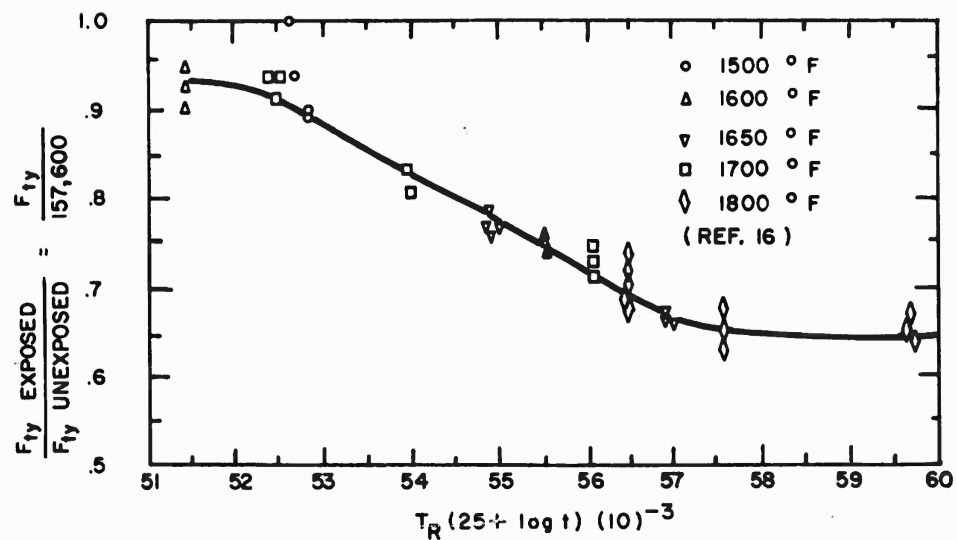
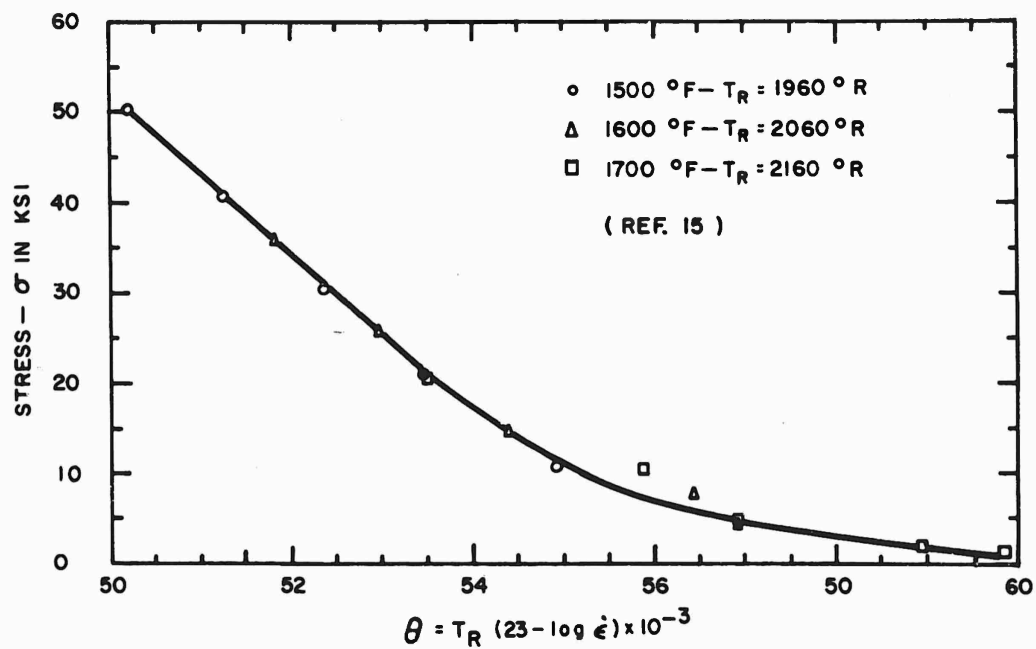


Figure 2. Parametric Creep Rate Plots of TZM and FS-85



a. Yield Strength Deterioration vs. Exposure



b. Creep Rate vs. Stress

Figure 3. Parametric Plots for Rene' 41

An estimate of the effect of thermal exposure upon the material constants can be obtained by noting the effect of the exposure upon the yield stress.

If  $\sigma_y' = x \sigma_y$

and assuming  $E_A' = E_A$

the following approximations result:

$$\sigma_o' = x \sigma_o$$

and  $\beta' = \beta/x$

$$\log \beta' = \log \beta - \log x \sim \log \beta$$

Primed constants refer to exposed material whose yield stress is x times the unexposed yield stresses. Values of x can be estimated from master "Larson-Miller Strength after Exposure" plots as exemplified by Figure 3a.

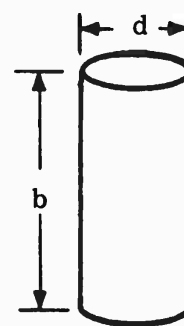
## B. COLUMNS

The calculations required to determine the load and stability indices are indicated in some detail for some column cross sections of up to 4 unknown dimensions. The results for other column cross sections, plates, and tubes can be obtained in a similar manner and are summarized in Table 1 for columns and in the appropriate sub-sections for some plate constructions and tubes.

The design would be obtained by computing the load index, determining the stress ratio from a  $\bar{P}$  vs.  $\sigma/\sigma_o$  plot, and determining the detail geometry from both  $\xi$  vs.  $\sigma/\sigma_o$  plots and the appropriate equations indicated below.

### 1. ONE UNKNOWN DIMENSION

Example - Solid circular column  
using load equation



#### Load Equation

$$P = A \sigma \quad (2a)$$

$$\text{Let } \xi_c = \left( \frac{\sigma}{\sigma_o} \right) / (E_T/E_A) \quad (\text{Fig. 4}) \quad (2b)$$

where values of the stability index ( $\xi_c$ ) as a function of the stress ratio ( $\sigma/\sigma_o$ ) are plotted in Figure 4 for various values of  $\log \beta$ .

$$\text{But } \sigma = C_c E_T \left( \frac{I}{A b^2} \right) \quad (2c)$$



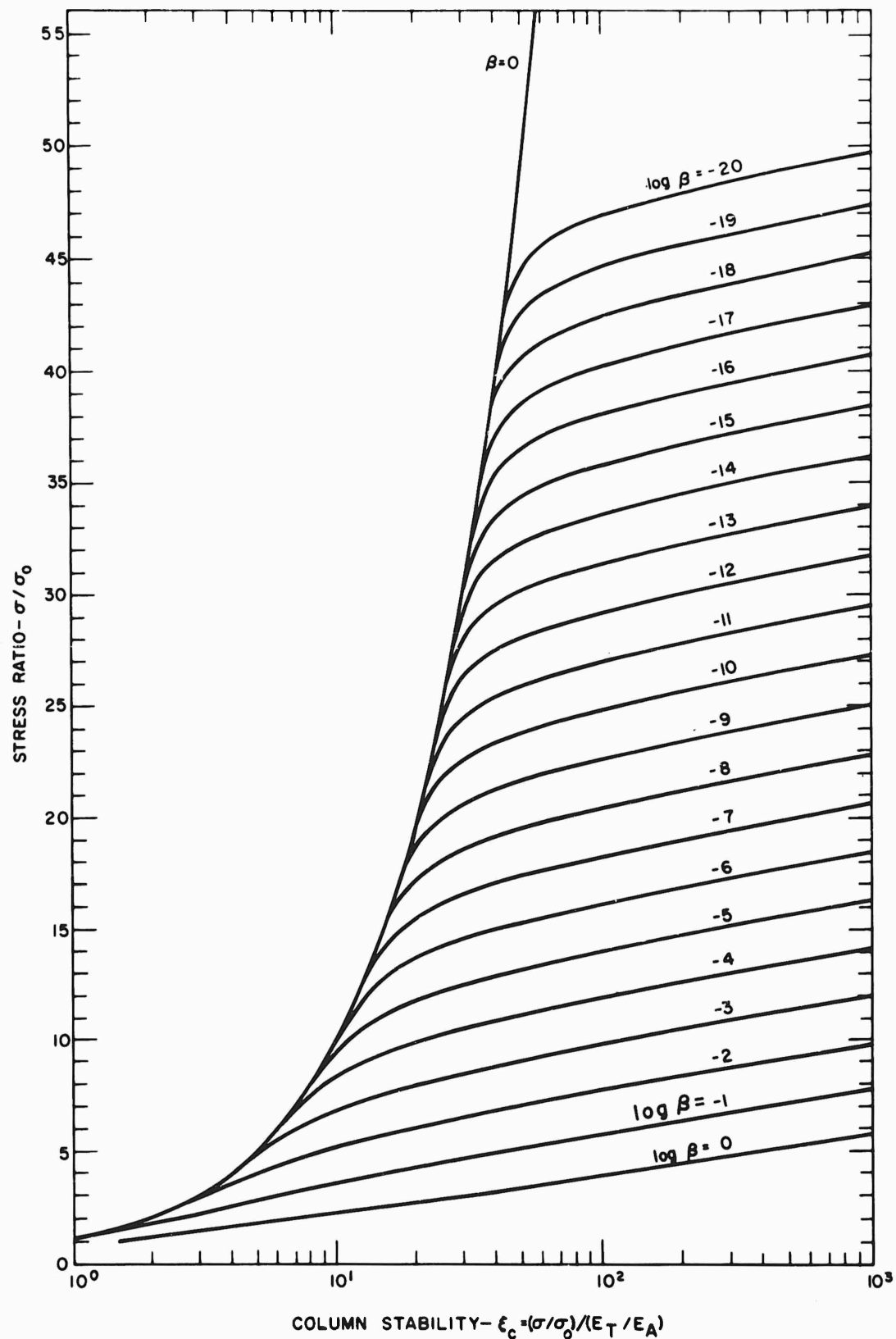


Figure 4. Stress Ratio vs. Column Stability Parameter

Where  $C_c$  is the end fixity of the column. Substituting Eq. (2c) into Eq. (2b) results in the stability index as a material-geometry parameter, giving

$$\xi_c = \frac{C_c}{16} \left( \frac{E_A}{\sigma_o} \right) \left( \frac{d}{b} \right)^2 = C_d \frac{E_A}{\sigma_o} \left( \frac{d}{b} \right)^2 \quad (2d)$$

$$\text{where } C_d = C_c (I/Ad^2) = C_c/16 \quad (2e)$$

$$\text{and } d = b \left( \frac{\xi_c \sigma_o}{C_d E_A} \right)^{1/2} \quad (3)$$

is obtained from Eq. (2d).

From Eqs. (2a) and (2d) we obtain

$$\frac{P}{b^2 \sigma_o} = \left( \frac{\pi}{4} \right) \left( \frac{d^2}{b^2} \right) \left( \frac{\sigma}{\sigma_o} \right) = \left( \frac{\pi}{4} \right) \left( \frac{\xi_c \sigma_o}{C_d E_A} \right) \left( \frac{\sigma}{\sigma_o} \right)$$

Rearranging terms so that the left-hand side of the equation is devoid of stability index and stress ratio terms, results in the following expression for the load index:

$$\bar{P} = \left( \frac{P}{b^2 \sigma_o} \right) \left( \frac{4}{\pi} \right) \left( \frac{C_d E_A}{\sigma_o} \right) = \xi_c \left( \frac{\sigma}{\sigma_o} \right) \quad (4)$$

This load index was not plotted since it was not deemed to be of sufficient interest in design and is only employed to illustrate the computing techniques to obtain load-material-geometry parameters ( $\bar{P}$ ) and material-geometry parameters ( $\xi$ ) that can be expressed as functions of the stress ratio ( $\sigma/\sigma_o$ ).

## 2. TWO UNKNOWN DIMENSIONS

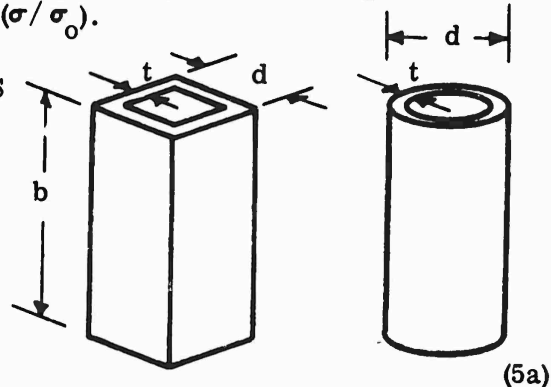
Examples - Circular or square tubes using stability and load equations.

### Stability Equation

$$\sigma_p = \sigma_c$$

Setting the local stability equal to the over-all stability results in

$$\sigma = C_t E_R \left( \frac{t}{d} \right)^n = C_c E_T \frac{I}{A b^2} \quad (5b)$$



where  $C_t$  and  $n$  are constants determined by the geometry.

Let  $n = 1$

$$\text{and } E_R = \sqrt{E_A E_T} \quad \text{for a circular tube (Reference 6)} \quad (6a)$$

Let  $n = 2$  for a plate-like element

$$\text{and } E_R = \left[ .428 + .572 \sqrt{.25 + .75 \frac{E_T}{E_S}} \right] E_S \quad (6b)$$

This is an average value for plates with various boundary conditions (See Table 31 and Fig. 176 of Reference 2).

$$\text{Let } A = \alpha_1 dt ; (\alpha_1 = \pi \text{ for a circular tube}) \quad (7a)$$

$$\text{and } I = \alpha_3 d^3 t ; (\alpha_3 = \pi/8 \text{ for a circular tube}) \quad (7b)$$

Substituting Eqs. (7a) and (7b) into Eq. (5b) results in

$$\sigma = C_t E_R \left( \frac{t}{d} \right)^n = C_c E_T \frac{\alpha_3 d^3 t}{\alpha_1 dt b^2} = C_d E_T \left( \frac{d}{b} \right)^2 \quad (8a)$$

$$\text{where } C_d = C_c \frac{I}{Ad^2} = \frac{\alpha_3}{\alpha_1} C_c \quad (8b)$$

Rearranging Eq. (8a) results in

$$\frac{t}{d} = \left[ \frac{C_d}{C_t} \frac{E_T}{E_R} \left( \frac{d}{b} \right)^2 \right]^{1/n} \quad (9)$$

Load Equation ( $P = A\sigma$ )

Employing the load equation with Eq. (7a) results in

$$P = \alpha_1 dt \sigma$$

Putting the equation in nondimensional form and substituting Eqs. (9) and (3) results in

$$\frac{P}{b^2 \sigma_o} = \alpha_1 \frac{d^2}{b^2} \frac{t}{d} \frac{\sigma}{\sigma_o} = \alpha_1 \frac{\xi_c \sigma_o}{C_d E_A} \left[ \frac{C_d}{C_t} \frac{E_T}{E_R} \frac{\xi_c \sigma_o}{C_d E_A} \right]^{1/n} \frac{\sigma}{\sigma_o}$$

Placing only stress ratio functions on the right hand side of the equation results in the load index

$$\bar{P} = \frac{P}{b^2 \sigma_o} \frac{E_A C_d}{\sigma_o a_1} \left( \frac{C_t E_A}{\sigma_o} \right)^{1/n} = (\xi_c)^{1 + \frac{1}{n}} \left( \frac{E_T}{E_R} \right)^{1/n} \frac{\sigma}{\sigma_o} \quad (10)$$

The following design equations result for columns with rectangular plate elements ( $n = 2$ ).

$$\begin{aligned} \bar{P} &= \frac{P}{b^2} \frac{(E_A)^{3/2}}{(\sigma_o)^{5/2}} \frac{C_d}{a_1} \sqrt{C_t} = \frac{P}{b^2} \frac{E_A^{3/2}}{\sigma_o^{5/2}} \frac{a_3}{a_1^2} C_c \sqrt{C_t} \\ &= \xi_c^{3/2} \left( \frac{E_T}{E_R} \right)^{1/2} \left( \frac{\sigma}{\sigma_o} \right) = \xi_c \xi_p^{1/2} \left( \frac{\sigma}{\sigma_o} \right) \end{aligned} \quad (11a)$$

This equation is plotted in Figure 6 for various values of  $\log \beta$ .

$$d = b \left( \frac{\xi_c \sigma_o}{C_d E_A} \right)^{1/2} = b \left( \frac{\xi_c \sigma_o}{C_c E_A} \frac{a_1}{a_3} \right)^{1/2} \quad (11b)$$

$$t = d \left( \frac{\xi_p \sigma_o}{C_t E_A} \right)^{1/2} \quad (11c)$$

$$\text{where } \xi_p = (\sigma/\sigma_o) / (E_R/E_A) = C_t \frac{E_A}{\sigma_o} \left( \frac{t}{d} \right)^2 \quad (\text{Fig. 5}) \quad (11d)$$

For a circular tube ( $n=1$ ),

$$\begin{aligned} \bar{P} &= \frac{P}{b^2} \frac{E_A^2}{\sigma_o^3} \frac{C_d C_t}{a_1} = \frac{P}{b^2} \frac{E_A^2}{\sigma_o^3} \frac{a_3}{a_1^2} C_c C_t = \xi_c^2 \left( \frac{E_T}{E_A E_R} \right) \left( \frac{\sigma}{\sigma_o} \right) \\ &= \xi_c^2 \left( \frac{E_T}{E_A} \right)^{1/2} \left( \frac{\sigma}{\sigma_o} \right) = \xi_c^{3/2} \left( \sigma/\sigma_o \right)^{3/2} \quad (\text{Fig. 7}) \end{aligned} \quad (12a)$$

$$d = b \left( \frac{\xi_c \sigma_o}{C_d E_A} \right)^{1/2} = b \left( \frac{\xi_c \sigma_o}{C_c E_A} \frac{a_1}{a_3} \right)^{1/2} \quad (11b)$$

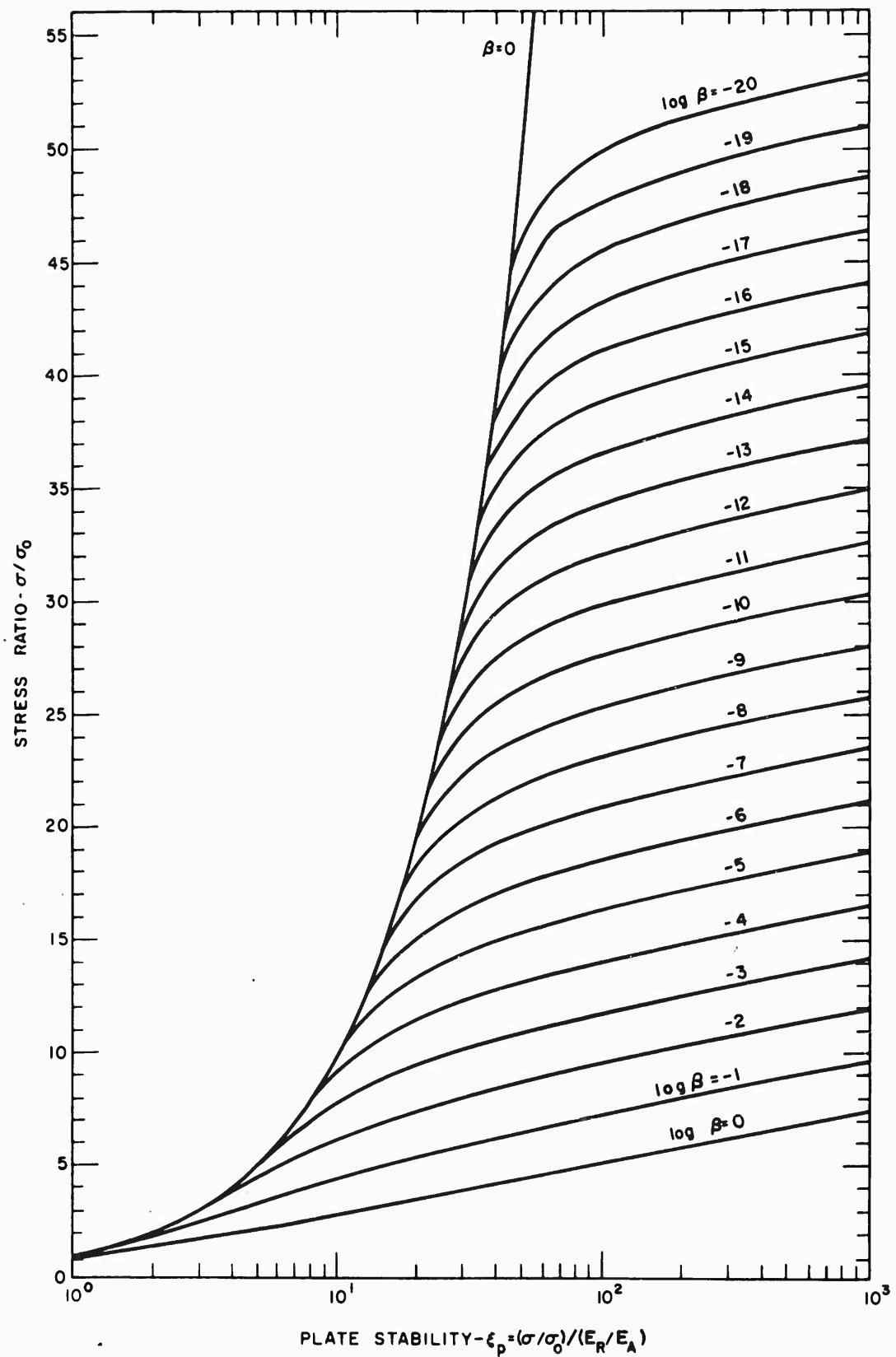


Figure 5. Stress Ratio vs. Plate Stability Parameter

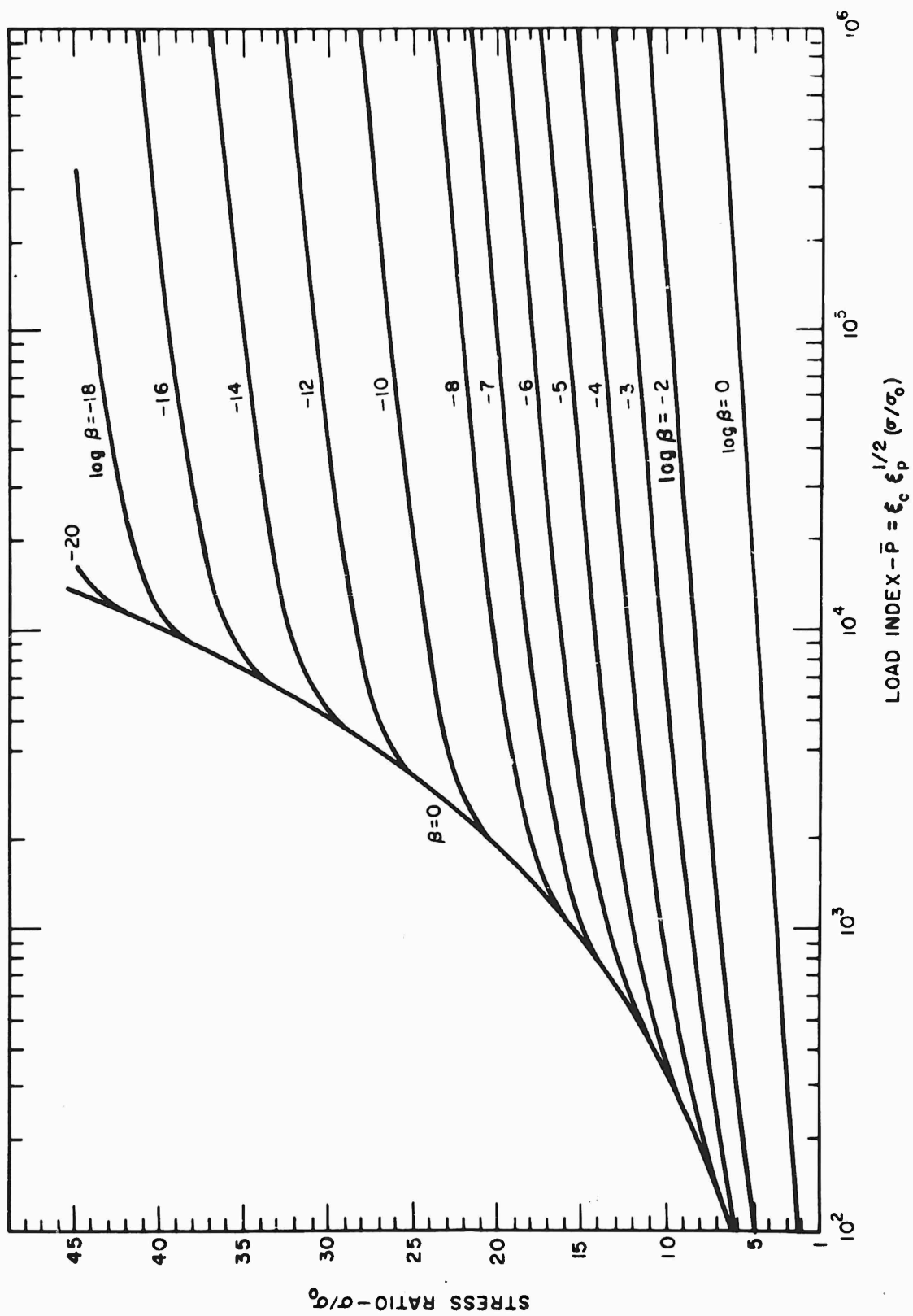


Figure 6. Stress Ratio vs. Load Index for a Column with Rectangular Plates

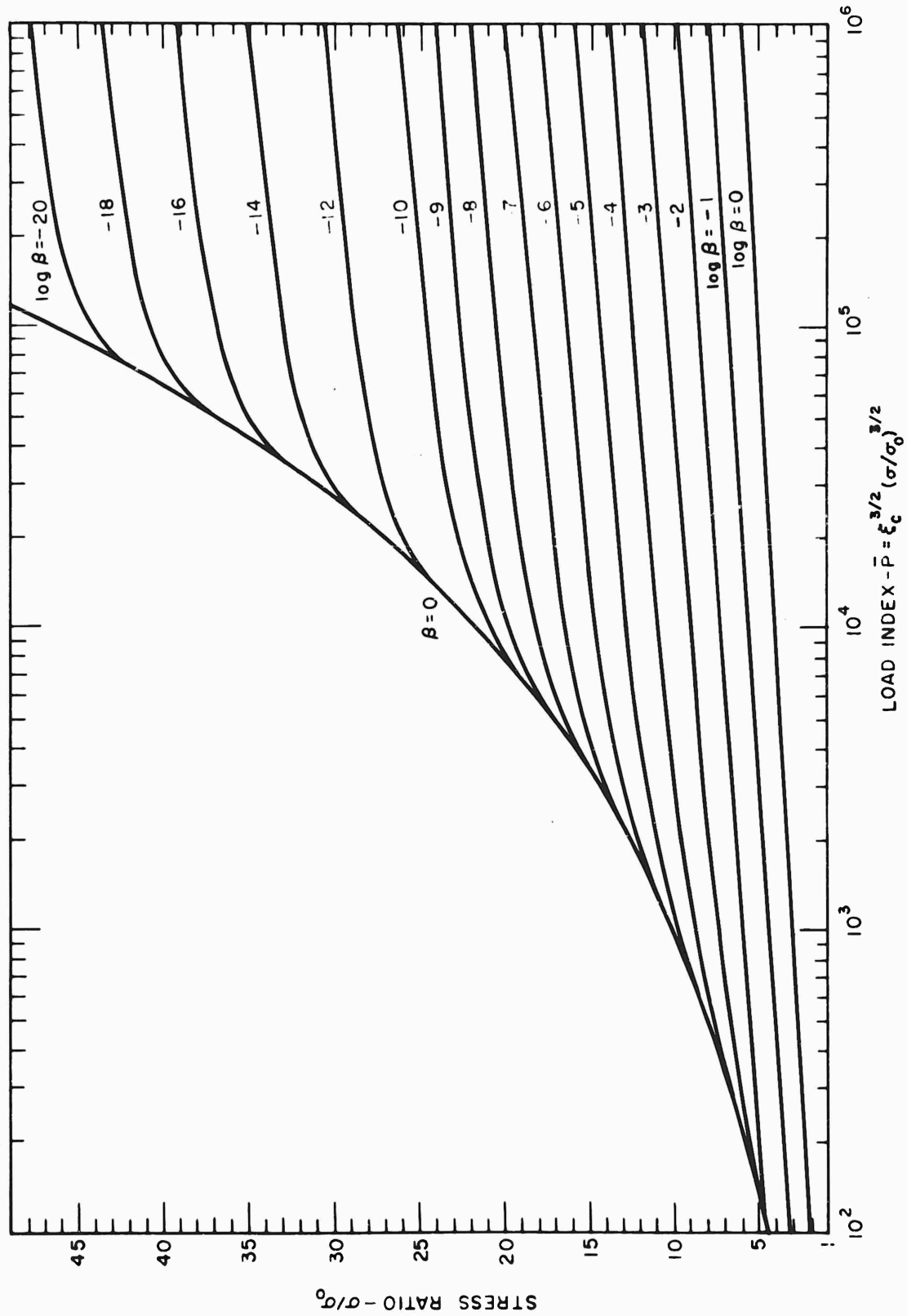
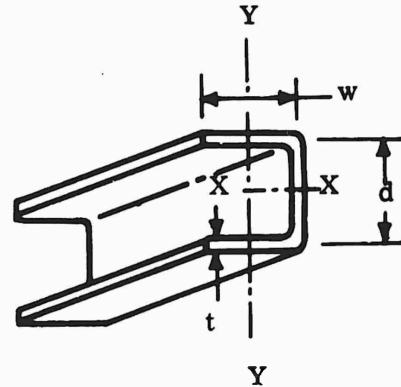


Figure 7. Stress Ratio vs. Load Index for a Tubular Column

$$t = d \frac{\sigma}{(C_t E_A) \sqrt{E_T/E_A}} = \frac{d(\sigma \sigma_o \xi_c)^{1/2}}{C_t E_A} \quad (12b)$$

### 3. THREE UNKNOWN DIMENSIONS

Examples - Sheet metal channels, angles, etc., using maximum over-all stability and stability and load equations.



Maximum Over-all Stability ( $C_{cx} I_{xx} = C_{cy} I_{yy}$ )  
(Equal stability about both bending axes)

Evaluating the inertias of the channel about both axes results in the following:

$$I_{xx} = \frac{1}{12} d^3 t + \frac{w t d^2}{2} = d^3 t \left( \frac{1}{12} + \frac{w}{2d} \right) \quad (13a)$$

$$\begin{aligned} I_{yy} &= 2 \frac{w^3 t}{12} + 2 (w t) \left( \frac{w}{2} \right)^2 - \frac{[2 (w t) (w/2)]^2}{2 w t + d t} \\ &= \frac{2}{3} w^3 t - \frac{w + t}{2w + d} w^3 t = w^3 t \left( \frac{2}{3} - \frac{1}{2 + d/w} \right) \end{aligned} \quad (13b)$$

For equal stability,

$$C_{cx} I_{xx} = C_{cy} I_{yy} \quad (13c)$$

where  $C_{cx}$  and  $C_{cy}$  are the end fixities for buckling of a column about the x and y axes, respectively.

Substituting Eqs. (13a) and (13b) in Eq. (13c) results in

$$C_{cx} d^3 t \left( \frac{1}{12} + \frac{w}{2d} \right) = C_{cy} w^3 t \left( \frac{2}{3} - \frac{1}{2 + d/w} \right)$$

$$\text{Let } \frac{w}{d} = y = z \quad (t/h) \quad (13d)$$

$$\therefore \frac{1}{12} + \frac{y}{2} = y^3 \left( \frac{y + 2}{3(2y + 1)} \right) \left( \frac{C_{cy}}{C_{cx}} \right) \quad (13e)$$

If  $\frac{C_{cy}}{C_{cx}} = 1$ , solving Eq. (13e) results in  $y = 1.366$



$$\text{Since } A = dt + 2 wt = dt \left( 1 + 2 \frac{w}{d} \right) = dt (1 + 2 y) \quad (14)$$

we obtain the coefficients which reduce this design to one with two characteristic dimensions similar to that described in the previous section. From Eqs. (14) and (13a) we obtain

$$\alpha_{1d} = (1 + 2y) = 3.732$$

$$\alpha_{3d} = \left( \frac{1}{12} + \frac{y}{2} \right) = .766$$

The detail design would be determined by employing Eqs. (11a), (11b), (11c), and (13a) provided that the web is most critical. The criteria for determining when the web is most critical is obtained as follows:

$$C_h E_R \left( \frac{h}{w} \right)^2 \geq C_t E_R \left( \frac{t}{d} \right)^2$$

$$\therefore \frac{h}{t} \geq (C_t / C_h)^{1/2} \left( \frac{w}{d} \right)$$

Substituting  $z = \frac{wh}{dt}$  results in

$$\left( \frac{h}{t} \right)^2 \sqrt{C_h / C_t} \geq z \quad (15)$$

The value of  $C_h$  can be increased, if desired, by adding a bead or reinforcement to the flange. This criteria is not satisfied in sheet metal construction with free flanges which can buckle about both axes. It is satisfied for all sections when buckling can occur about the X-axis only (see Subsection B. 4). For the case illustrated, the flange is more critical than the web since, from Eq. (15),

$$\left( \frac{h}{t} \right)^2 (C_h / C_t)^{1/2} = 1 \left( \frac{.388}{3.62} \right)^{1/2} = .329 < \frac{y}{(t/h)} = \frac{1.366}{1} = 1.366$$

From Eqs. (14) and (13a) we obtain

$$A = wt \left( \frac{d}{w} + 2 \right) = wt \left( \frac{1}{y} + 2 \right) = 2.732 wt = \alpha_{1w} wt$$

$$I = w^3 t \left( \frac{2}{3} - \frac{1}{2 + 1/y} \right) = .301 w^3 t = \alpha_{3w} w^3 t$$

This results in similar expressions for the design using  $w$  as the characteristic dimension, i.e.,

$$\bar{P} = \left( \frac{P}{b^2} \right) \left( \frac{E_A}{\sigma_o} \right)^{3/2} \left( \frac{\alpha_3}{\alpha_1} \right) (C_c) (C_h)^{1/2} \quad (16a)$$

$$w = b \left( \frac{\xi_c \sigma_o \alpha_1}{C_c E_A \alpha_3} \right)^{1/2} \quad (16b)$$

$$t = w \left( \frac{\xi_p \sigma_o}{C_h E_A} \right)^{1/2} \quad (16c)$$

$$d = w/y \quad (16d)$$

Values of  $z$ ,  $\alpha_{1d}$ , or  $\alpha_{1w}$ , and  $\alpha_{3d}$  or  $\alpha_{3w}$  for various cross sections with  $C_{cy}/C_{cx}$  equal to 1 (i.e.,  $I_{xx} = I_{yy}$ ) and 4 (i.e.,  $I_{xx} = 4I_{yy}$ ) are presented in Table 1. Note that the design procedure is identical to that described in Sub-section 2 except that the geometry constants ( $\alpha_{1w}$ ,  $\alpha_{3w}$ , and  $C_h$ ) are employed to solve for  $w$  rather than  $d$ .

#### 4. FOUR OR MORE UNKNOWN DIMENSIONS

Example - Extruded or machined channels, etc., using symmetry, maximum over-all stability, and the stability and load equations.

Symmetry (Equal stability and max.  $I$ )

$$w_1 = w_2 = w$$

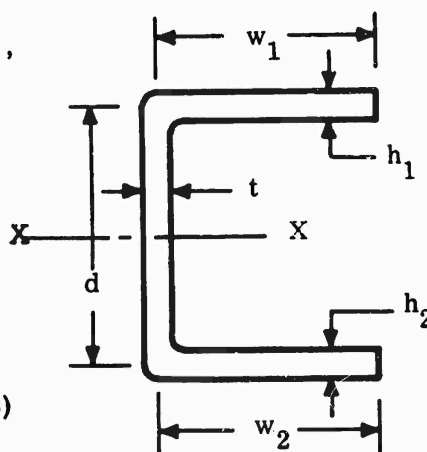
$$h_1 = h_2 = h$$

Maximum Over-all Stability  
(Maximum inertia [ $I_{xx}$ ] about only bending axis)

$$A = dt + 2 wh = dt (1 + 2z) \quad (17a)$$

$$I = \frac{1}{12} d^3 t + 2 wh \left( \frac{d}{2} \right)^2 = d^3 t \left( \frac{1}{12} + z/2 \right) \quad (17b)$$

$$\text{where } z = \frac{wh}{dt} \quad (17c)$$



To determine the mass distribution which will maximize  $I$  for a stationary  $A$  and  $t/d$  ratio, we first determine the relationship which makes the  $A$  and  $t/d$  ratio stationary for an incremental change in  $z$ .

$$\left( \text{i.e., } \frac{\delta A}{\delta z} = \frac{\delta (t/d)}{\delta z} = 0 \right)$$

$$\text{Since } \frac{\delta A}{\delta z} = \frac{\delta \left[ (t/d) (d^2) (1 + 2z) \right]}{\delta z} = 0 \quad (18a)$$

it follows that

$$\frac{\delta A}{\delta z} = \frac{\delta(t/d)}{\delta z} \left[ d^2 (1 + 2z) \right] + \frac{\delta d^2}{\delta z} \left( \frac{t}{d} \right) (1 + 2z) + \left( \frac{t}{d} \right) (d^2) (2) = 0$$

but for maximum stability of element

$$\frac{\delta(t/d)}{\delta z} = 0$$

$$\therefore \frac{\delta d^2}{\delta z} (1 + 2z) + 2d^2 = 0$$

$$\frac{\delta d^2}{d^2} = - \frac{\delta z}{1 + 2z}$$

$$\log d^2 = - \log (1 + 2z) + c$$

$$\log d^2 (1 + 2z) = c$$

$$\therefore d^2 (1 + 2z) = e^c = \text{constant for stationary area} \quad (18b)$$

For maximum over-all stability, the incremental change in I for a change in z should be zero.

$$\frac{\delta I}{\delta z} = \frac{\delta \left[ (d^4) (t/d) (1/12 + z/2) \right]}{\delta z} = \frac{\delta \left[ \frac{(e^{2c}) (t/d) (1/12 + z/2)}{(1 + 2z)^2} \right]}{\delta z} = 0 \quad (18c)$$

This results in

$$\frac{(1 + 2z)^2 (1/2) - (1/12 + z/2) (2) (1 + 2z) (2)}{(1 + 2z)^4} = 0$$

$$\text{and } 1/6 = z \quad (18d)$$

Substituting in Eqs. (17a) and (17b)

$$\alpha_1 = 1 + 2z = 1.333 \quad (\text{Table 1}) \quad (18e)$$

$$\alpha_3 = \frac{1}{12} + z/2 = .167 \quad (\text{Table 1}) \quad (18f)$$

Utilizing the equal stability of elements (provided the  $h/t$  ratio is not specified) results in

$$\frac{h}{w} = (t/d) (C_t/C_h)^{1/2} \quad (19a)$$

but from Eq. (17c)  $h = z \frac{td}{w}$  (19b)

$$\therefore \frac{ztd}{w^2} = (t/d) (C_t/C_h)^{1/2}$$

and  $w = d (z)^{1/2} (C_h/C_t)^{1/4}$  (20a)

Similarly,

$$h = t (z)^{1/2} (C_t/C_h)^{1/4} \quad (20b)$$

Values of  $z$ ,  $\alpha_1$ ,  $\alpha_3$ , and  $h/t$  are presented in Table 1 for typical machined or sheet metal sections.

The above analysis is for a column which can only buckle about one axis, and can be applied to sheet metal constructions as well as machined sections. The value of  $z$  which optimizes the cross section does not change. Thus values of  $\alpha_1$  and  $\alpha_3$  can be determined even when the thickness ratio is specified as in sheet metal constructions. All the sections summarized in Table 1 for sheet metal construction which can bend about the  $x$  axis, only, satisfy the criteria of Eq. (15). Thus the web is the critical element and Eqs. (11a), (11b), (11c), and (13d) define the detail design. The case of a machined section with unspecified  $h/t$  ratio need not be investigated as to the characteristic dimensions since the criteria of Eq. (15) is automatically satisfied by Eqs. (20a) and (20b) which results in the web and flanges being equally stable.

### C. PLATES

The basic difference between the column and plate is the restraint in the transverse direction due to the Poisson's ratio ( $\nu$ ) and the edge fixities of the unloaded sides. If the unloaded ends are free, then the plate acts as a column with the bending stiffness increase by a factor of the order of  $1/(1-\nu^2)$ . If the unloaded ends are restrained and the aspect ratio is significant ( $a/b > 1$ ) then the width of the plate, rather than the length, becomes the characteristic buckling dimension ( $b$ ) which determines the stability. It cannot, in this case, be treated as parallel columns.

Many types of plates can be fabricated. This report will consider a limited number of such types of construction. The unreinforced plate, the corrugated plate, the integrally stiffened plate, and the sandwich plate constructions will be examined.

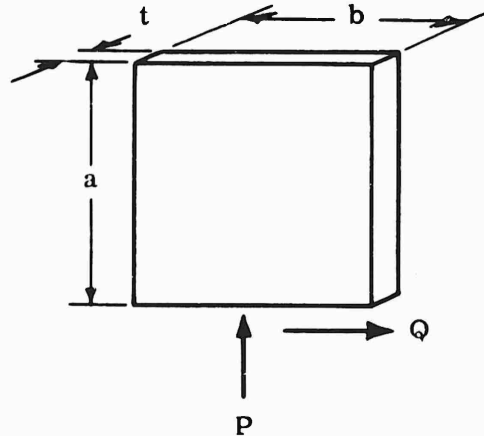
The sandwich plate differs from the others in structural design in that the stability stress can be assigned and the plate designed so as to attain this stability stress. The other constructions require the determination of the "optimum" stress level which will provide the minimum area to resist the applied load. A lower stability stress would require more area to withstand the load and would weigh more than the minimum weight. A higher stability stress cannot be obtained without increasing the area or taking it away from one element to increase the stability of another which will decrease the controlling stability stress.

The sandwich construction has the design characteristic described above because it employs a core which does not resist the applied compression load. The sandwich construction is very efficient for low load intensities ( $P/b^2 \sigma_o$ ), where the built-up constructions have low "optimum" stress levels, but it becomes less efficient than built-up constructions as the "optimum" stress increases to the order of the stress in the sandwich construction. Corrugations, and then reinforced panels, approach higher optimum stresses at lower load intensities than the unreinforced plate. The shear deformation due to axial load is relatively small for non-sandwich type constructions and its effect upon the stability is ignored except for the sandwich construction. It should be noted that non-structural details necessary for these various types of constructions may overshadow the difference in the minimum weight designs.

### 1. UNREINFORCED PLATE

The unreinforced plate contains only one unknown dimension, the thickness "t". Employing the load equation, we obtain.

$$\begin{aligned} P &= A \sigma \\ &= t b \sigma \end{aligned} \quad (21a)$$



Dividing Eq. (21a) by  $b^2 \sigma_o$ , to make the equation nondimensional, results in

$$\frac{P}{b^2 \sigma_o} = \left( \frac{t}{b} \right) \left( \frac{\sigma}{\sigma_o} \right) \quad (21b)$$

Since  $\sigma = C_t E_R \left( \frac{t}{b} \right)^2$ , where  $C_t = \frac{\pi^2}{12(1-\nu^2)} \left( \frac{a}{nb} + \frac{nb}{a} \right)^2$  for simple supported ends (see Table 36 of Reference 2 and Figures 14 to 20 of Reference 4 for values of  $1.08 C_t$ ),

$$\text{we obtain } \xi_p = (\sigma/\sigma_o)/(E_R/E_A) = C_t \frac{E_A}{\sigma_o} \left( \frac{t}{b} \right)^2 \quad (11d)$$

$$\text{and } \frac{t}{b} = \sqrt{\frac{\xi_p \sigma_o}{C_t E_A}} \quad (11c)$$

Substituting in Eq. (21b) results in

$$\frac{P}{b^2 \sigma_0} = \left( \frac{\xi_p \sigma_0}{C_t E_A} \right)^{1/2} \left( \frac{\sigma}{\sigma_0} \right)$$

$$\therefore \bar{P} = \frac{P}{b^2 \sigma_0} \left( \frac{C_t E_A}{\sigma_0} \right)^{1/2} = \left( \xi_p \right)^{1/2} \left( \frac{\sigma}{\sigma_0} \right) \text{ (Fig. 8)} \quad (22a)$$

and from Eq. (11c)

$$t = b \left( \frac{\xi_p \sigma_0}{C_t E_A} \right)^{1/2} \quad (22b)$$

A plate in shear can be handled in a similar manner, i.e.,

$$Q = A\tau = t b \tau$$

$$\frac{Q}{b^2 \sigma_0} = \left( \frac{t}{b} \right) \left( \frac{\tau}{\sigma_0} \right)$$

$$\text{but } \tau = C_\tau E_R \left( \frac{t}{b} \right)^2$$

where  $C_\tau \sim \frac{\pi^2}{12(1-\nu^2)} \left( 5.34 + \frac{4b^2}{a^2} \right)$  for simple supported sides (See Eqs. 735 and 736 of Ref 2). Assuming an invariant octahedral stress-strain law results in the transformation

$$\tau = \frac{\sigma/\sqrt{3}}{2(1+\nu)\epsilon} \quad \left[ \begin{array}{l} \text{Eq. 739 of Reference 2 and} \\ \text{Section 3 of Reference 7} \end{array} \right]$$

$$\text{and } \gamma = \frac{2(1+\nu)\epsilon}{\sqrt{3}}$$

This is employed to obtain the shear stress-strain curve from the uniaxial stress-strain curve and results in

$$\xi_p = (\sigma/\sigma_0)/(E_R/E_A) = (\tau\sqrt{3}/\sigma_0)/(E_R/E_A) = \sqrt{3} C_\tau \left( \frac{E_A}{\sigma_0} \right) \left( \frac{t}{b} \right)^2 \quad (23a)$$

$$\therefore t = b \left[ \frac{\xi_p \sigma_0}{\sqrt{3} C_\tau E_A} \right]^{1/2} \quad (23b)$$

$$\text{and } \bar{P} = \frac{Q}{b^2 \sigma_0} \left( \frac{\sqrt{3} C_\tau E_A}{\sigma_0} \right)^{1/2} = \sqrt{\xi_p} \quad \frac{\sigma}{\sigma_0} = \sqrt{\xi_p} \left( \frac{\tau\sqrt{3}}{\sigma_0} \right) \text{ (Fig. 8)} \quad (24)$$

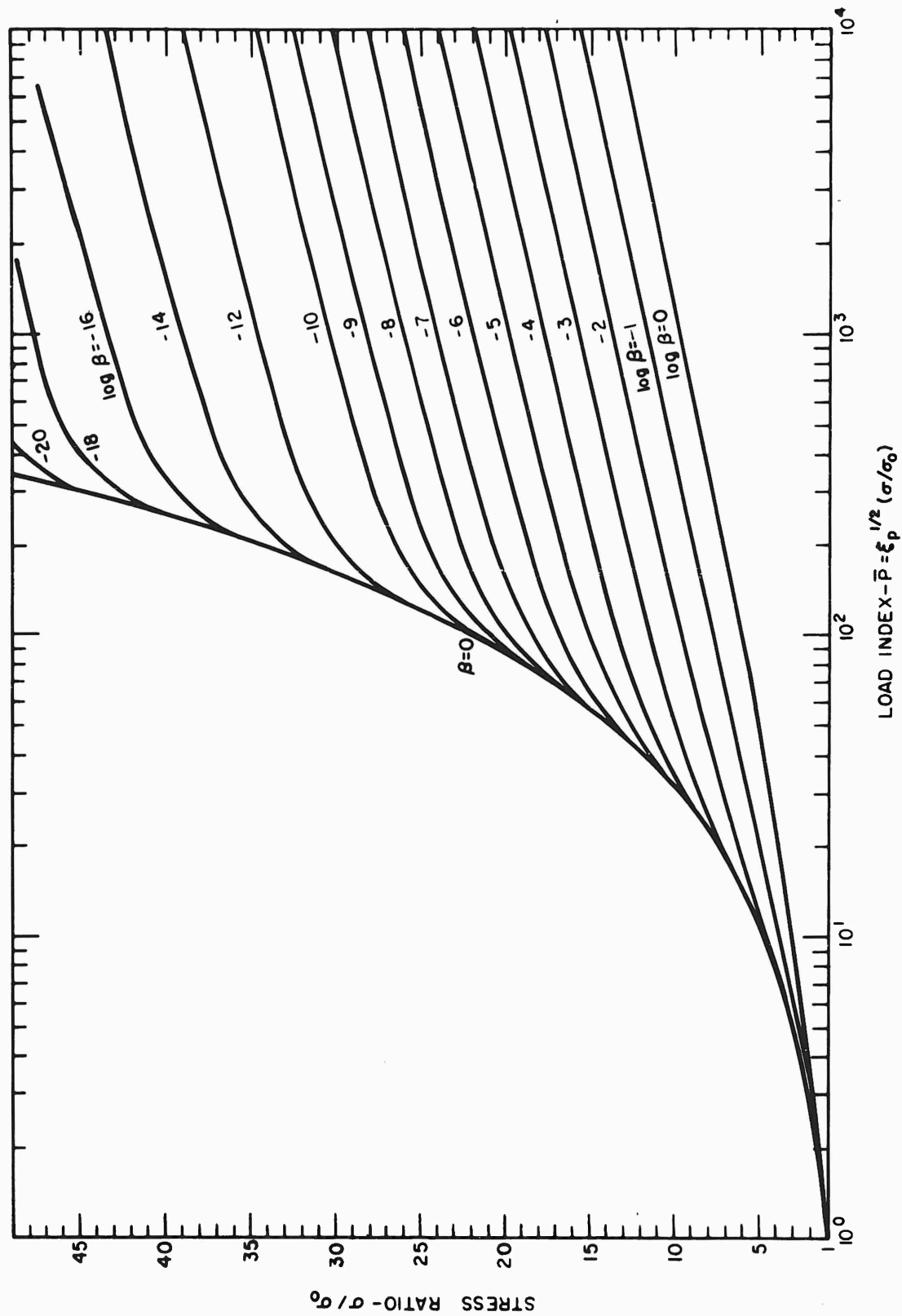


Figure 8. Stress Ratio vs. Load Index for an Unreinforced Plate

Thus the same design graph can be employed. It should be noted that the use of the design graph would result in solutions for  $\frac{\tau\sqrt{3}}{\sigma_0}$  rather than  $\tau/\sigma_0$  and that the average  $E_R$  used for plates in compression was employed.

## 2. CORRUGATED PLATE

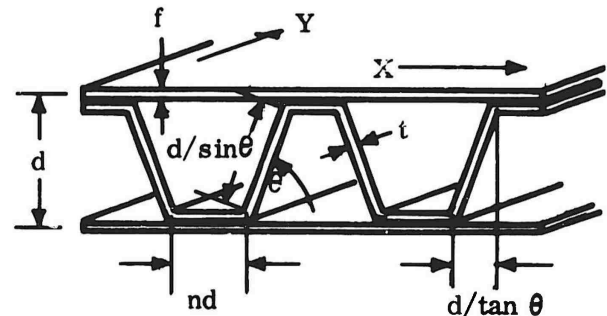
Plate construction consisting of corrugations must be considered as orthotropic plate in that the cross-sectional properties vary in different directions. The bending stiffnesses of the corrugated plate about axes parallel ( $D_{yy}$ ) and perpendicular ( $D_{xx}$ ) to the longitudinal axis

of the corrugations are not difficult to determine. The torsional stiffness is more difficult to evaluate. It is assumed that the torsional stiffness ( $GI_{xy}$ ) is associated with the weaker of the

two bending stiffnesses, [i.e.,  $D_{xy} = 1/2 (\nu_x D_{yy} + \nu_y D_{xx}) + 2 G I_{xy}$  can be approximated by  $D_{yy}$  (see Eq. 203 of Ref. 1)]. This is a good approximation for corrugated plate with two faces (almost isotropic) since the torsional stiffness of a multicellular box is approximately equal to the enveloping box. In the case of one or no faces, the torsional stiffness can be viewed as two springs in series (since the torsional moment must be taken in both directions). Since the stiffness of the weaker spring is a good estimate of the stiffness of the two springs in series, we again conclude that  $D_{xy} \sim D_{yy}$ .

The corrugated sandwich shown in the sketch above has as many as five unknown dimensions. The variables  $\theta$  and  $nd$  are not always at the discretion of the designer but may be particularized because of fabrication requirements. Discrete corrugation angles  $\theta$  and minimum flats ( $nd$ ) for joining may be specified to the designer who must consider these details when he seeks to obtain a minimum weight design. The type of design equations employed for the column still apply, however, and are utilized.

From specified values of  $n$  and  $\theta$  and employing equal stability of the elements, it is possible to express the area and inertia about both axes in terms of two characteristic dimensions, "d" and "t". Employing the load and stability equations described in Paragraphs a. and b. of Subsection II-A-1, it is then possible to develop design graphs. The double-faced corrugation panel must be considered separate from the single-faced and no-faced corrugations because of a difference in form of the over-all stability equations. The values of the geometric constants which express the area and inertia will be presented in terms of  $n$  and  $\theta$ . Methods of obtaining the best values of  $n$  and  $\theta$  will be discussed in the Appendix.





a. Double-Faced Corrugations in Compression

The local stability of the face and corrugation web elements is employed to obtain a relationship between the face and corrugation web thicknesses. It is assumed that the flat is sufficiently small so as to be more stable than the web. Values of  $\sqrt{C_t/C_f}$  of 1 (equal end fixities) and of 1.14 (obtained from Figure 5a of Reference 20 in which moment distribution was employed) are recommended.

$$\text{Since } \sigma_f = C_f E_R \left( \frac{f}{2 (nd + d/\tan\theta)} \right)^2 = C_t E_R \left( \frac{t}{d/\sin\theta} \right)^2 = \sigma_t \quad (25a)$$

$$\text{then } \frac{f}{t} = 2 (n \sin \theta + \cos \theta) \sqrt{C_t/C_f} \quad (25b)$$

The geometry can then be expressed as

$$A_x/\text{in.} = \alpha_1 t \quad (26a)$$

$$I_{xx}/\text{in.} = \alpha_4 t d^2 \quad (26b)$$

$$I_{yy}/\text{in.} = \alpha_5 t d^2 \quad (26c)$$

$$\text{where } \alpha_{12c} = \frac{n \sin \theta + 1}{n \sin \theta + \cos \theta} + 4 (C_t/C_f)^{1/2} (n \sin \theta + \cos \theta) \quad (26d)$$

$$\alpha_{42c} = \frac{(n/4) \sin \theta + 1/12}{n \sin \theta + \cos \theta} + (C_t/C_f)^{1/2} (n \sin \theta + \cos \theta) \quad (26e)$$

$$\text{and } \alpha_{52c} = \sqrt{C_t/C_f} (n \sin \theta + \cos \theta) \quad (26f)$$

where  $\alpha_{x2c}$  = Geometry factor for double faced corrugations in compression.

Employing over-all stability equations such as found in Reference 8 and in Eq. 233 of Reference 1, and equating this stability to the local stability of the corrugated web, we obtain, noting that A, D, and I are per inch of width,

$$\sigma_p = \frac{P/b}{A} = k \left( \frac{\sqrt{D_{xx} D_{yy} + D_{xy}}}{b^2 A} \right) \sim K E_R \left( \frac{\sqrt{I_{xx} I_{yy} + I_{xy}}}{b^2 A} \right) \quad (27a)$$

where  $k = K(1-\nu^2) \sim 2\pi^2$  for simple supported plate of infinite aspect ratio (See Reference 8 for other boundary conditions). Substituting Eqs. (26) into Eq. (27a) and equating this to the local stability results in

$$\sigma_p = \frac{K E_R (\sqrt{\alpha_4 \alpha_5} + \alpha_5)}{\alpha_1} \left( \frac{d}{b} \right)^2 = C_t E_R \left( \frac{t}{d/\sin\theta} \right)^2 = \sigma_t \quad (27b)$$

Solving for  $d/b$ , we obtain

$$\frac{d}{b} = (\sin \theta) \left( \frac{C_t a_1}{K(\sqrt{a_4 a_5} + a_5)} \right)^{1/2} \left( \frac{t}{d} \right) \quad (27c)$$

From the load equation ( $P = \sigma A b$ ), we obtain

$$\frac{P}{b^2 \sigma_o} = \left( \frac{\sigma}{\sigma_o} \right) \left( \frac{A}{b} \right) = \left( \frac{\sigma}{\sigma_o} \right) \left( \frac{a_1 t}{b} \right) = (a_1) \left( \frac{\sigma}{\sigma_o} \right) \left( \frac{t}{d} \right) \left( \frac{d}{b} \right) \quad (28a)$$

Substituting Eq. (27c) in Eq. (28a) we obtain

$$\frac{P}{b^2 \sigma_o} = a_1 \sin \theta \left( \frac{C_t a_1}{K(\sqrt{a_4 a_5} + a_5)} \right)^{1/2} \left( \frac{t}{d} \right)^2 \left( \frac{\sigma}{\sigma_o} \right) \quad (28b)$$

but 
$$\left( \frac{t}{d} \right)^2 = \frac{\xi_p \sigma_o}{C_t E_A \sin^2 \theta} \quad (28c)$$

and manipulating Eq. (28b) results in

$$\bar{P} = \left( \frac{P}{b^2 \sigma_o} \right) \left( \frac{E_A \sin \theta}{\sigma_o} \right) \left( \frac{C_t K (\sqrt{a_4 a_5} + a_5)}{a_1^3} \right)^{1/2} = \xi_p \left( \frac{\sigma}{\sigma_o} \right) \quad (\text{Fig. 9}) \quad (28d)$$

The detail geometry is as follows:

$$d = b \left[ \frac{a_1}{K(\sqrt{a_4 a_5} + a_5)} \frac{\xi_p \sigma_o}{E_A} \right]^{1/2} \quad (29a)$$

$$t = \frac{d}{\sin \theta} \left( \frac{\xi_p \sigma_o}{C_t E_A} \right)^{1/2} \quad (29b)$$

$$f = 2 t (n \sin \theta + \cos \theta) \sqrt{C_t / C_f} \quad (29c)$$

The manipulation of Eq. (28a) could as easily have resulted in an expression of the load in terms of the " $d/b$ " ratio rather than the " $t/d$ " ratio. The technique employed was to obtain results similar to those with less than two faces where the plate stress can not be expressed directly as a function of " $d/b$ " ratio; see Eq. (33b).

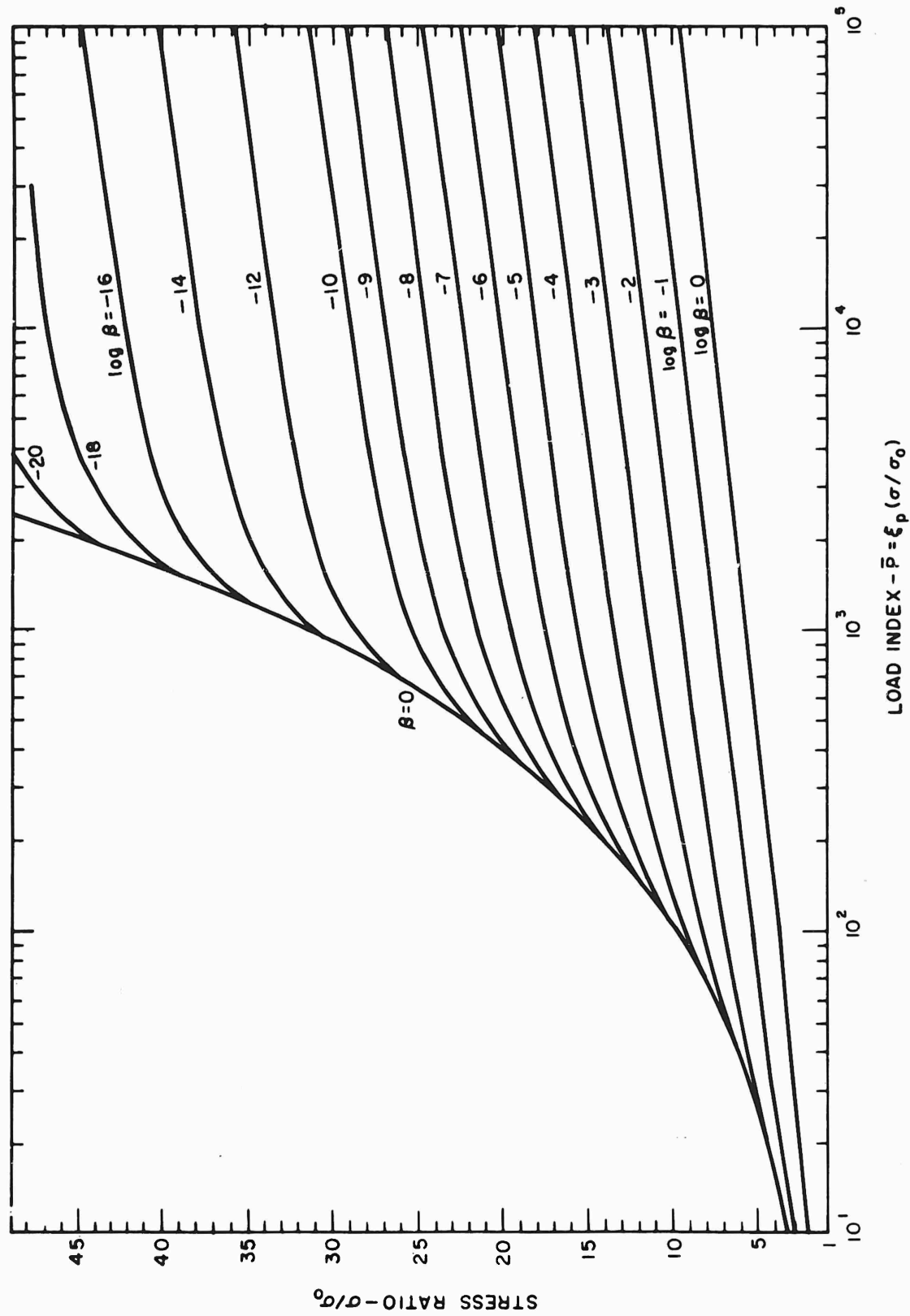


Figure 9. Stress Ratio vs. Load Index for a Corrugated Sandwich Plate

b. No Faces or Single-Face Corrugations In Compression

For these types of construction, the following cross-sectional properties apply:

$$A = \alpha_1 t \quad (30a)$$

$$I_{xx} = \alpha_4 t d^2 \quad (30b)$$

$$I_{yy} = \alpha_5 t^3 \quad (30c)$$

$$I_{xx} \gg I_{yy} \quad (30d)$$

Equation (25b) applies to the "f/t" ratio for single-face corrugations and is not needed for the case of no faces since  $f = 0$  is no longer an unknown dimension.

For one face, we obtain

$$\alpha_{11c} = \frac{n \sin \theta + 1}{n \sin \theta + \cos \theta} + 2 \sqrt{C_t/C_f} (n \sin \theta + \cos \theta) \quad (31a)$$

$$\alpha_{41c} = \frac{(n/4) \sin \theta + 1/12}{n \sin \theta + \cos \theta} + \frac{(1/2) \sqrt{C_t/C_f} (n \sin \theta + 1)}{\alpha_{11}} \quad (31b)$$

and 
$$\alpha_{51c} = \frac{1}{12} \left[ 1 + 2 \sqrt{C_t/C_f} (n \sin \theta + \cos \theta) \right]^3 \quad (31c)$$

For no faces, we obtain

$$\alpha_{10c} = \frac{n \sin \theta + 1}{n \sin \theta + \cos \theta} \quad (32a)$$

$$\alpha_{40c} = \frac{(n/4) \sin \theta + 1/12}{n \sin \theta + \cos \theta} \quad (32b)$$

and 
$$\alpha_{50c} = \frac{1}{12} \quad (32c)$$

where  $\alpha_{x1c}$  = Geometry factor for single faced corrugation in compression.

The larger inertia about the x axis is employed to simplify the overall stability equation

$$\sigma_p = \frac{KE_R \left( \sqrt{I_{xx} I_{yy}} + I_{yy} \right)}{b^2 A} \sim \frac{KE_R \sqrt{I_{xx} I_{yy}}}{b^2 A} \quad (33a)$$

$$\therefore \sigma_p = \frac{K E_R \sqrt{a_4 a_5}}{a_1} \frac{t d}{b^2} \quad (33b)$$

Employing equal stability to evaluate  $d/b$  in terms of  $t/d$  results in

$$\frac{d}{b} = \left( \frac{C_t a_1 \sin^2 \theta}{K \sqrt{a_4 a_5}} \right)^{1/2} \left( \frac{t}{d} \right)^{1/2} \quad (34)$$

From the load equation ( $P = \sigma A b$ ), we obtain

$$\bar{P} = \frac{P}{b^2 \sigma_o} \left( \frac{K \sqrt{a_4 a_5} \sin \theta}{a_1^3} \right)^{1/2} \left( \frac{C_t E_A}{\sigma_o} \right)^{3/4} = \xi_p^{3/4} (\sigma / \sigma_o) \text{ (Fig. 10)} \quad (35)$$

and the following formulae for the detail geometry:

$$d = b \left( \frac{C_t a_1 \sin \theta}{K \sqrt{a_4 a_5}} \right)^{1/2} \left( \frac{\xi_p \sigma_o}{C_t E_A} \right)^{1/4} \quad (36a)$$

$$t = (d / \sin \theta) \left( \frac{\xi_p \sigma_o}{C_t E_A} \right)^{1/2} \quad (36b)$$

$$f = 2 t (n \sin \theta + \cos \theta) \sqrt{C_t / C_f} \quad (36c)$$

### c. Corrugation Panels in Shear

Corrugation panels in shear require a somewhat more complicated approach. The stability of a corrugation panel in shear is not as well defined as in compression. Equation 235 of Reference 1 is employed to define the stability in shear. In addition, the area of the corrugated web is not as efficient as the faces in carrying the shear load. The shear strain (and therefore stress) in the corrugations must be smaller than that in the faces. This is because the deformations from node to node, which join the faces to the core, must be equal to ensure compatibility of the assembly but the load path from node to node is longer via the corrugation web than via the face. For this reason the corrugation web can be made to buckle at a lower stress than the faces. The relationship between the faces and core is obtained by making the faces and webs buckle simultaneously when the stresses are properly distributed.

To obtain the  $f/t$  ratio, use is made of the compatibility equation

$$\gamma_f (nd + d / \tan \theta) = \gamma_t (nd + d / \sin \theta) \quad (37a)$$

$$\text{resulting in } \frac{\tau_f}{\tau_t} = \frac{n \sin \theta + 1}{n \sin \theta + \cos \theta} \quad (37b)$$

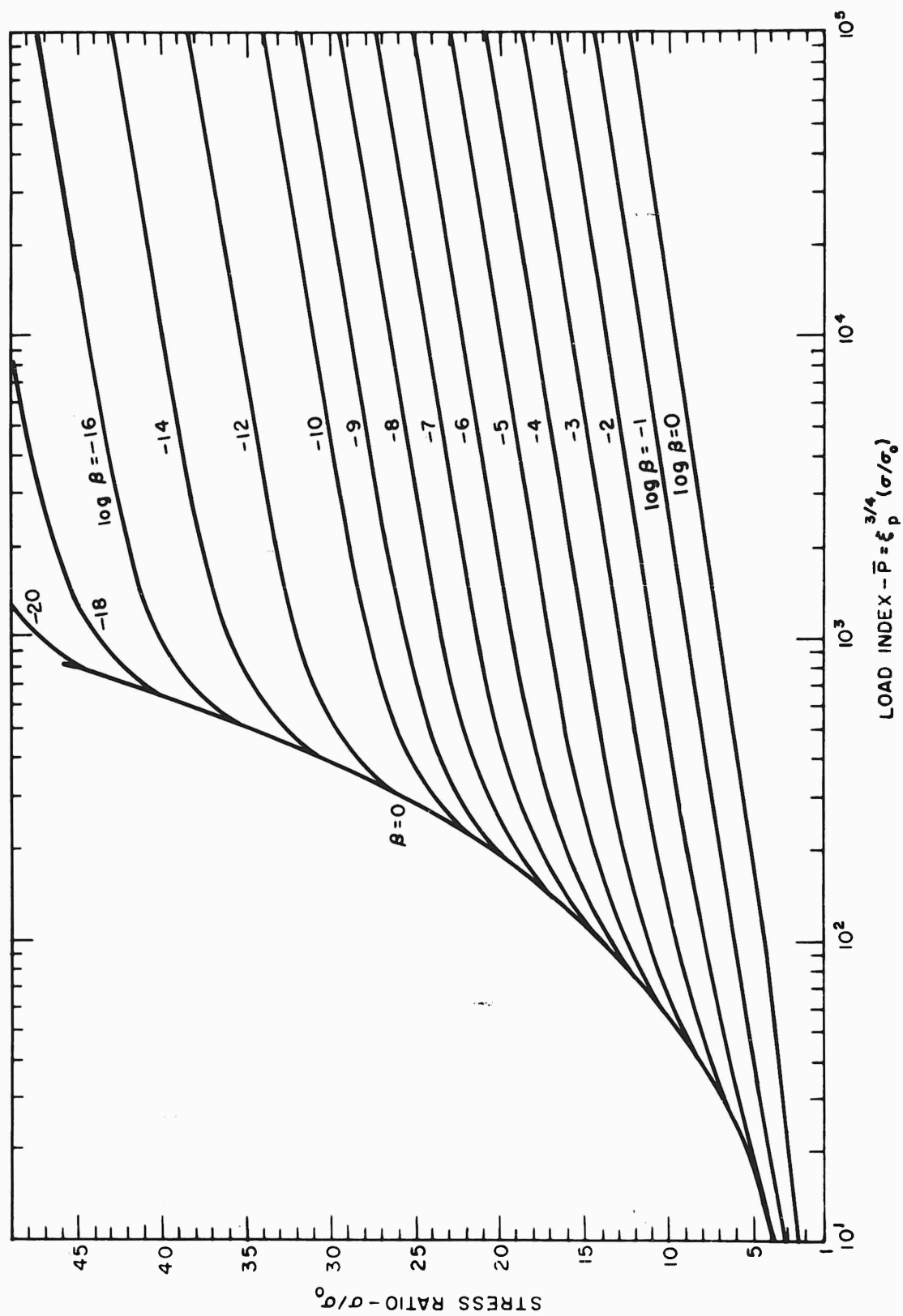


Figure 10. Stress Ratio vs. Load Index for an Orthotropic Plate

The simultaneous instability criteria yields

$$\frac{\tau_f}{\tau_t} = \frac{C_f E_R \left[ \frac{f}{2(nd + d/\tan \theta)} \right]^2}{C_t E_R \left( \frac{t}{d/\sin \theta} \right)^2} = \frac{C_f}{C_t} \left[ \frac{1}{2(n \sin \theta + \cos \theta)} (f/t) \right]^2 \quad (38)$$

This result is approximate because of the assumption that the effective moduli for the face and web are equal. Combining Eqs. (37b) and (38) results in

$$\frac{f}{t} = 2 \sqrt{(C_t/C_f) (n \sin \theta + 1) (n \sin \theta + \cos \theta)} = \alpha_7 \quad (39)$$

where  $C_t$  and  $C_f$  refer to the stability constant for web and face panels in shear. The thickness ratio is then employed to obtain the area and inertia of the plate in terms of  $t$  and  $d$ . The over-all stability equation defined by Eq. 235 of Reference 1 is then employed giving

$$\frac{Q}{b} = \frac{4k(D_{yy} D_{xx}^3)^{1/4}}{b^2} = \frac{4k E_R}{(1 - \nu^2) b^2} (I_{yy} I_{xx}^3)^{1/4} \quad (40a)$$

$$\text{where } k \sim 8 + 5 \left( \frac{D_{yy}}{D_{xx}} \right)^{1/2} = 8 + 5 \left( \frac{I_{yy}}{I_{xx}} \right)^{1/2} \quad \text{for simple supports and infinite}$$

aspect ratio (Fig. 203 of Reference 1).

#### 1). No Faces or Single Face Corrugation in Shear

$$\text{Let } A_x = \alpha_1 t$$

$$I_{xx} = \alpha_4 t d^2$$

$$I_{yy} = \alpha_5 t^3$$

$$\text{and } K = \frac{4k}{1 - \nu_x \nu_y} \sim 32 \quad \text{for simple supports since } I_{xx} \gg I_{yy} \text{ and } 1 - \nu_x \nu_y \sim 1.$$

From Eq. (40a), we have

$$\frac{Q}{b} = \frac{K E_R}{b^2} [I_{yy} I_{xx}^3]^{1/4} = \frac{K (\alpha_5 \alpha_4^3)^{1/4} (E_R t)^{3/2} (d)^{3/2}}{b^2} \quad (41a)$$

$$\text{but } \frac{Q}{b} = \tau_f f + \tau_t t = \tau_t t \left[ \left( \frac{\tau_f}{\tau_t} \right) \left( \frac{f}{t} \right) + 1 \right] = t \tau_t (\alpha_8) \quad (41b)$$

$$\text{where } \alpha_8 = \left[ \left( \frac{\tau_f}{\tau_t} \right) \left( \frac{f}{t} \right) + 1 \right] = \left( \frac{n \sin \theta + 1}{n \sin \theta + \cos \theta} \alpha_7 + 1 \right) \quad (41c)$$

is obtained from Eqs. (37b) and (39).

Combining Eqs. (41a) and (41b) results in

$$\tau_t = \frac{Q}{\alpha_8 t b} = K E_R \frac{t^{1/2} d^{3/2}}{b^2} \frac{(\alpha_5 \alpha_4^3)^{1/4}}{\alpha_8} \quad (42)$$

Equating this to the stability of the web  $\left[ \tau_t = C_t E_R \left( \frac{t}{d/\sin \theta} \right)^2 \right]$  results in

$$\frac{t}{b} = \left[ \frac{\alpha_8 C_t \sin^2 \theta}{K (\alpha_5 \alpha_4^3)^{1/4}} \right]^{1/2} \left( \frac{t}{d} \right)^{7/4} = \alpha_9 \left( \frac{t}{d} \right)^{7/4} \quad (43)$$

Using the load equation, we obtain,

$$\frac{Q}{b^2 \sigma_o} = \alpha_8 \frac{\tau_o}{\sigma_o} \frac{t}{b} = \frac{\alpha_8}{\sqrt{3}} \left( \frac{\tau \sqrt{3}}{\sigma_o} \right) \alpha_9 \left( \frac{t}{d} \right)^{7/4}$$

$$\frac{Q}{b^2 \sigma_o} = \frac{\alpha_8}{\sqrt{3}} \left( \frac{\tau \sqrt{3}}{\sigma_o} \right) \alpha_9 \left( \frac{\xi_s \sigma_o}{\sin^2 \theta E_A C_t \sqrt{3}} \right)^{7/8} \quad (44a)$$

$$\therefore \bar{P} = \frac{Q}{b^2 \sigma_o} \frac{\sqrt{3}}{\alpha_8 \alpha_9} \left( \frac{\sin^2 \theta E_A C_t \sqrt{3}}{\sigma_o} \right)^{7/8} = \frac{\tau \sqrt{3}}{\sigma_o} (\xi_s)^{7/8} \quad (44b)$$

(Fig. 11)

$$\text{where } \xi_s = (\sigma/\sigma_o) / (E_S/E_A) = \frac{E_A \epsilon}{\sigma_o} \quad (\text{Fig. 12}) \quad (45)$$

The effective modulus was approximated with the secant modulus in accordance with Reference 9. The average value  $E_R = E_S (.428 + .572 \sqrt{.25 + .75 E_T/E_S})$  was employed for unreinforced plates to avoid the need of another design curve. This is justified by the fact that the correct form of  $E_R$  is in doubt and the differences in the design curves are slight.



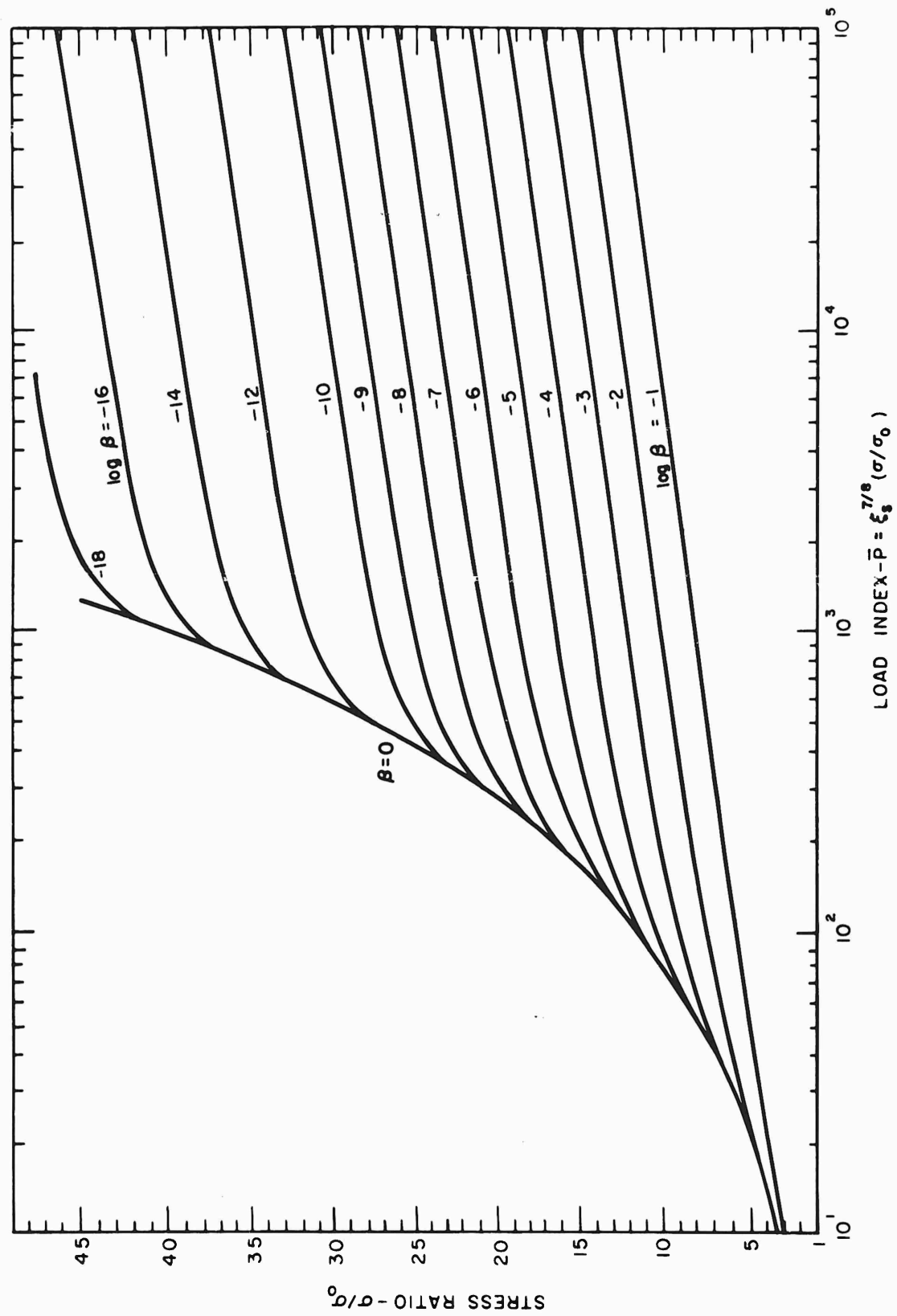


Figure 11. Stress Ratio vs. Load Index for a Corrugated Plate in Shear

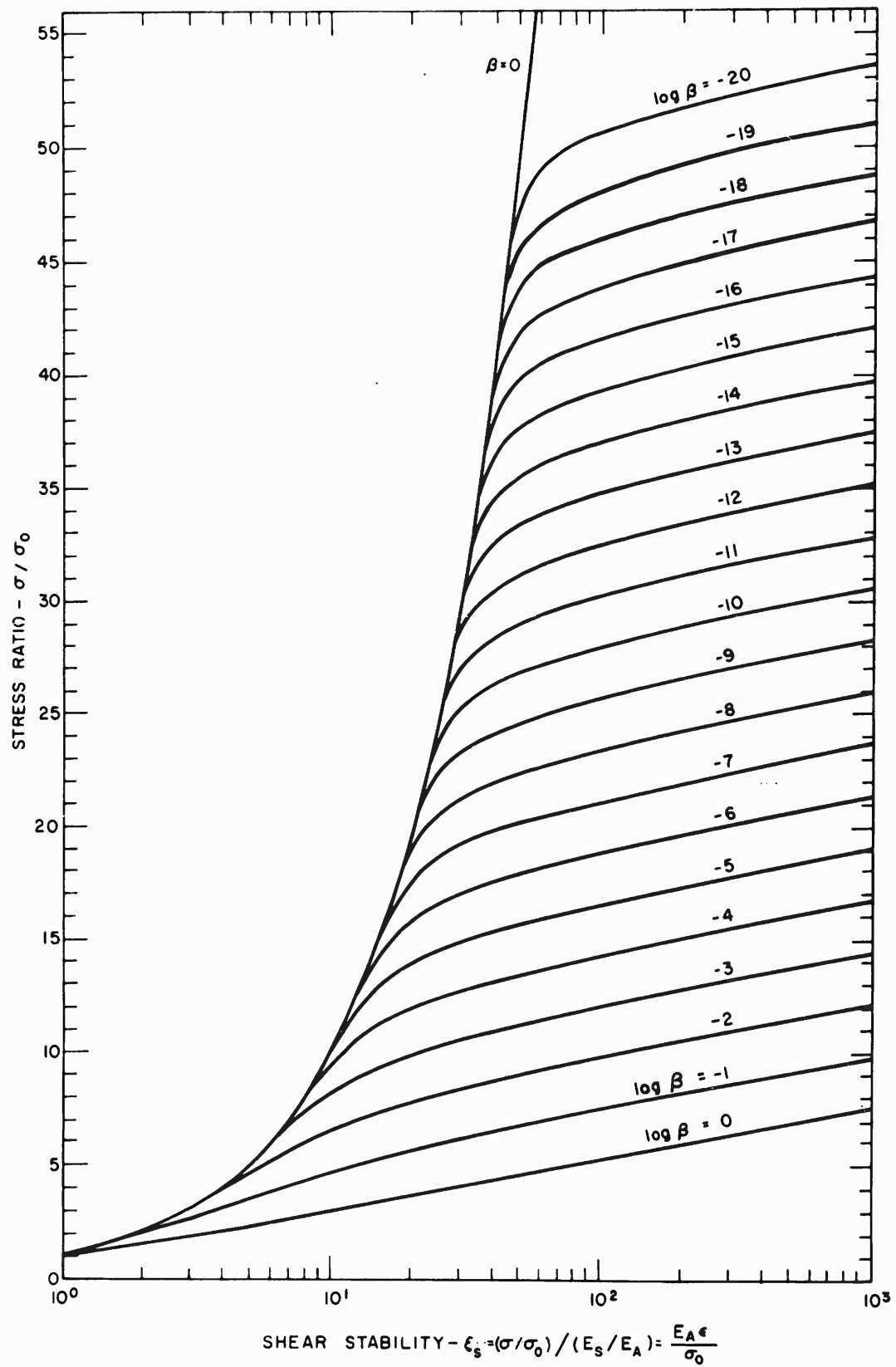


Figure 12. Nondimensional Stress-Strain Curves

Values of the constants are as follows:

$$\alpha_{10s} = \frac{n \sin \theta + 1}{n \sin \theta + \cos \theta} \quad (46a)$$

$$\alpha_{40s} = \frac{(n/4) \sin \theta + 1/12}{n \sin \theta + \cos \theta} \quad (46b)$$

$$\alpha_{50s} = 1/12 \quad (46c)$$

$$\alpha_{80} = 1 \quad (46d)$$

$$\alpha_{90} = \left[ \frac{\alpha_{80} C_t \sin^2 \theta}{K(\alpha_5 \alpha_4^3)^{1/4}} \right]^{1/2} \quad (46e)$$

where  $\alpha_{x0s}$  = geometry factor for corrugation with no faces in shear.

$$\alpha_7 = 2 \sqrt{\frac{C_t}{C_f}} (n \sin \theta + 1) (n \sin \theta + \cos \theta) \quad (39)$$

$$\alpha_{11s} = \frac{n \sin \theta + 1}{n \sin \theta + \cos \theta} + \alpha_7 \quad (47a)$$

$$\alpha_{41s} = \frac{(n/4) \sin \theta + 1/12}{n \sin \theta + \cos \theta} + \frac{\alpha_7 \alpha_{10}}{4 \alpha_{11}} \quad (47b)$$

$$\alpha_{51s} = \frac{1}{12} (1 + \alpha_7)^3 \quad (47c)$$

$$\alpha_{81} = \left( \frac{n \sin \theta + 1}{n \sin \theta + \cos \theta} \right) \alpha_7 + 1 \quad (41c)$$

$$\alpha_{91} = \left[ \frac{\alpha_{81} C_t \sin^2 \theta}{K(\alpha_5 \alpha_4^3)^{1/4}} \right]^{1/2} \quad (47d)$$

The detail geometry is obtained from:

$$t = b \alpha_9 \left( \frac{\xi_s \sigma_o}{\sin^2 \theta E_A C_t \sqrt{3}} \right)^{7/8} \quad (48a)$$

$$d = t \left( \frac{E_A C_t \sqrt{3} \sin^2 \theta}{\sigma_o \xi_s} \right)^{1/2} \quad (48b)$$

$$f = t a_7 \quad (f = 0 \text{ for no faces}) \quad (48c)$$

$$W/\rho = t a_1 \quad (48d)$$

## 2). Double-Face Corrugations in Shear

The results for double-face corrugations in shear are obtained in a similar manner to that for corrugation with one face in shear with the exceptions that the  $I_{yy}$  inertia is defined in terms of  $td^2$  rather than  $t^3$  and the stability constant is modified by the ratio of the inertias.

$$\text{Let} \quad A_x = a_{12} t$$

$$I_{xx} = a_{42} t d^2$$

$$I_{yy} = a_{52} t d^2$$

$$K \sim 4 \left( 8 + 5 \sqrt{\frac{I_{yy}}{I_{xx}}} \right) / (1 - \nu^2) \quad \text{for simple supports}$$

Expressions similar to Eqs. (42), (43), (44b), (47) and (48) can then be obtained with the above definitions of the geometry.

$$\tau_t = \frac{4}{1 - \nu^2} \frac{\left( 8 + 5 \sqrt{\frac{a_{52}}{a_{42}}} \right) (a_{52} a_{42}^3)^{1/4}}{a_{82}} E_R \left( \frac{d}{b} \right)^2 = C_t E_R \left( \frac{t \sin \theta}{d} \right)^2 \quad (49)$$

$$\frac{d}{b} = \left[ \frac{C_t \sin^2 \theta a_{82}}{\frac{4}{1 - \nu^2} \left( 8 + 5 \sqrt{a_{52}/a_{42}} \right) (a_{52} a_{42}^3)^{1/4}} \right]^{1/2} \quad \left( \frac{t}{d} \right) = a_{92} \left( \frac{t}{d} \right) \quad (50)$$

$$\bar{P} = \frac{Q}{b^2 \sigma_o} \frac{3 \sin^2 \theta}{a_{82} a_{92}} \frac{C_t E_A}{\sigma_o} = \left( \frac{\tau \sqrt{3}}{\sigma_o} \right) \xi_p \quad (\text{Fig. 9}) \quad (51a)$$

$$t = \frac{a_{92} b}{\sin^2 \theta} \left( \frac{\xi_p \sigma_o}{\sqrt{3} C_t E_A} \right) \quad (51b)$$

$$d = \frac{a_{92} b}{\sin \theta} \left( \frac{\xi_p \sigma_o}{\sqrt{3} C_t E_A} \right)^{1/2} \quad (51c)$$

$$f = \alpha_7 t \quad (51d)$$

$$W/\rho = \alpha_{12} t \quad (51e)$$

where

$$\alpha_{12s} = \frac{n \sin \theta + 1}{n \sin \theta + \cos \theta} + 2 \alpha_7 \quad (51f)$$

$$\alpha_{42s} = \frac{(n \sin \theta / 4) + 1/12}{n \sin \theta + \cos \theta} + \frac{\alpha_7}{2} \quad (51g)$$

$$\alpha_{52s} = \alpha_7^{1/2} \quad (51h)$$

$$\alpha_7 = 2 \left[ (C_t/C_f) (n \sin \theta + 1) (n \sin \theta + \cos \theta) \right]^{1/2} \quad (39)$$

$$\alpha_{82} = (2 \alpha_7) \frac{n \sin \theta + 1}{n \sin \theta + \cos \theta} + 1 \quad (51i)$$

$$\alpha_{92} = \left[ \frac{\alpha_{82} C_t \sin^2 \theta}{\left( \frac{4}{1-\nu^2} \right) \left( 8 + 5 \sqrt{\frac{\alpha_{52s}}{\alpha_{42s}}} \right) (\alpha_{52s} \alpha_{42s}^3)^{1/4}} \right]^{1/2} \quad (51j)$$

The stability index  $\xi_p$  is employed rather than  $\xi_s$  in order to utilize Figure 9 which was obtained for a double-faced corrugation in compression. The present state of the art does not warrant refining the design procedure any further. The technique is versatile enough, however, to develop new design curves whenever experimental and analytical investigations present more reliable stability equations.

The Appendix presents a technique for determining the corrugation angle  $\theta$  for given values of  $n$  which would result in minimum weight of the plate. The results of this analysis are presented in Figures A-1a to A-2b together with the resulting values of the geometry coefficients  $\alpha$ . These can be employed wherever the fabrication requirements do not dictate the values of  $\theta$  and  $n$ . A possible design technique is to assume a value of  $n$  in order to determine the appropriate geometric constants and to design a minimum weight structure. The detail design is then reviewed to obtain a better estimate of  $n$  consistent with the requirements of a minimum flat for joining and a minimum bending radius for the corrugation thickness. This process can be repeated until the assumed value of  $n$  is in satisfactory agreement with the value of  $n$  required for fabrication.

### 3. REINFORCED PLATE

A plate is reinforced for the purpose of working to a higher stability stress level by modifying the buckling pattern of the plate. Reinforcing a plate by transverse stiffeners will not be too effective unless the stiffeners are spaced closer than the width of the plate so as to force buckle waves shorter than those for the unreinforced plate. A more efficient construction is usually obtained by introducing longitudinal stiffeners. These stiffeners not only carry a portion of the compression

load but they attempt to subdivide the plate into smaller panels with smaller buckle waves. The longitudinal stiffeners can be viewed as intermediate "elastic" supports for the plate. If the bending stiffness of the stiffener is sufficiently large relative to the plate, then it can act as a node provided it is also stable as a column. Orthotropic plate theory, similar to that employed for corrugated plate, will be utilized in the design of reinforced plate.

A typical integrally stiffened plate is shown in the accompanying sketch. The similarity of repeated portions of the reinforced plate with column sections is apparent. It can be shown that in order to obtain maximum stability, the geometric distribution of area in the cross section will be similar to a column for maximum inertia about one axis.

The requirement of equal stability of the elements of the cross section permits expressing the area and inertia in terms of two characteristic dimensions. From Eq. (20) we have

$$w = d (z)^{1/2} (C_h/C_t)^{1/4} \quad (20a)$$

$$\text{and} \quad h = t (z)^{1/2} (C_t/C_h)^{1/4} \quad (20b)$$

The area and inertia are then evaluated utilizing the relationships for columns

$$(A_c = \alpha_1 dt \text{ and } I_c = \alpha_3 d^3 t).$$

$$\text{Area/in.} = A_p/b = [n (A_c) + wh] / b = (n\alpha_1 + z) dt/b = \alpha_7 dt/b \quad (52a)$$

$$(1 - \nu^2) \frac{D_{xx}}{E_R} = I_{xx} \sim n I_c/b = n \alpha_3 d^3 t/b = \alpha_4 d^3 t/b \quad (52b)$$

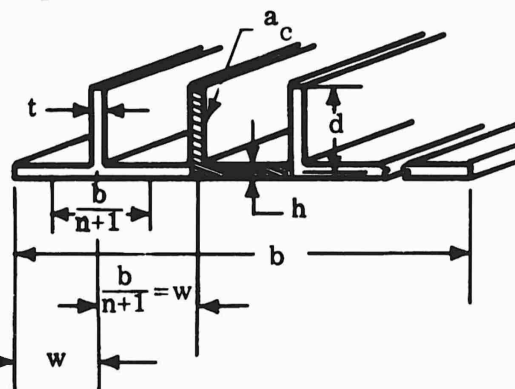
$$(1 - \nu^2) \frac{D_{yy}}{E_R} = I_{yy} = h^3/12 = (z \sqrt{C_t/C_h})^{3/2} (t^3/12) = \alpha_5 t^3 \quad (52c)$$

$$\text{where } \alpha_7 = n \alpha_1 + z \quad (52d)$$

$$\alpha_4 = n \alpha_3 \quad (52e)$$

$$\alpha_5 = (z \sqrt{C_t/C_h})^{3/2}/12 \quad (52f)$$

and  $n = \text{number of stiffeners.}$



Employing Eq. (33a) for an orthotropic plate with  $I_{xx} \gg I_{yy}$ , we obtain the stability stress of the plate:

$$\sigma_p = \frac{K E_R \sqrt{I_{xx} I_{yy}}}{b^2 A} = \frac{K E_R \sqrt{a_4 a_5}}{a_7} \left( \frac{t}{b} \right) \left( \frac{d}{b} \right)^{1/2} \quad (53)$$

Equating the local stability of the element to this stress results in

$$\left( \frac{d}{b} \right) = \left( \frac{a_7 C_t}{K \sqrt{a_4 a_5}} \frac{t}{d} \right)^{2/3} \quad (54)$$

The load equation results in

$$\bar{P} = \frac{P}{b^2 \sigma_o a_7} \left( \frac{K \sqrt{a_4 a_5}}{C_t a_7} \right)^{4/3} \left( \frac{C_t E_A}{\sigma_o} \right)^{7/6} = \left( \xi_p^{7/6} \right) \left( \frac{\sigma}{\sigma_o} \right) \text{ (Fig. 13a)} \quad (55)$$

with the detail geometry determined as follows:

$$d = b \left( \frac{C_t a_7}{K \sqrt{a_4 a_5}} \right)^{2/3} \left( \frac{\xi_p \sigma_o}{C_t E_A} \right)^{1/3} \quad (56a)$$

$$t = d \left( \frac{\xi_p \sigma_o}{C_t E_A} \right)^{1/2} \quad (56b)$$

$$h = t \sqrt{z \sqrt{C_t / C_h}} \quad (56c)$$

$$\frac{W}{\rho} = a_7 dt \quad (56d)$$

The load index is not unique since the  $(d/b)$  ratio can be solved for in terms of the  $(t/b)$  ratio as well as the  $(t/d)$  ratio. This would result in

$$\bar{P}' = \frac{P}{b^2 \sigma_o} \left( \frac{E_A}{\sigma_o} \right)^{3/2} \frac{K^2 a_4 a_5^{2/3}}{a_7^{3(n+1)} (12)^{1/3} C_h^{1/2}} = \left( \xi_p^{3/2} \right) \left( \frac{\sigma}{\sigma_o} \right) \text{ (Fig. 13b)} \quad (56e)$$

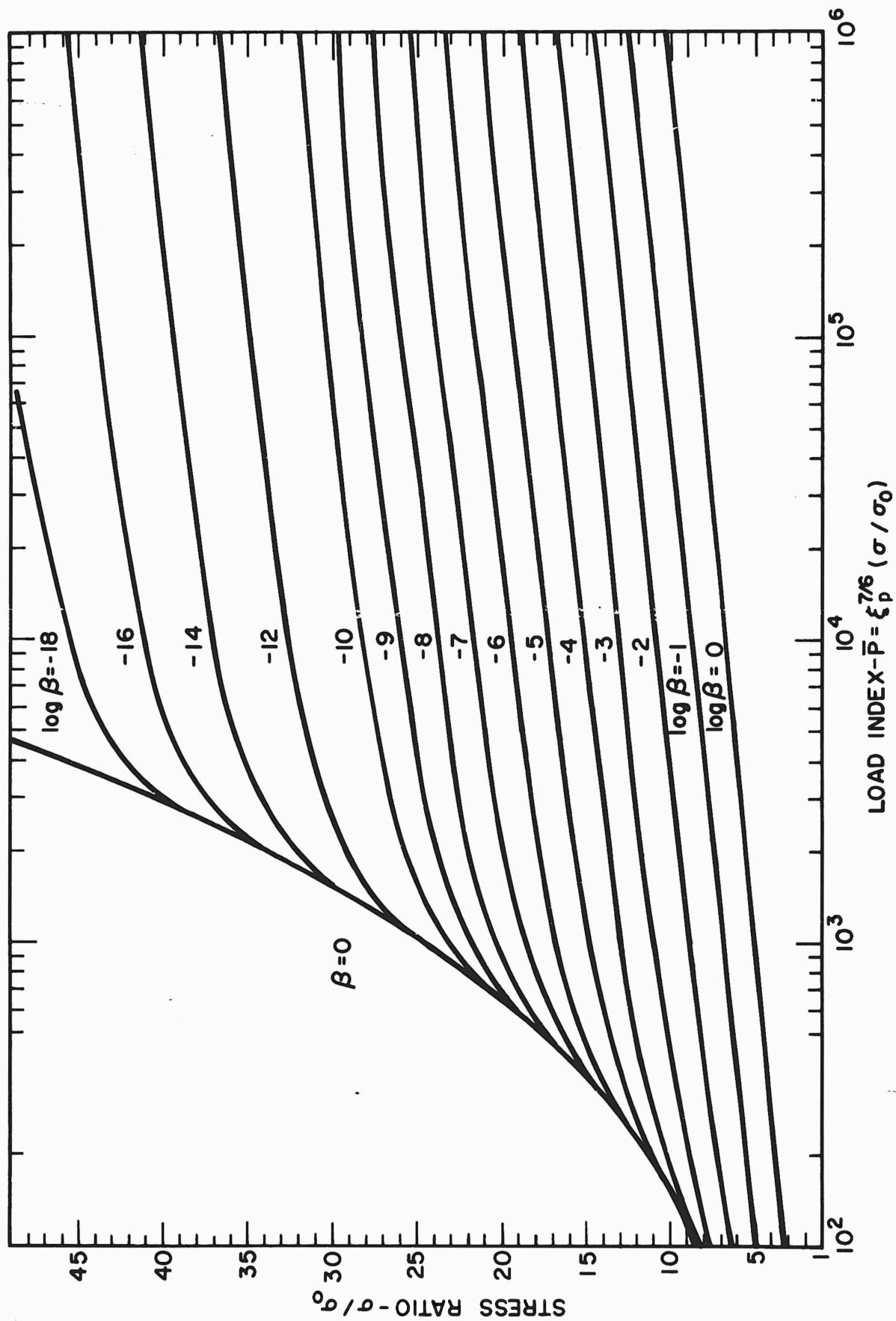


Figure 13a. Stress Ratio vs. Load Index for an Integrally Stiffened Plate



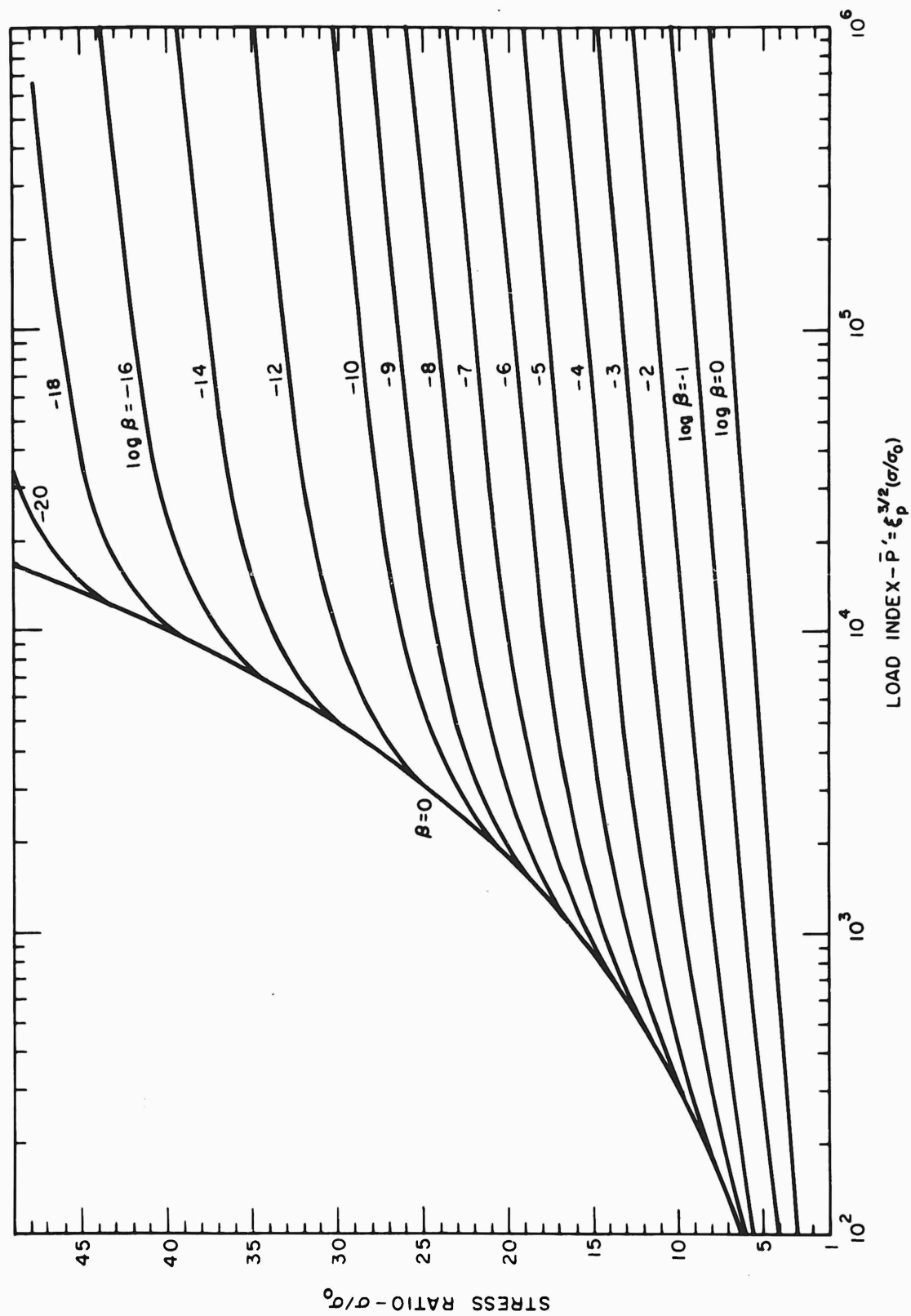


Figure 13b. Stress Ratio vs. Load Index for an Integrally Stiffened Plate

The design of the structure requires a knowledge of the distribution of area ( $z = wh/dt$ ) between the plate and the stiffening elements. The distribution should be arranged so that the product  $D_{xx} D_{yy}$  is a maximum when the area and stability thickness ratio are stationary. This would result in a maximum stability stress. Considering a typical reinforced portion of the plate, we can resolve the product of the bending stiffness to

$$D_{xx} D_{yy} \sim \left[ \frac{E_R^2}{12(1-\nu^2)^2} (C_t/C_h)^{3/2} \left( \frac{b}{n+1} \right)^2 \right] \alpha_3 d^3 t \quad (57a)$$

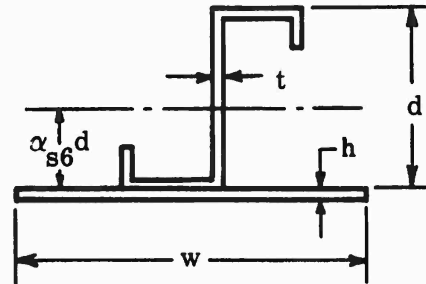
For a given number of stiffeners the value of the terms multiplying  $\alpha_3 d^3 t$  is stationary and we arrive at the conclusion that the area distribution which maximizes the inertia of the column section ( $\alpha_3 d^3 t$ ) will also maximize the over-all stability stress of the reinforced plate. These values of  $z = wh/dt$  correspond to values presented in Table 1, when the moment of inertia ( $I_{xx}$ ) of the column section is maximized, for angles (see shaded area of sketch above) or for channels (if stiffener has area above the web). This is because the area of the skin assumed acting with the stiffener is "wh" and not "2 wh". Any stiffener area (wh) above the web should be distributed so that the area is stable to a stress equal to or greater than the stability stress of the web. Note that the  $C_h$  for the base is for a supported plate while the  $C_h$  and  $C_t$  of the upper flange and web may be for a flange or a supported plate.

If the plate is stiffened by stringers then the optimum distribution of area will depend upon the cross-sectional properties of the stiffener. Assuming a stringer whose cross-sectional properties are defined as

$$\text{Area} = A_s = \alpha_{s1} dt \quad (57b)$$

$$\text{Inertia} = I_s = \alpha_{s3} d^3 t \quad (57c)$$

$$\text{Centroidal distance} = c = \alpha_{s6} d \quad (57d)$$



and where all the elements of the stringer are at least as stable as the web (dt). Then employing the technique of maximizing the inertia of the sheet-stringer combination for a stationary area, results in

$$z_s = \frac{wh}{dt} = \frac{a_{s1} (a_{s1}^2 a_{s6}^2 - 2a_{s3})}{2 (a_{s1}^2 a_{s6}^2 + a_{s3})} \quad (57e)$$

which can be employed to calculate values of

$$a_7 = n (a_{s1} + z_s) + z_s \quad (57f)$$

$$a_4 = n \left( a_{s3} + \frac{a_{s1}^2 a_{s6}^2}{a_{s1} + z_s} \right) \quad (57g)$$

and

$$a_5 = \left[ z_s (C_t/C_h)^{1/2} \right]^{3/2} \quad (57h)$$

to be substituted in Eqs. (55) and (56e).

The above design procedure assumes that reinforced plate buckles as an orthotropic plate. The dimensions of the plate, however, may be such as to enforce another type of deflection pattern. If the plate is very short so that it will not buckle except as individual smaller plates, then

$$\frac{P}{b^2 \sigma_0} = \frac{A_p \sigma}{b^2 \sigma_0} = \frac{a_7 dt \sigma}{b^2 \sigma_0} = a_7 \left( \frac{t}{d} \right) \left( \frac{d}{b} \right)^2 \left( \frac{\sigma}{\sigma_0} \right) \quad (58a)$$

$$\text{but } \frac{b}{n+1} = w = d \sqrt{z \sqrt{C_h/C_t}} \quad (20a)$$

which results in

$$\frac{d}{b} = \frac{1}{(n+1) \sqrt{z \sqrt{C_h/C_t}}} \quad (58b)$$

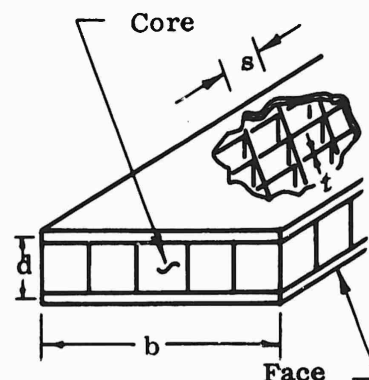
$$\therefore \bar{P} = \frac{P}{b^2 \sigma_0} \left( \frac{(n+1)^2 z \sqrt{C_h/C_t}}{a_7} \right) \left( \frac{C_t E A}{\sigma_0} \right)^{1/2} = \left( \xi_p^{1/2} \right) \left( \frac{\sigma}{\sigma_0} \right) \text{ (Fig. 8) } (58c)$$

If the plate is sufficiently wide so that the side supports do not significantly restrain the center of the panel, then the design procedures developed for columns would be applicable for a plate with a few stiffeners.

It is recommended that the stability stress level be evaluated for all the modes of failure described, whenever the designer has any doubts, and to base the design upon the lowest stability stress obtained.

#### 4. SANDWICH PLATES

A typical honeycomb sandwich plate is shown in the accompanying sketch. Each component of the sandwich must be capable of doing its assigned task. Failure of any component can precipitate instability of the assembly at a stress lower than the design stress. The facing material provides the load carrying medium of the structure and must be stiff and continuous. The core material must have enough stiffness to stabilize the individual faces against buckling; restrain the faces from deforming independently of each other (the large bending stiffness to weight ratio is dependent upon the faces and core acting together); and to carry lateral loads and shears (lateral deflections of the plate cause a lateral component of the axial load). The core is connected to the faces by means of a bonding agent which must be capable of transmitting the loads between the faces and the core. For minimum weight design the core and bond should be as light as possible (consistent with their ability to do their assigned tasks), and the faces should have the highest stress to density ratio in the expected environment.



The design curves presented in this study are based upon an analysis presented in Reference 21 for square cell core and they should be sufficiently accurate for hexcel core. The problem of face wrinkling, for which no acceptable design procedures exist, was empirically resolved by making the thickness of the core cell greater than 10 percent of the face thickness ( $t > .1 f$ ). This criteria can be readily modified without affecting the design curves. The definition of effective stability modulus ( $E_R$ ) was avoided since disagreement exists as to the proper modulus. The design procedure permits the designer to select any definition he believes to be appropriate.

The analysis of the stability of the honeycomb sandwich is similar to the analysis of unreinforced plate with the exception that the effect of shearing energy upon the stability cannot be ignored. The general equation employed (as, for example, in References 7, 8, and 21) is as follows:

$$\sigma_{cr} = \frac{\sigma_{crm}}{1 + \frac{P_{crm}}{P_{crs}}} = \frac{K E_R (I/Ab^2)}{1 + \frac{K (I/Ab^2) A E_R}{A_s G_R}} \quad (59)$$

where subscript crm refers to stability due to bending and no shear  
 and subscript crs refers to stability due to shear and no bending  
 $A_s$  = shear area of sandwich  $\sim (\rho_c/\rho_f)/2 \sim t/s$ . (The other symbols are defined elsewhere.) Manipulation of this equation under the assumptions that the faces are small with respect to the depth of the sandwich ( $f \ll d$ ) and that the effective shear modulus is proportional to the effective stability modulus

$$\left[ E_R/G_R = 2(1+\nu) \right]$$

results in the following

$$K \frac{d}{b} = (1+\nu) \left( \frac{P}{b^2 \sigma} \right) \left( \frac{s}{t} \right) (K \bar{\epsilon}) + \sqrt{\left[ (1+\nu) \left( \frac{P}{b^2 \sigma} \right) \left( \frac{s}{t} \right) (K \bar{\epsilon}) \right]^2 + 4 K \bar{\epsilon}} \quad (60a)$$

(Eq. 13.2 of Reference 21)

$$\text{where } \bar{\epsilon} = \sigma/E_R \quad (60b)$$

$$\text{and } K = \frac{\pi^2 k}{1-\nu^2} \quad (60c)$$

where  $k$  is the standard stability constant for plates presented in various texts, References 1 to 8, (e.g.,  $K = \frac{\pi^2 4}{1-\nu^2} = 43.5$  for a simply supported plate of infinite aspect ratio).

Plots of this equation are presented in Figures 14a to 14d for given values of  $t/s$ . Entering with the known abscissa  $(P/b^2 \sigma)$  and proceeding to the proper curve  $\bar{\epsilon} = \sigma/E_R$ , results in the ordinate  $(K d/b)$  which can be employed to solve for the minimum depth which will stabilize the faces to the selected stress. The proper value of  $t/s$  is obtained by selecting an available  $s$  and  $t$  where  $t \geq .1 f$  (this ratio can be modified) and  $s \leq 2f/(3 \epsilon)^{2/3}$ . These requirements can be satisfied with the aid of Figure 15 which also indicates the available cores.

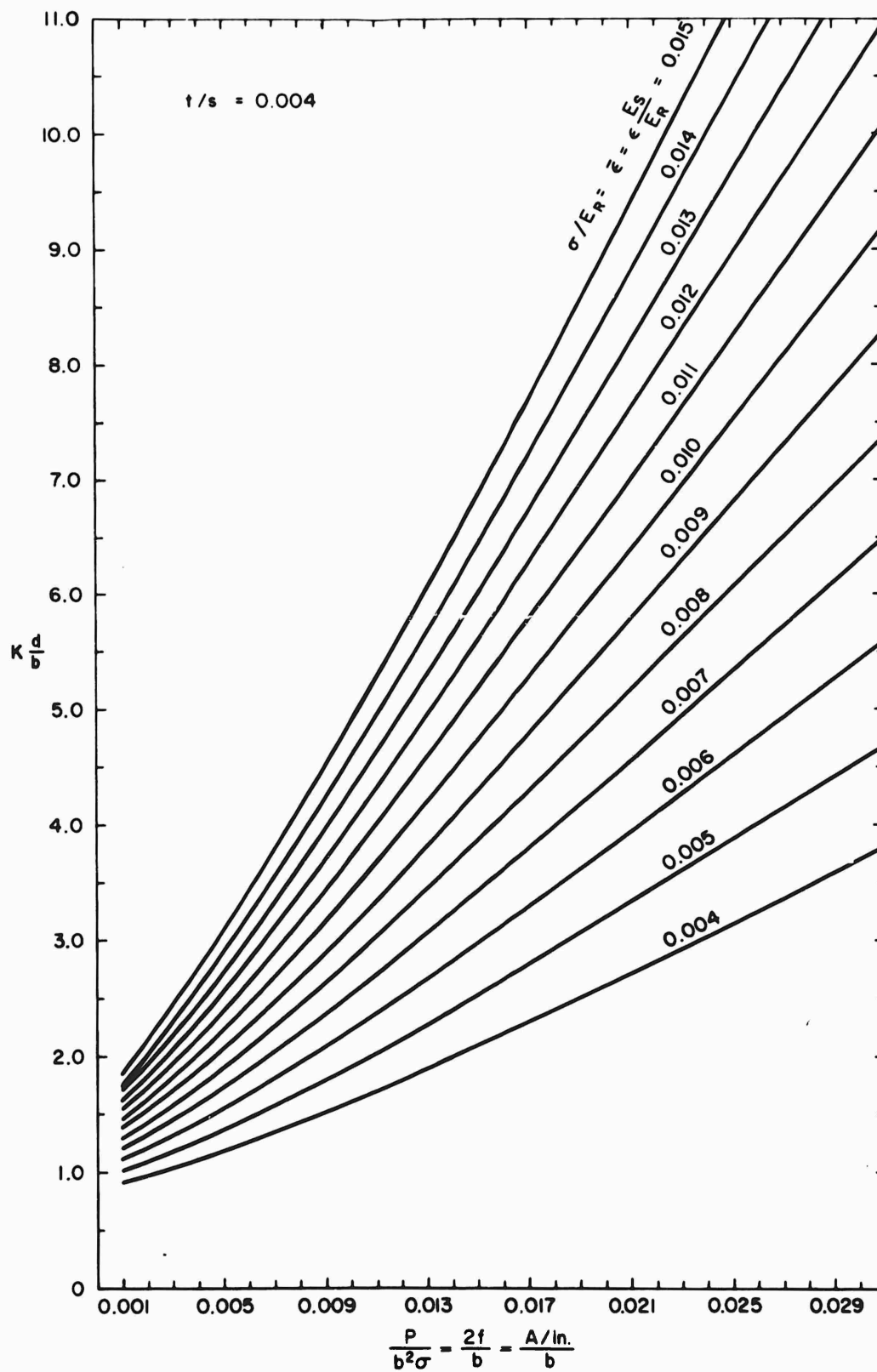


Figure 14a. Design Curves for Honeycomb Sandwich (  $t/s = 0.004$  )

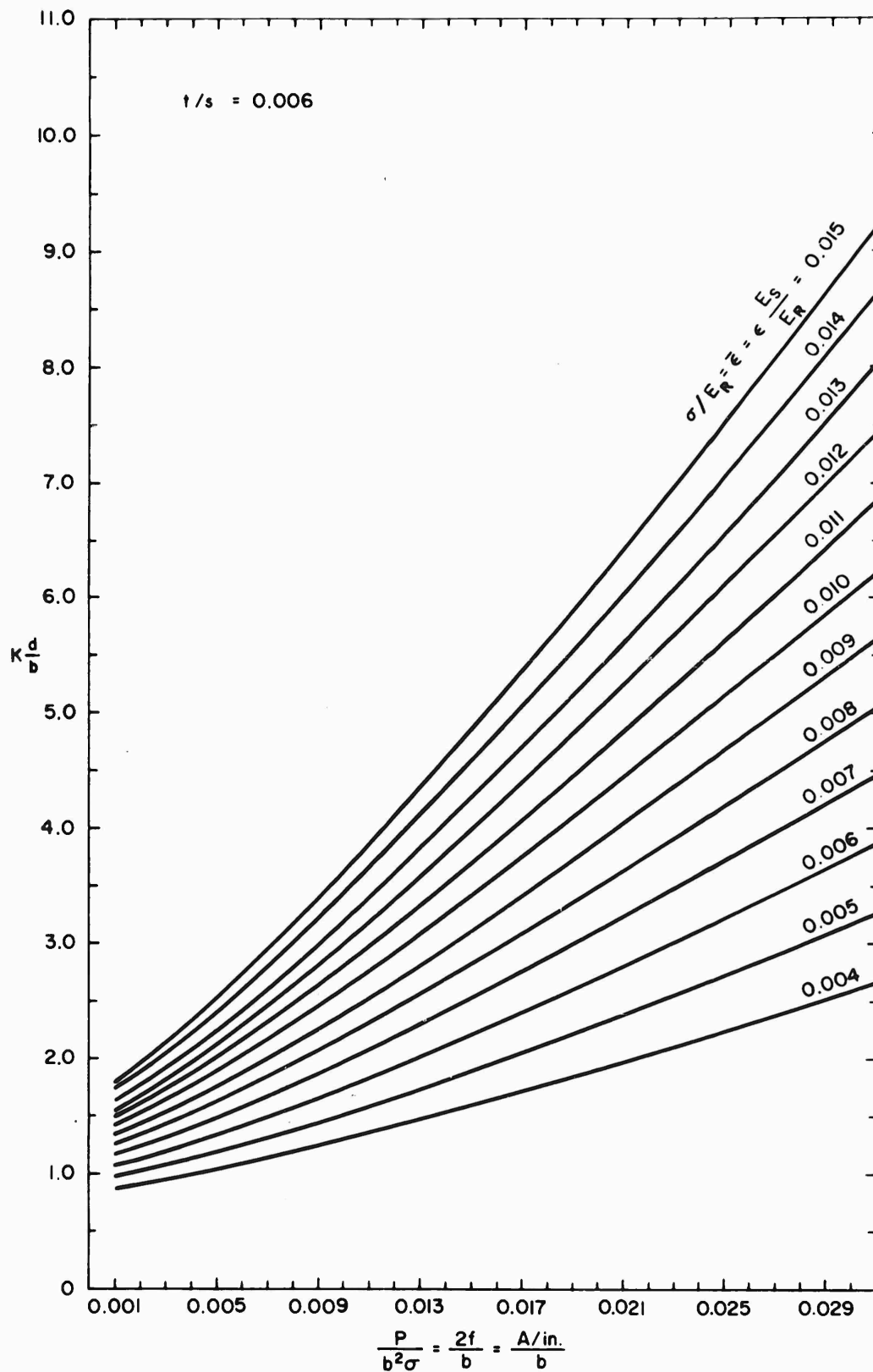


Figure 14b. Design Curves for Honeycomb Sandwich ( $t/s = 0.006$ )

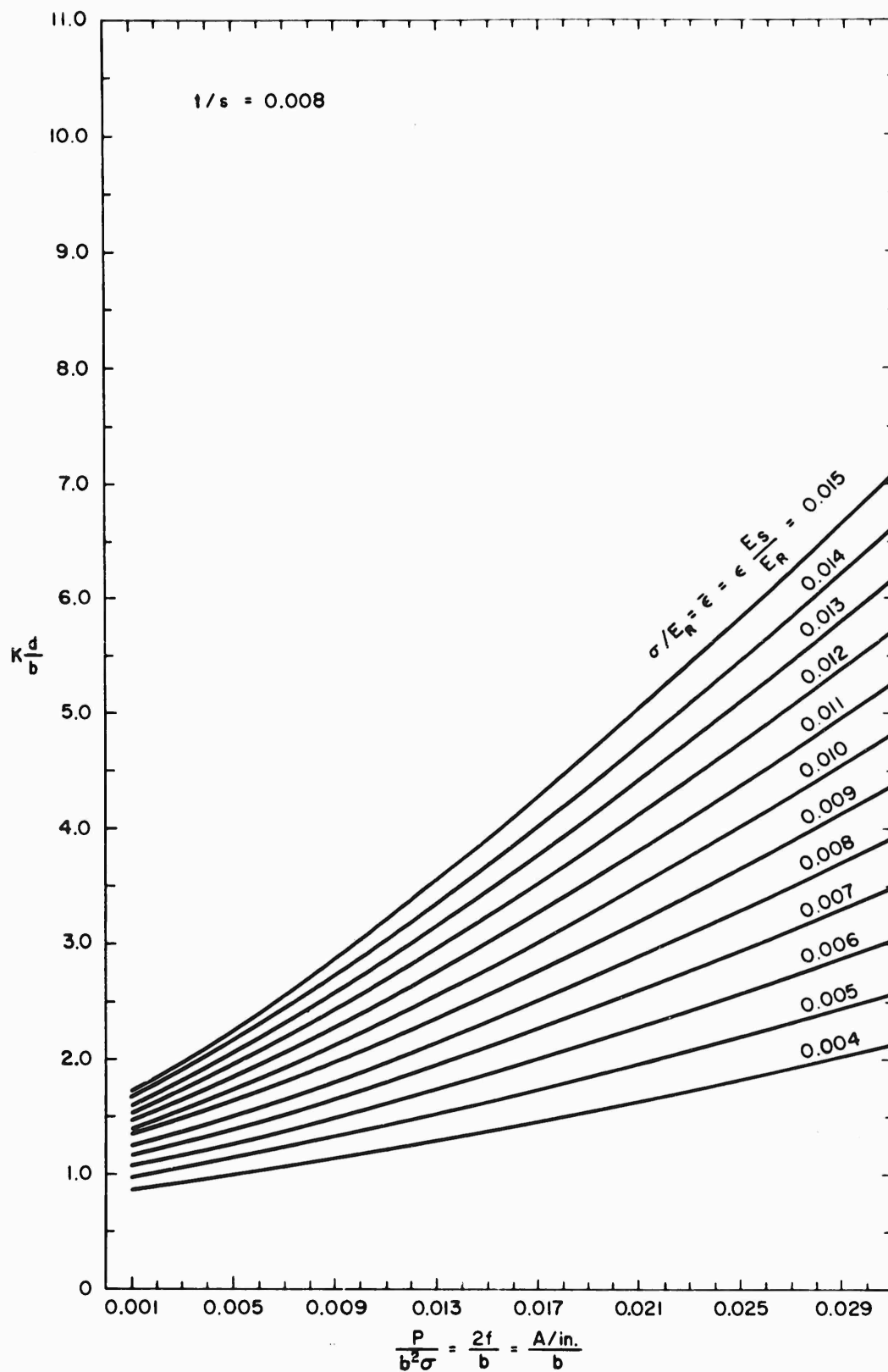


Figure 14c. Design Curves for Honeycomb Sandwich ( $t/s = 0.008$ )



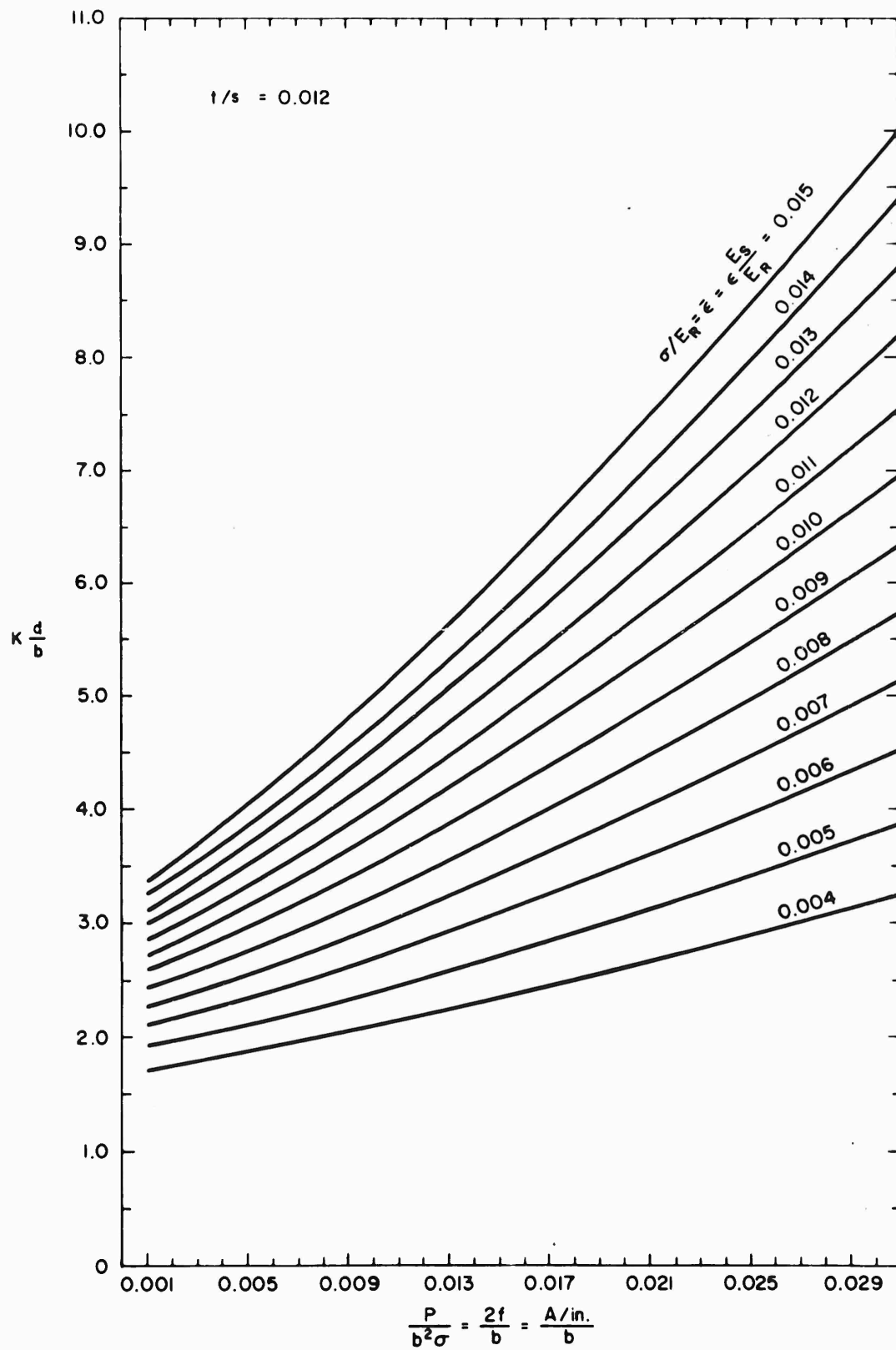


Figure 14d. Design Curves for Honeycomb Sandwich ( $t/s = 0.012$ )

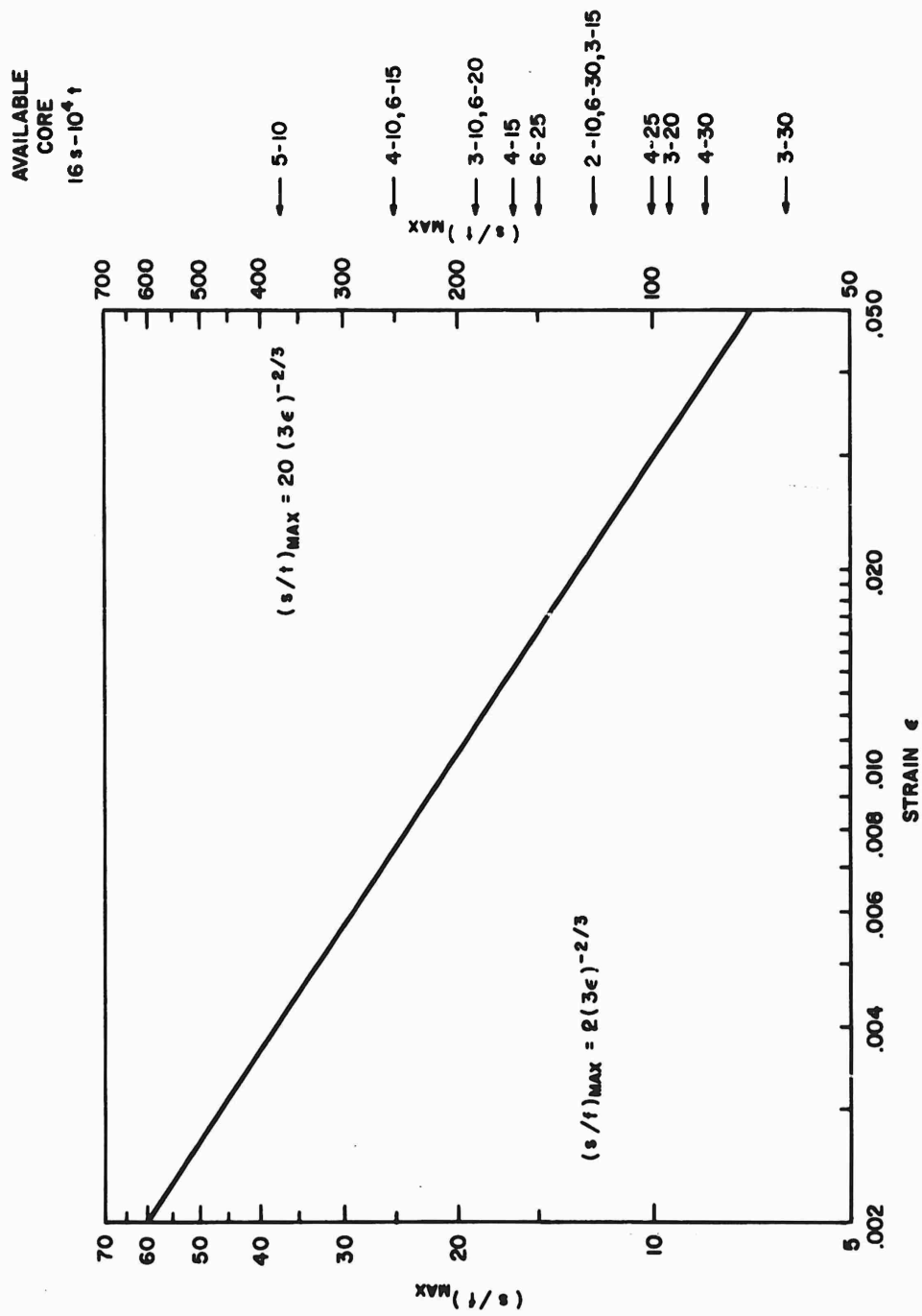


Figure 15. Core Size Required to Stabilize the Faces

The design procedure can be described as follows:

- ( 1 ) Select a design stress  $\sigma$  and a material ( $E_A, \sigma_o, \beta$ )
- ( 2 ) Enter Figures 12 and 4 with  $\sigma/\sigma_o$  in order to determine  $\xi_s$  and  $\xi_c$
- ( 3 ) Calculate  $E_S$  and  $E_T$ :

$$E_S = E_A \left[ (\sigma/\sigma_o) / \xi_s \right] \quad (61a)$$

$$E_T = E_A \left[ (\sigma/\sigma_o) / \xi_c \right] \quad (61b)$$

- ( 4 ) With the appropriate effective modulus formula, determine  $E_R$ , where  $E_R = E_R(E_S, E_T)$

- ( 5 ) Calculate  $\bar{\epsilon}$  and  $\epsilon$

$$\text{where } \bar{\epsilon} = \sigma/E_R \quad (60b)$$

$$\text{and } \epsilon = \sigma/E_S \quad (61c)$$

- ( 6 ) Enter Figure 15 with  $\epsilon$  and determine an available  $t/s$  which stabilizes

$$\text{the faces. Where } t \geq (.1)f = (.1) \frac{P}{2b\sigma} \quad (62a)$$

$$\text{and } s \leq 2f/(3\epsilon)^{2/3} \quad (62b)$$

- ( 7 ) Enter Figure 14 for the appropriate value of  $t/s$  with  $P/b^2\sigma$  and  $\bar{\epsilon}$  and determine  $K \frac{d}{b}$ .

- ( 8 ) Calculate the depth of core required

$$d_c = (K d/b) (b/K) - f \quad (63)$$

An analysis of the weight of the sandwich indicates that the weight of the bond is fairly independent of the design, the weight of the faces is dependent upon the face density ( $\rho_f$ ) and stability stress ( $\sigma$ ), and the weight of the core increases with core density ( $\rho_c$ ). This would suggest that the honeycomb sandwich be constructed with faces of the highest stress to density ratio and the lightest core that satisfies the core requirements.

Figures 14a to 14d indicate that the depth of core increases with the  $2f/b$  ratio. A minimum weight design would result if the face thickness is made as small as possible consistent with other requirements, such as required torsional stiffness, etc., and if the remaining required axial load carrying area were distributed at the supports so as to preclude instability.

For plate-like structures the minimum weight occurs for equal faces. For box-like structures in bending, however, a more efficient design can occur with thicker outer faces.

In some cases, selecting the allowable compressive stress does not result in a minimum weight design. This can occur if the load intensity ( $P/b^2\sigma_o$ ) is too small or the available core which satisfies the core specifications is too heavy. An analysis, such as performed in Reference 21, indicates that the design stress which results in minimum weight satisfies the following:

$$\frac{\delta \bar{\epsilon}}{\delta \sigma} = \frac{P}{b^2 \sigma^2} \frac{\rho_f}{\rho_c \sqrt{K \bar{\epsilon}}} \quad (\text{Eq. 20 of Ref. 21}) \quad (64a)$$

Plotting

$$\frac{P}{b^2 \sigma_o} \frac{\rho_f}{\rho_c \sqrt{K}} \left( \frac{E_A}{\sigma_o} \right)^{3/2} = \left( \frac{\sigma}{\sigma_o} \right)^{5/2} \left( \frac{E_A}{E_R} \right)^{1/2} \left[ \frac{E_A}{E_R} + \left( \frac{\sigma}{\sigma_o} \right) \frac{\delta(E_A/E_R)}{\delta(\sigma/\sigma_o)} \right] \quad (64b)$$

as a function of  $\sigma/\sigma_o$  can be employed to obtain a graphical solution of the optimum stress ratio  $\sigma/\sigma_o$ . No attempt was made in this report to present such curves since the value of  $E_R$  was not defined.

If  $E_R = E_S$ , Eq. (64b) reduces to

$$\frac{P}{b^2 \sigma_o} \frac{\rho_f}{\rho_c \sqrt{K}} \left( \frac{E_A}{\sigma_o} \right)^{3/2} = \left( \frac{\sigma}{\sigma_o} \right)^{5/2} \left( \frac{E_A}{E_S} \right)^{1/2} \left( \frac{E_A}{E_T} \right) \quad (64c)$$

If the optimum stress is low then a good approximation (upper bound) would be to assume that  $E_R = E_A$ . This results in

$$\sigma^{5/2} = \frac{P}{b^2} \left( \frac{E_A^{3/2} \rho_f}{\sqrt{K} \rho_c} \right) \quad (64d)$$

## D. TUBES IN TORSION

Tubes in torsion can be designed in the manner described for compression members. Two types of problems will be considered. The first is a tube (e.g., control rod) where the diameter (d) wall thickness (t) are determined by considering the local and over-all stabilities. The second is for a cylindrical tube (e.g., fuselage) where the thickness must be determined by considering the local stability.

### 1. LONG TUBE

The over-all stability of a tube in torsion is obtained by the use of Eq. 107 of Reference 1. This results in

$$T = \frac{2\sqrt{C_c}}{l} EI \sim \frac{\pi}{4} \sqrt{C_c} E_R \frac{d^3 t}{l} \quad (65a)$$

$$\tau = \frac{T}{2A_o t} = (E_R/2) \sqrt{C_c} (d/l) \quad (65b)$$

where  $A_o = \frac{\pi}{4} d^2$  is the area enclosed by the median curve (65c)

and  $t \ll d$ .

The local stability is determined by the use of Eqs. (A6) and (A7) of Reference 5, i.e.,

$$\tau = \frac{k_t^2 \pi^2 E_R 2^{3/4}}{12 (1-\nu^2)^{5/8}} \left(\frac{t}{d}\right)^{5/4} \left(\frac{d}{l}\right)^{1/2} = K E_R \left(\frac{t}{d}\right)^{5/4} \left(\frac{d}{l}\right)^{1/2} \quad (66a)$$

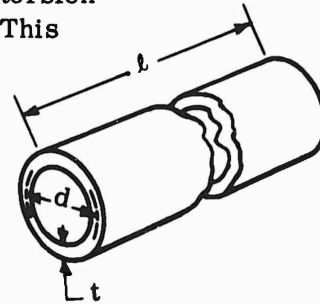
where  $K = 2^{3/4} \pi^2 k_t / 12 (1-\nu^2)^{5/8}$  (66b)

$$k_t = .85 F \text{ for simple supports}$$

$$k_t = .93 F \text{ for clamped supports}$$

$$F = \text{Factor to correlate theory and tests} \sim .84 \text{ (Reference 5).}$$

The effective modulus is assumed to be the secant modulus ( $E_R = E_S$ ) for a tube in torsion.



Equating the two stabilities results in

$$\tau = \frac{T}{2A_0 t} = \frac{E_R}{2} \sqrt{C_c} \left( \frac{d}{l} \right) = K E_R \left( \frac{t}{d} \right)^{5/4} \left( \frac{d}{l} \right)^{1/2} \quad (67a)$$

$$\text{and} \quad \left( \frac{\sqrt{C_c}}{2K} \right)^{4/5} \left( \frac{d}{l} \right)^{2/5} = \left( \frac{t}{d} \right) \quad (67b)$$

$$\text{The load equation } (T = \frac{\pi}{2} d^2 t \tau) \quad (68)$$

expressed in nondimensional form becomes

$$\frac{T}{l^3 \sigma_0} = \frac{\pi}{2\sqrt{3}} \left( \frac{d}{l} \right)^3 \left( \frac{t}{d} \right) \frac{\tau\sqrt{3}}{\sigma_0} = \frac{\pi}{2\sqrt{3}} \left( \frac{\sqrt{C_c}}{2K} \right)^{4/5} \left( \frac{d}{l} \right)^{17/5} \frac{\tau\sqrt{3}}{\sigma_0} \quad (69a)$$

but from Eq. (65c), we have

$$\left( \frac{d}{l} \right) = \frac{2\tau}{E_S \sqrt{C_c}} = \frac{(\tau\sqrt{3})/\sigma_0}{(E_S/E_A) \left( \frac{\sqrt{3C_c}}{2} \frac{E_A}{\sigma_0} \right)} = \frac{\xi_s}{\frac{E_A}{2\sigma_0} \sqrt{3C_c}} \quad (69b)$$

$$\therefore \bar{P} = \frac{T}{l^3 \sigma_0} \frac{2\sqrt{3}}{\pi} \left( \frac{E_A}{2\sigma_0} \sqrt{3C_c} \right)^{17/5} \left( \frac{\sqrt{C_c}}{2K} \right)^{-4/5} = \left( \xi_s^{17/5} \right) \left( \frac{\tau\sqrt{3}}{\sigma_0} \right) \quad (69c)$$

(Fig. 16)

The detail geometry is obtained as follows:

$$d = \frac{l \xi_s}{\frac{E_A}{2\sigma_0} \sqrt{3C_c}} \quad (70a)$$

$$\text{and} \quad t = \frac{d^{7/5}}{l^{2/5}} \left( \frac{\sqrt{C_c}}{2K} \right)^{4/5} \quad (70b)$$

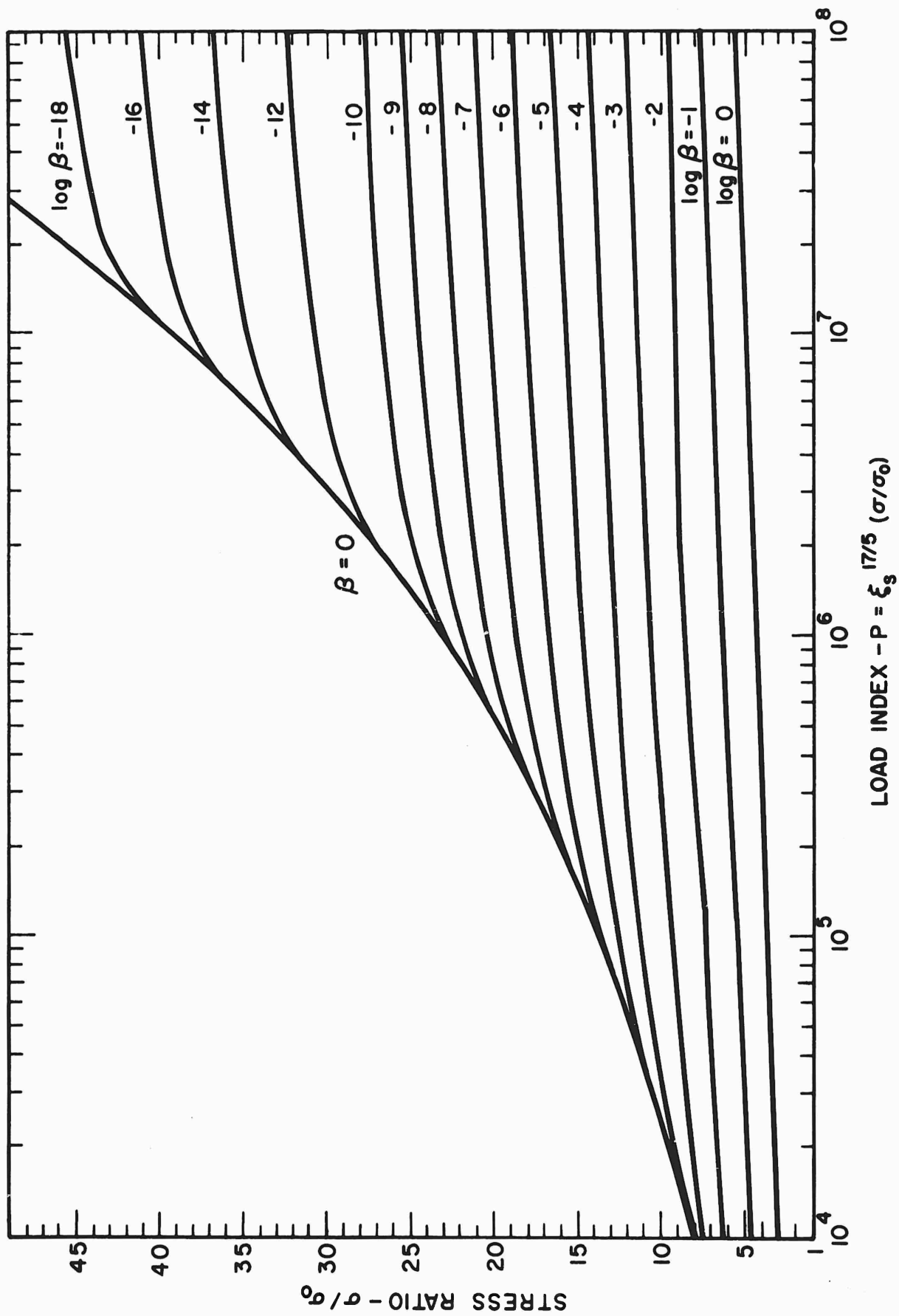


Figure 16. Stress Ratio vs. Load Index for Tube in Torsion

## 2. CYLINDRICAL TUBE

In many cases the tube is not too long and over-all stability does not determine the design. The following design approach can be employed for the case of a monocoque fuselage when the length and diameter are prescribed and it is desired to determine the minimum wall thickness to preclude local instability. The load equation is

$$T = \frac{\pi}{2} d^2 t \tau \quad (68)$$

but from Eq. (66a) we have

$$t = \left( \frac{\tau}{E_S} \right)^{4/5} \frac{l^{2/5} d^{3/5}}{K^{4/5}} \quad (71a)$$

Substituting Eq. (71a) into Eq. (68) and transforming to nondimensional form results in

$$\frac{T}{l^3 \sigma_o} = \frac{\pi}{2\sqrt{3} K^{4/5}} \left( \frac{d}{l} \right)^{13/5} \left( \frac{\tau\sqrt{3}}{E_S/E_A} \right)^{4/5} \left( \frac{\sigma_o}{\sqrt{3} E_A} \right)^{4/5} \left( \frac{\tau\sqrt{3}}{\sigma_o} \right) \quad (71b)$$

$$\text{and } \bar{P} = \frac{T}{l^3 \sigma_o} \frac{2\sqrt{3} K^{4/5}}{\pi} \left( \frac{l}{d} \right)^{13/5} \left( \frac{\sqrt{3} E_A}{\sigma_o} \right)^{4/5} = \left( \xi_s^{4/5} \right) \left( \frac{\tau\sqrt{3}}{\sigma_o} \right) \text{ (Fig. 17)} \quad (72)$$

The value of  $t$  can be determined by the equation

$$t = \frac{T}{\frac{\pi}{2} d^2 \left( \frac{\tau\sqrt{3}}{\sigma_o} \right) \frac{\sigma_o}{\sqrt{3}}} \quad (73)$$

after the value of  $\frac{\tau\sqrt{3}}{\sigma_o} = \sigma/\sigma_o$  is determined from the graph.

## E. BENDING OF BEAMS AND BEAM-LIKE PLATES

The minimum weight design of a beam is not as apparent as a column. In a column the axial stress in the member is independent of the distribution of the area in the cross section. This does not apply to a beam since an area redistribution will generally change the stress distribution. A redistribution of a given area of the beam



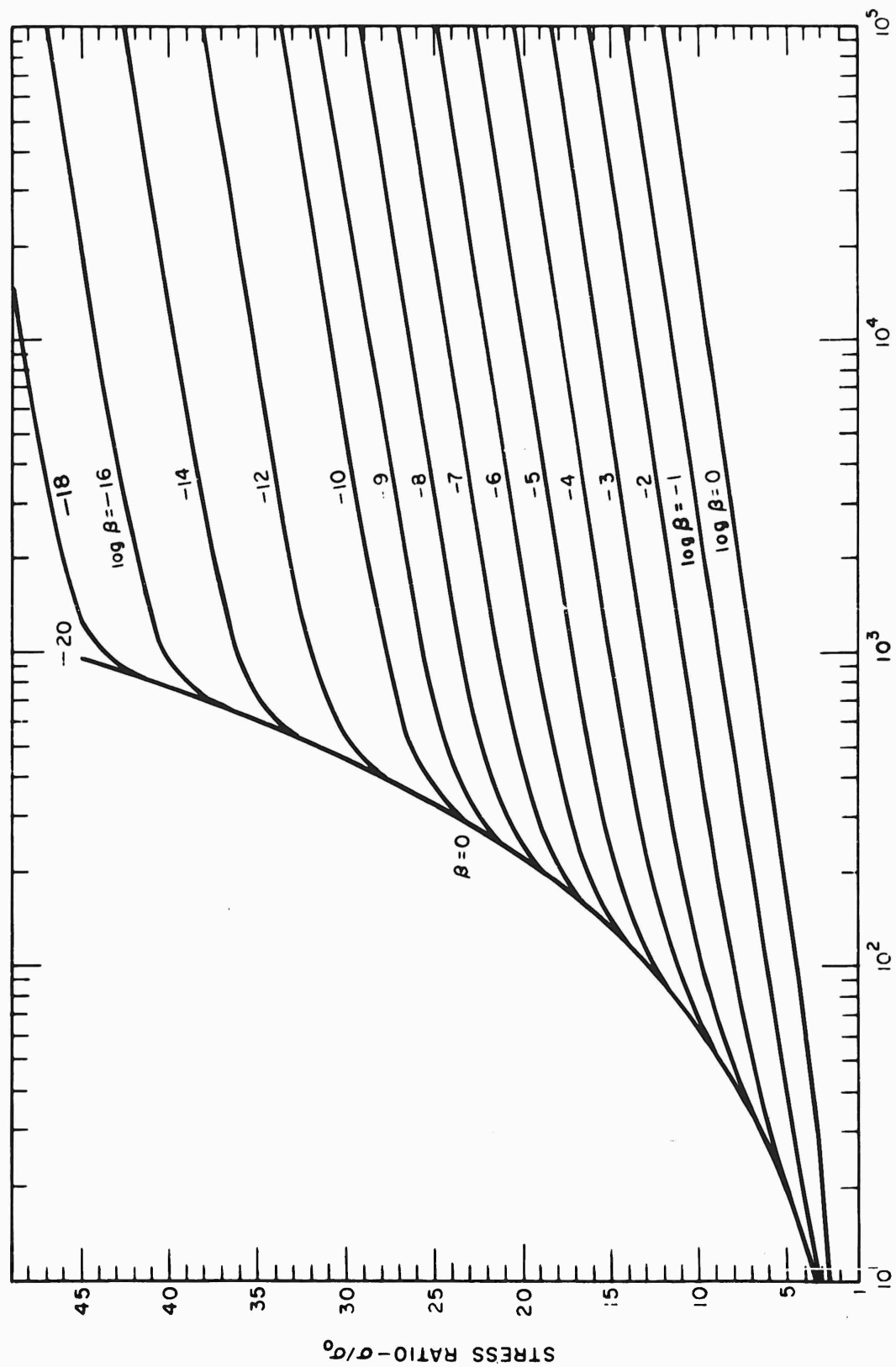


Figure 17. Stress Ratio vs. Load Index for Cylinder in Torsion

may decrease the stability of an element to increase another but it may also reduce the resulting stresses so that the elements remain stable for larger moments. Thus increasing the web of a beam at the expense of the flange will increase the allowable applied moment of a beam of constant area up to a point after which the loss of stability overrides the decrease in stress. The problem posed is how to determine this point so as to design a beam to resist a given moment with a minimum weight.

The technique employed is to examine a beam which fails because the compression stress exceeds the buckling of an element of the beam. Consider any beam: The area, the inertia, and the extreme fiber distance can be expressed in terms of two characteristic web dimensions  $d$  and  $t$  and a ratio of flange area to web area ( $z = wh/dt$ ). As an example, the cross-sectional properties of the channel section can be represented as follows:

$$A = \alpha_1 dt = (1 + 2z) dt$$

$$I = \alpha_3 d^3 t = (1/12 + z/2) d^3 t$$

$$c = \alpha_6 d = (1/2) d$$

The assumption is made that the extreme fiber stress can be calculated with sufficient accuracy by employing linear bending theory (i.e.,  $\sigma = Mc/I$ ). This should be satisfactory for optimum structures such as I-beams where the moment carrying capacity is primarily concentrated in the flanges. In addition, it is assumed that the stress-strain relationship is the same in tension and compression and that the neutral axis does not shift even when the stresses become nonlinear.

The load equation is therefore

$$M = \frac{\sigma I}{c} = \frac{\sigma \alpha_3 d^3 t}{\alpha_6 d} = \frac{\alpha_3}{\alpha_6} d^2 t \sigma \quad (74a)$$

Letting  $t/d = \left( \frac{\xi_p \sigma_o}{C_t E_A} \right)^{1/2}$  define the thickness ratio which becomes unstable at the design stress results in a load index

$$\frac{\alpha_6 M}{\alpha_3 \sigma_o d^3} \left( \frac{E_A C_t}{\sigma_o} \right)^{1/2} = \frac{\sigma}{\sigma_o} \sqrt{\xi_p} \quad (74b)$$

Similarly, the area can be expressed as an area index.

$$\frac{A \left( \frac{E_A C_t}{\sigma_o} \right)^{1/2}}{a_1 d^2} = \sqrt{\xi_p} \quad (74c)$$

For a given material and geometry, the area and weight of the beam are proportional to  $d^2 \sqrt{\xi_p}$  whereas the moment carried by this beam is proportional to  $d^3 \sqrt{\xi_p} (\sigma/\sigma_o)$ . Solving for  $d$  in Eq. (74b) and substituting the resulting solution into Eq. (74c) results in

$$\frac{A \left( \frac{E_A C_t}{\sigma_o} \right)^{1/2}}{a_1} = \left[ \frac{\frac{a_6 M}{a_3 \sigma_o} \left( \frac{E_A C_t}{\sigma_o} \right)^{1/2}}{\left( \frac{\sigma}{\sigma_o} \sqrt{\xi_p} \right)} \right]^{2/3} \sqrt{\xi_p} \quad (75a)$$

$$\text{Letting } \frac{a_6 M}{a_3 \sigma_o} \left( \frac{E_A C_t}{\sigma_o} \right)^{1/2} = X \quad (75b)$$

$$\text{and } \left( \frac{\sigma}{\sigma_o} \sqrt{\xi_p} \right)^{-2/3} = d_o^2 \quad (75c)$$

results in

$$\frac{A \left( \frac{E_A C_t}{\sigma_o} \right)^{1/2}}{a_1 X^{2/3}} = d_o^2 \sqrt{\xi_p} = \left( \frac{\sqrt{\xi_p}}{\left( \frac{\sigma}{\sigma_o} \sqrt{\xi_p} \right)} \right)^{2/3} \quad (75d)$$

This equation can be plotted to determine the value of  $\sigma/\sigma_o$  that would minimize this expression which is proportional to the weight of the structure for a given material, applied moment, and geometry. (See Fig. 18 for a typical plot for a corrugation plate beam).

The above analysis indicates that the optimum value of the extreme fiber stress ratio  $\sigma/\sigma_o$ , which would minimize the weight of a given beam of a given material, depends only upon the stress-strain relationship. The area distribution ( $z$ ) and the boundary conditions ( $C_t$ ) do not affect this optimum stress ratio.

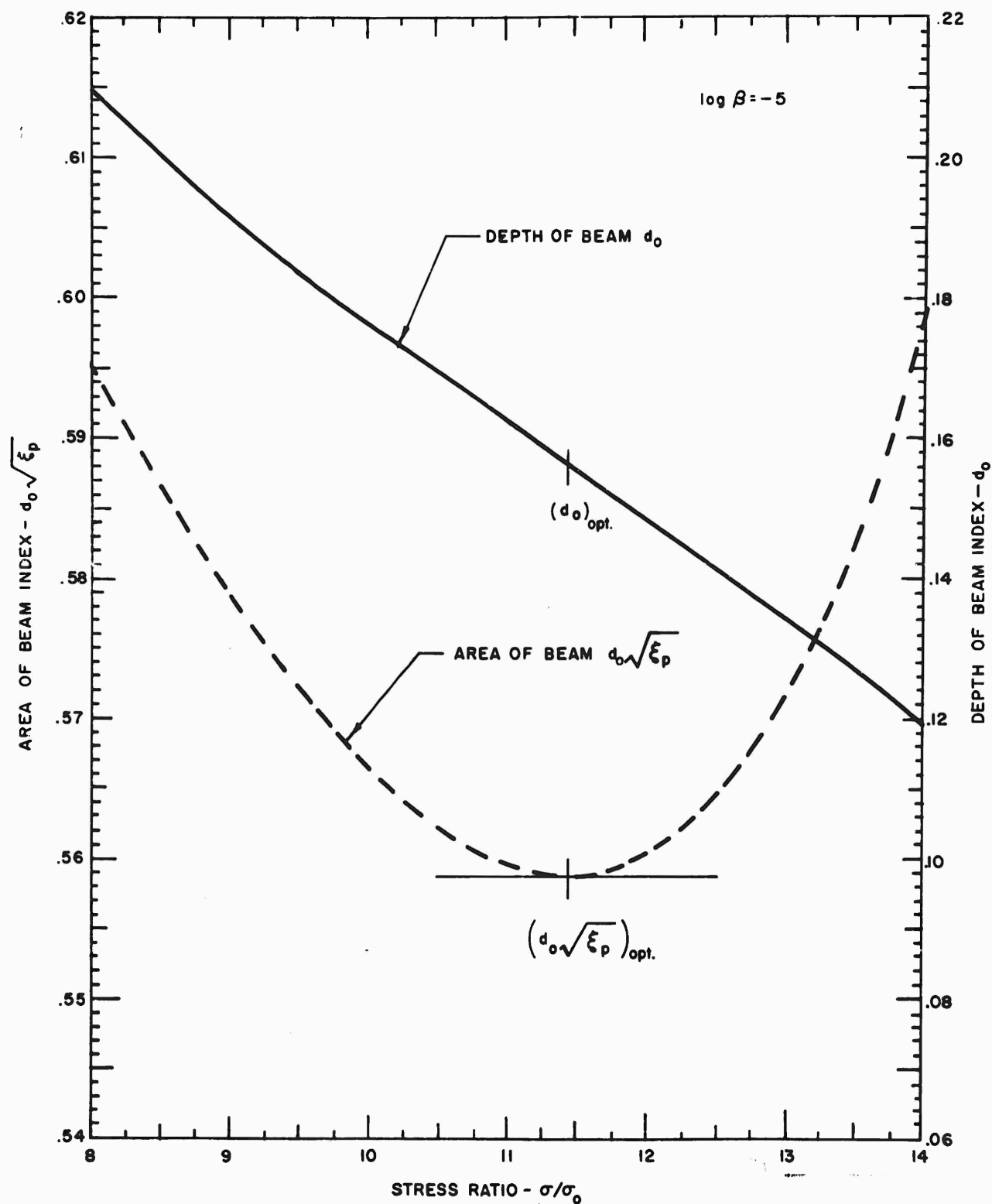


Figure 18. Typical Plot of Area Index vs. Stress Ratio

The other questions that must be resolved are what is the distribution of the area in the cross section and what are the elemental dimensions that would result in minimum weight when stressed to this optimum stress. The approach is to examine various types of distributions and to determine which would result in a minimum weight for a given moment. A complementary procedure is to note that a cross section which can resist a higher moment can be reduced in weight to take the required moment. It is immediately obvious that an area distribution which would maximize the section modulus ( $I/a_0 d$ ) while maintaining the area and thickness ratios would reduce the stress level and result in a minimum weight. The technique is similar to that of columns (maximum  $I_{xx}$ ) in solving for the area distribution  $z$ . Sections of constant thickness, such as bent-up sheet, can be determined in this manner. Sections of variable thickness require some additional defining conditions. In an arbitrary cross section the flange elements can be less stable, equally stable, or more stable than the web element. If the flange is less stable, then some area could be removed from the web and added to the flange; this would increase the moment carrying capacity of the beam. If the flange is more stable, then area could be removed from the flange and employed to increase the depth of the web. This would increase the section modulus and moment carrying capacity of the beam. This suggests that a minimum weight beam would have the flanges and webs equally stable up to the optimum stress.

Thus the design of beam sections is somewhat similar to columns. The requirements of maximum section modulus and equal stability result in defining the cross-sectional properties in terms of two characteristic dimensions  $d$  and  $t$ . The optimum stress ratio ( $\sigma/\sigma_0$ ) required to solve for  $d$  and  $t$ , however, can be determined as a function of the nonlinearity of the stress-strain relationship of the material ( $\beta$ ), and is presented in Figure 19. There is no need to resort to a  $\bar{P}$  vs.  $\sigma/\sigma_0$  plot to determine this stress ratio.

## 1. BEAMS

The design procedure for beams is straightforward provided stability designs the cross section. The description of the cross section in terms of the web dimensions is determined by maximizing the section modulus for a stationary area and thickness ratio. Values for typical sections are shown in Table 2. The optimum stress ratio is determined with the aid of Figure 19 and the beam is designed for this stress.

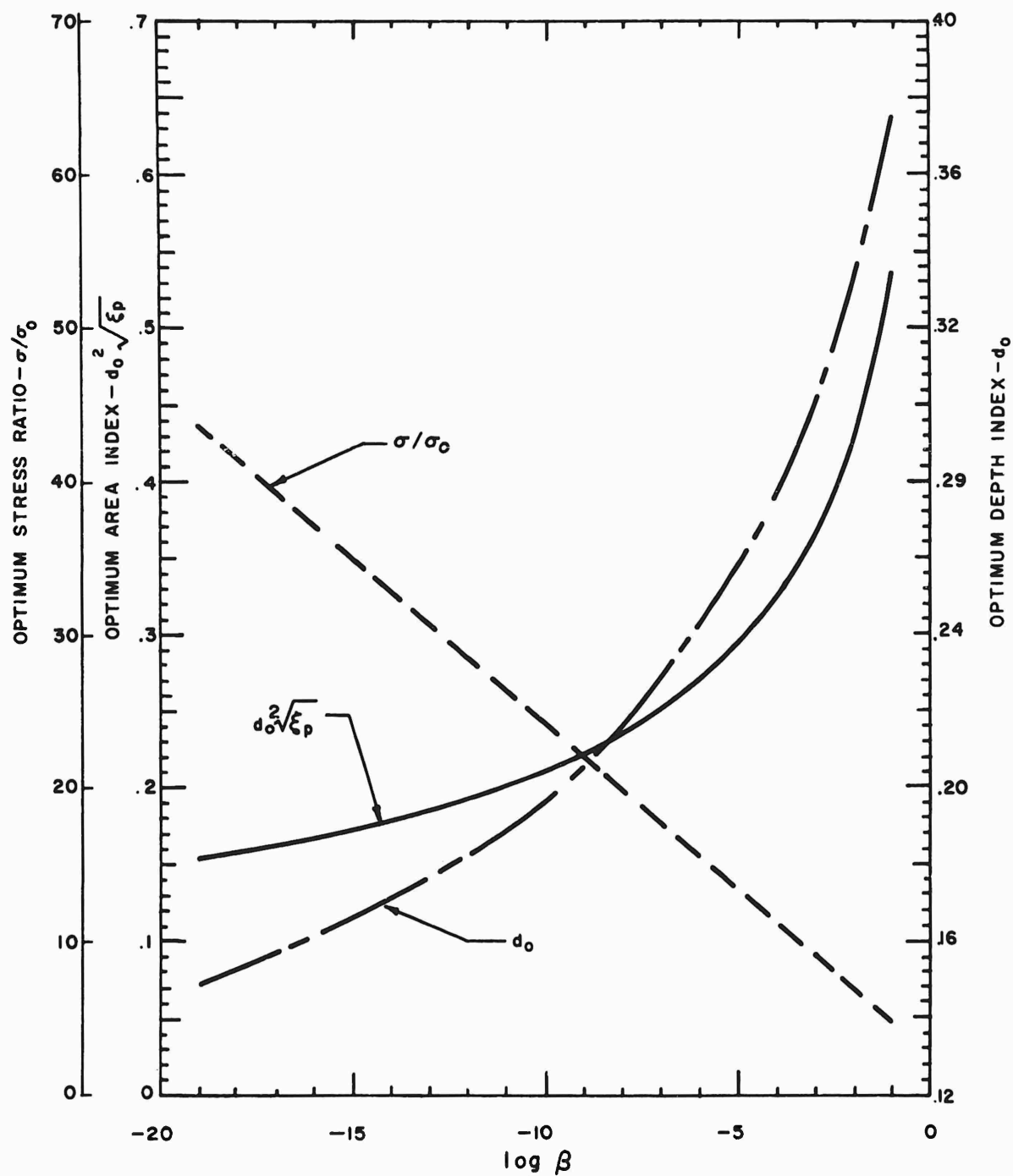


Figure 19. Optimum Stress, Depth, and Area Indices of a Beam

TABLE 2 - GEOMETRIC FACTOR FOR BEAMS IN BENDING

Section (Bending about x axis, see Table 1)	$z^*$	$\alpha_1$	$\alpha_3$	$\alpha_6$
	wh/dt	A/dt	$I/d^3t$	c/d
I-Beam	.250	2.000	.333	.500
Channel	.500	2.000	.333	.500
Tee	.625	2.250	.222	.222**
Angle (Sheet stiffener)	1.250	2.250	.222	.222**

\* The flange may have to be stiffened for bent-up sheet to ensure that  $C_h \geq C_t (z t/h)^2$

where  $C_h$  = stability constant for flange in compression

$C_t$  = stability constant for web in bending

$$(C_t = \frac{\pi^2 k}{12(1-\nu^2)} \text{ where } k \text{ is defined in various}$$

texts, e.g., References 2 and 4).

\*\* Flange in compression.

The design equations then become

$$d = \frac{\left( \frac{\alpha_6 M \sqrt{E_R C_t}}{\alpha_3 \sigma^{3/2}} \right)^{1/3}}{\left[ \frac{\alpha_6 M}{\alpha_3 \sigma} \left( \frac{E_A C_t}{\xi_p \sigma_o} \right)^{1/2} \right]^{1/3}} \quad (76a)$$

$$t = d \left( \frac{\sigma}{E_R C_t} \right)^{1/2} = \left( \frac{\alpha_6 M}{\alpha_3 E_R C_t} \right)^{1/3} = d \left( \frac{\xi_p \sigma_o}{E_A C_t} \right)^{1/2} \quad (76b)$$

$$\text{where } \sigma = (\sigma/\sigma_o) \sigma_o \quad (\sigma/\sigma_o \text{ obtained from Fig. 18}) \quad (76c)$$

$$E_R = E_A (\sigma/\sigma_o)/\xi_p \quad (\xi_p \text{ obtained from Fig. 5}) \quad (76d)$$

If the beam is of sheet metal, then

$$w = d (z t/h) \quad (77a)$$

If the beam is machined, then

$$w = d (z)^{1/2} (C_h/C_t)^{1/4} \quad (77b)$$

$$\text{and } h = t (z)^{1/2} (C_t/C_h)^{1/4} \quad (77c)$$

The weight of the structure is

$$W = \rho a_1 dt \quad (77d)$$

and must be compared for various materials.

If the allowable compressive stress is lower than the optimum stress e.g., if tension, creep, or fatigue governs), then a possible design procedure is to employ the same equations to obtain a beam of maximum section modulus that is stable up to the allowable stress. Equal stability of the elements will result in an optimum weight as indicated in the previous discussion.

## 2. CORRUGATION PLATE BEAMS

The design procedure for corrugation plate is identical to that described for beams with the exception that the moment and cross-sectional properties are given per inch of width, i.e.,

$$A = a_1 t$$

$$I = a_4 d^2 t$$

$$c = a_6 d$$

This results in

$$\frac{A \left( \frac{E_A C_t}{\sigma_o} \right)^{1/2}}{a_1 X^{1/2}} = \frac{\sqrt{\xi_p}}{\left( \frac{\sigma}{\sigma_o} \sqrt{\xi_p} \right)^{1/2}} = d_o \sqrt{\xi_p} \quad (78a)$$



$$\text{where } X = \frac{a_6 M}{a_4 \sigma_o} \left( \frac{E_A C_t}{\sigma_o} \right)^{1/2} \quad (78b)$$

$$\text{and } d_o = \left[ (\sigma/\sigma_o) \sqrt{\xi_p} \right]^{-1/2}$$

A typical plot of  $d_o \sqrt{\xi_p}$  as a function of  $\sigma/\sigma_o$  is shown in Figure 18. The results of such plots are then employed to obtain a plot (Figure 20) of the optimum stress ratio ( $\sigma/\sigma_o$ ), depth ( $d_o$ ), and area index ( $d_o \sqrt{\xi_p}$ ) as a function of  $\beta$ .

The values of  $a_1$ ,  $a_4$ , and  $a_6$  vary as a function of  $n$  and  $\theta$  and are formulated by Eqs. (26), (31) and (32).

The resulting design equations are

$$d = \left( \frac{a_6 M \sqrt{E_R C_t}}{a_4 \sigma^{3/2}} \right)^{1/2} \quad (79a)$$

$$t = d \left( \frac{\sigma}{E_R C_t} \right)^{1/2} = \left( \frac{a_6 M}{a_4 \sqrt{\sigma E_R C_t}} \right)^{1/2} \quad (79b)$$

$$f = 2t (n \sin \theta + \cos \theta) \sqrt{C_t/C_f} \quad (79c)$$

$$\text{and } W = a_1 t \rho \quad (79d)$$

## F. COMBINED LOADING CONDITIONS

Structures are frequently subjected to more than one type of loading. The combination of loads must be considered in designing the structure since it affects the stability. The addition of a tension load would tend to restrict the lateral deflections and increase the stability while a compression load would have the opposite effect. The effect upon the stability of loads causing different stress systems is usually expressed by an interaction equation. The interaction equation is a relationship between the ratios of the applied stresses to the buckling stresses (acting alone). When the loads cause stresses in the same direction they are usually added numerically and compared to the critical stress.

### 1. INTERACTION EQUATIONS

The interaction equations can be employed to obtain a modification factor to apply to the load index in the design procedures described previously. A typical interaction equation is as follows:

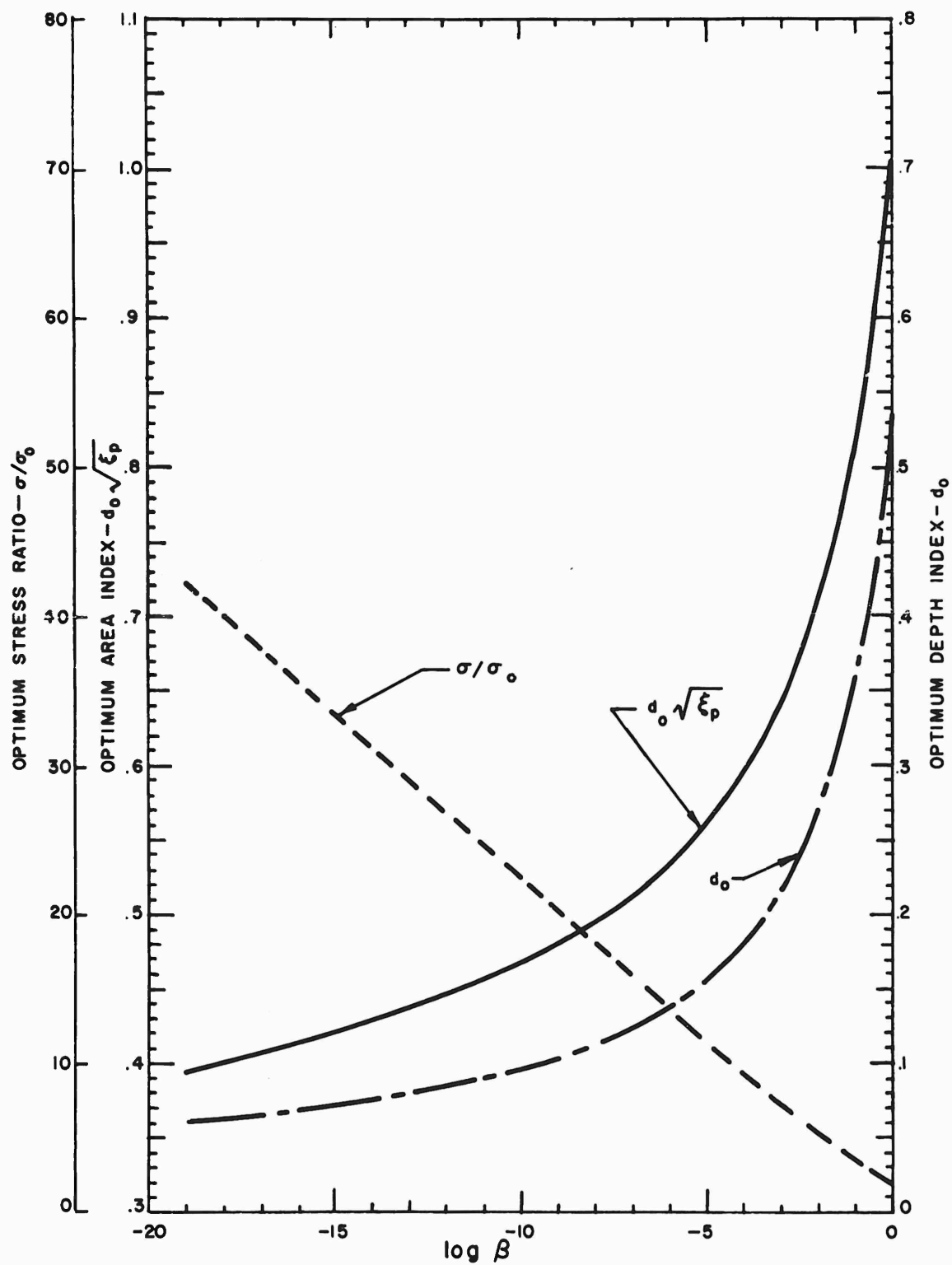


Figure 20. Optimum Stress, Depth, and Area Indices of a Corrugated Plate

$$\left(\frac{\sigma_1}{\sigma_{cr_1}}\right) + \left(\frac{\sigma_2}{\sigma_{cr_2}}\right)^n = 1 \quad (80)$$

The ratio of stresses is usually known since the stresses are proportional to the known applied loads and the corresponding resisting areas, i.e.,

$$\sigma_1 = P_1/A_1$$

$$\sigma_2 = P_2/A_2$$

$$\therefore \frac{\sigma_2}{\sigma_1} = \frac{P_2}{P_1} \frac{A_1}{A_2} = x \quad (81a)$$

The ratio of the critical stresses is known provided the stability equations are similar in form, i.e.,

$$\sigma_{cr_1} = C_1 E_R (t/d)^2$$

$$\sigma_{cr_2} = C_2 E_R (t/d)^2$$

$$\therefore \frac{\sigma_{cr_2}}{\sigma_{cr_1}} = \frac{C_2}{C_1} = y \quad (81b)$$

Substituting Eqs. (81a) and (81b) in Eq. (80) results in

$$\left(\frac{x}{y}\right)^n \left(\frac{\sigma_1}{\sigma_{cr_1}}\right)^n + \left(\frac{\sigma_1}{\sigma_{cr_1}}\right) = 1 \quad (81c)$$

This equation can be solved for the stress ratio  $\sigma_1/\sigma_{cr_1}$ . The structure could then be designed for a load equal to  $P_1/(\sigma_1/\sigma_{cr_1})$ . This would be a structure which would not become unstable when the loads  $P_1$  or  $P_2$  were applied but would become unstable when both loads were applied simultaneously.

The technique can be readily applied to the cover of a box beam subjected simultaneously to bending and torsion. The cover will have an axial load equal to the moment divided by the height of the box ( $P = M/h$ ) and a shear load equal to the twisting moment divided by twice the height of the box ( $Q = T/2h$ ). The interaction equation for a plate in compression and shear (Eq. 55 of Reference 4) is usually given as

$$\left(\frac{\sigma}{\sigma_{cr}}\right)^2 + \left(\frac{\tau}{\tau_{cr}}\right)^2 = 1 \quad (82a)$$

Since the areas are the same, we obtain from Eq. (81a)

$$x = \frac{\tau}{\sigma} = \frac{Q}{P} = \frac{T}{2M}$$

A comparison of the stability equations results in

$$y = \frac{\tau_{cr}}{\sigma_{cr}} = \frac{C_{\tau} E_R (t/d)^2}{C_t E_R (t/d)^2} \sim \frac{C_{\tau}}{C_t}$$

Eq. (81c) then becomes

$$\left(\frac{x}{y}\right)^2 \left(\frac{\sigma}{\sigma_{cr}}\right)^2 + \left(\frac{\sigma}{\sigma_{cr}}\right)^2 = 1$$

and the solution is

$$\frac{\sigma}{\sigma_{cr}} = \frac{\left(1 + 4\left(\frac{x}{y}\right)^2\right)^{1/2} - 1}{2\left(\frac{x}{y}\right)^2} = \frac{\left(1 + 4\left(\frac{Q}{P} \frac{C_t}{C_{\tau}}\right)^2\right)^{1/2} - 1}{2\left(\frac{Q}{P} \frac{C_t}{C_{\tau}}\right)^2} \quad (82b)$$

This results in the following modified load index for unreinforced plates:

$$\bar{P} = \frac{P}{b^2 \sigma_o} \left(\frac{C_t E_A}{\sigma_o}\right)^{1/2} \left[ \frac{2\left(\frac{Q}{P} \frac{C_t}{C_{\tau}}\right)^2}{\left(1 + 4\left(\frac{Q}{P} \frac{C_t}{C_{\tau}}\right)^2\right)^{1/2} - 1} \right] \quad (82c)$$

## 2. COMBINED AXIAL LOAD AND BENDING OF BEAMS

The design of beams subjected to combined axial load and bending can be treated in a manner similar to beams in pure bending provided the axial load is not too large. Employing the assumptions of linear stress distribution and non-shifting of the neutral axis, results in the following stress equations:

$$\sigma = \frac{M c}{I} + \frac{P}{A} = \frac{M a_6}{a_3 d^2 t} + \frac{P}{a_1 t d} \quad (83a)$$

$$\frac{a_6 M}{a_3 d^3 \sigma_o} \left( 1 + \frac{a_3 P d}{a_1 a_6 M} \right) \left( \frac{E_A C_t}{\sigma_o} \right)^{1/2} = \frac{\sigma}{\sigma_o} \sqrt{\xi_p} \quad (83b)$$

$$\frac{A}{a_1 d^2} \left( \frac{E_A C_t}{\sigma_o} \right)^{1/2} = \sqrt{\xi_p} \quad (83c)$$

If the expression  $\frac{a_3 P d}{a_1 a_6 M}$  is small compared to 1 then the equations

are identical with Eqs. (75) for pure bending and the optimum stress ratio, which does not change, can be obtained from Figure 19. Assuming that the optimum stress ratio does not change significantly results in the following design equation which must be solved for d:

$$\left( \frac{d}{d_o} \right)^3 = \frac{a_6 M}{a_3 \sigma_o} \left( 1 + \frac{a_3}{a_1 a_6} \frac{P d_o (d/d_o)}{M} \right) \left( \frac{E_A C_t}{\sigma_o} \right)^{1/2} \quad (84a)$$

$$\text{Letting } \frac{a_6 M}{a_3 \sigma_o} \left( \frac{E_A C_t}{\sigma_o} \right)^{1/2} = b \quad (84b)$$

$$\text{and } \frac{a}{b} = \frac{a_3 P}{a_1 a_6 M} \quad (84c)$$

$$\text{results in } \left( \frac{d}{d_o} \right)^3 = b \left[ 1 + \frac{a d_o}{b} \left( \frac{d}{d_o} \right) \right] \quad (84d)$$

which is solved graphically in Figure 21 for  $(d/d_o)$  knowing the value of  $b$  and  $a d_o/b$ . The design technique is to determine values of  $b$ ,  $a$ , and  $d_o$  knowing the material, the loads, and the geometric distribution. With this information the depth is calculated from which all the other dimensions are obtained with the aid of Eqs. (76b), (77a), (77b), and (77c). It is necessary to either assume that the value of  $C_t$  does not change because of the axial load or else to employ an iterative technique. This would require assuming a value of  $C_t$ , calculating the geometry and stress distribution and determining the corresponding  $C_t$  for the web (e.g., Table 34 of Reference 2). This process would then be repeated until the assumed and calculated values agreed to a satisfactory degree.

The same design technique can be employed with corrugated plates subjected to bending and axial loads. The design equation becomes

$$\left(\frac{d}{d_o}\right)^2 = b \left[ 1 + \frac{a d_o}{b} \left(\frac{d}{d_o}\right) \right] \quad (85a)$$

$$\text{where } b = \frac{a_6 M}{a_4 \sigma_o} \left( \frac{E_A C_t}{\sigma_o} \right)^{1/2} \quad (85b)$$

$$\text{and } \frac{a}{b} = \frac{a_4}{a_1 a_6} \frac{P}{M} \quad (85c)$$

This can be solved directly as

$$\frac{d}{d_o} = \frac{\frac{a d_o}{b} + \left[ \left( \frac{a d_o}{b} \right)^2 + 4 b \right]^{1/2}}{2} \quad (85d)$$

or graphically as shown in Figure 22. The detail design is then obtained from Eqs. (85d), (79b) and (79c).

#### G. DESIGN HINTS

Errors can be introduced into the design because of reading and interpolating the design graphs. In order to minimize these errors it is wise to incorporate check calculations. The largest errors occur in estimating the values of stability parameter

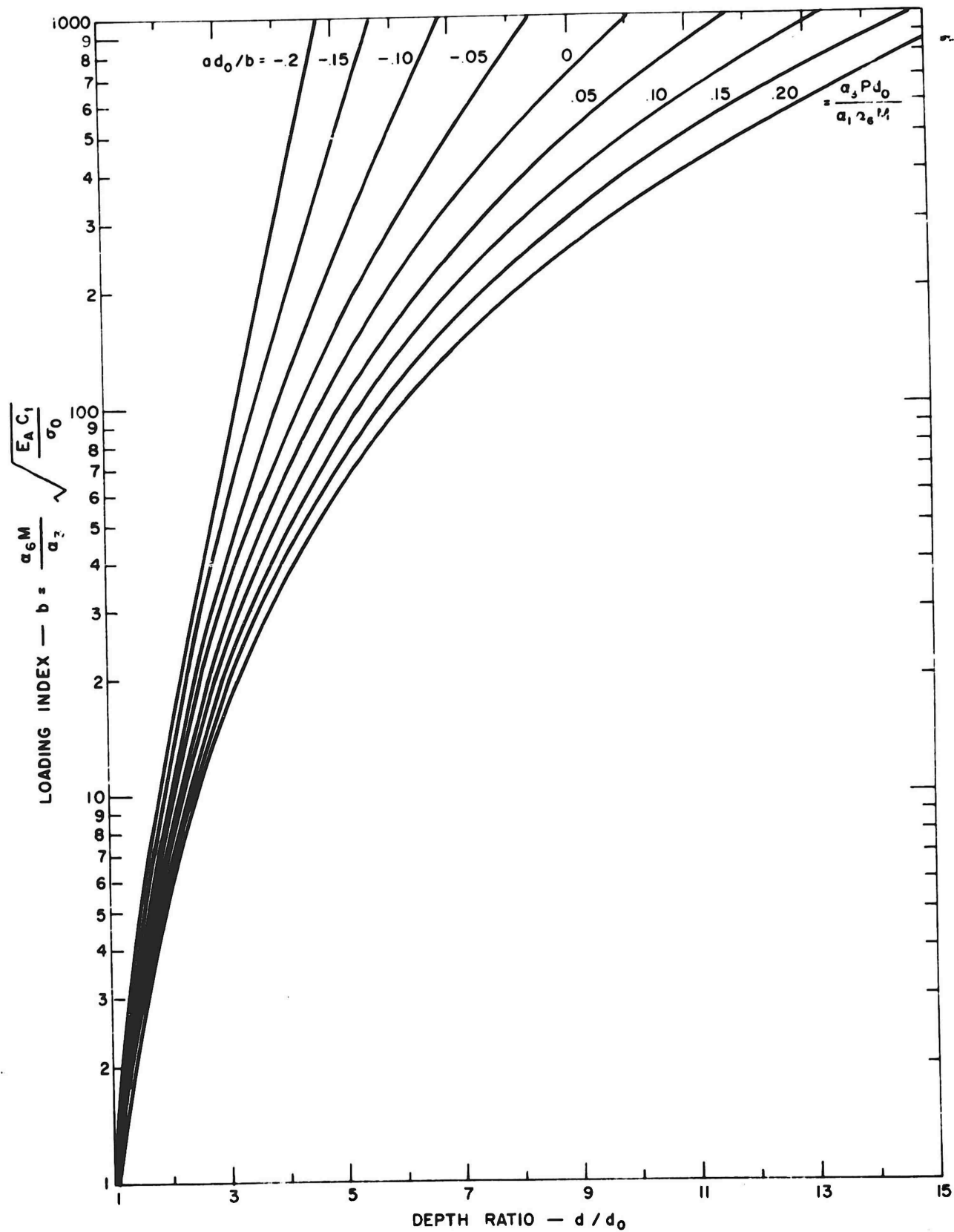


Figure 21. Depth Ratio of a Beam Subjected to Bending and Axial Loads

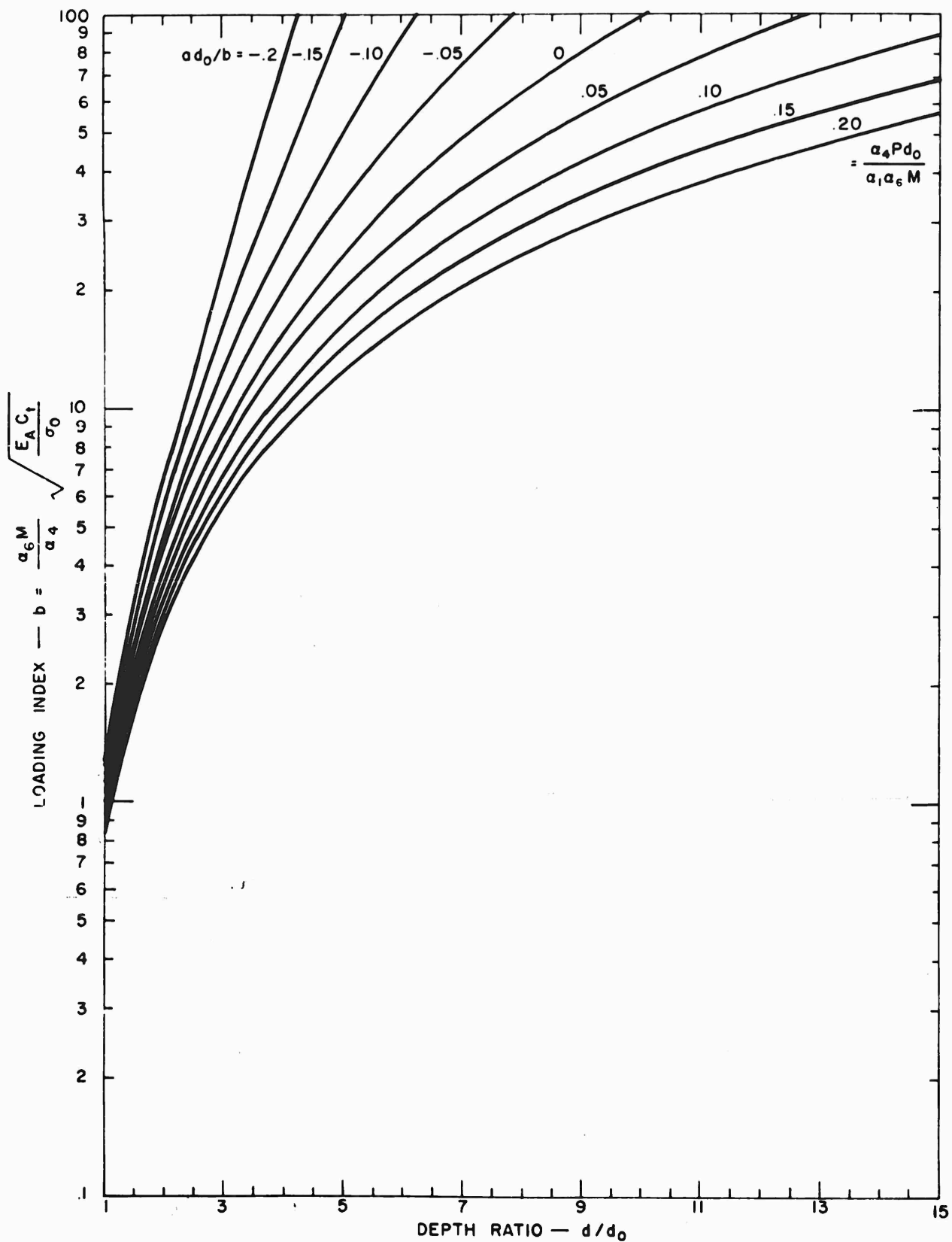


Figure 22. Depth Ratio of a Corrugated Plate Subjected to Bending and Axial Loads



$\xi$  whenever  $\log \beta$  is not a negative integer. In the elastic range (low load indices) the stability parameter is equal to the stress ratio ( $\xi_c = \xi_p = \xi_s = \sigma/\sigma_o$ ) but as the material becomes plastic (larger load indices) then the incremental changes of the values of  $\sigma/\sigma_o$ ,  $\xi_s$ ,  $\xi_p$  and  $\xi_c$  increase in the order given.

Having calculated the load index  $\bar{P}$  from the appropriate formula, the designer enters the appropriate curves to obtain values of  $\sigma/\sigma_o$ ,  $\xi_s$ ,  $\xi_p$ , and  $\xi_c$ . If the graphical results indicate that the stress is elastic ( $\sigma/\sigma_o = \xi$ ) then the exact value of  $\sigma/\sigma_o$  can be obtained by the solution of the load index equation (e. g., Eq. (44b);  $\bar{P} = (\xi_s^{7/8})(\sigma/\sigma_o) = (\sigma/\sigma_o)^{15/8}$  for a corrugated panel in shear) and will serve as a check upon the graphical result. If the graphical result indicates that the stress is plastic ( $\sigma/\sigma_o \neq \xi$ ) then calculating the load index by means of the stress ratio and stability parameters would serve as a check upon the graphical interpolation. The least sensitive parameters, coupled with the load index, can be employed to obtain a better estimate of the most sensitive parameter. For example,

$$\xi_c = \frac{\bar{P}}{\left(\frac{\sigma}{\sigma_o}\right)\sqrt{\xi_p}}$$

can be employed from Eq. (10b) to obtain or check the column stability parameter  $\xi_c$ . Greater accuracy in reading the design graphs can be obtained by enlarging the scales for the particular type of construction, material, and loads of interest. The possibility of having to design for materials which have high stress ratios (e. g., structural steel) resulted in the design curves presented in this report.

The minimum weight design must be increased in area if the allowable stress is less than the stability stress that corresponds to a minimum weight. A method of increasing the area so that the stability of the different modes of failure remains equal is recommended. This will result in the most stable structure for a given area and will permit a maximum increase of the applied load if the allowable stresses should ever be increased. If the allowable stress is predicated upon the permissible creep strain in a column then maintaining equal stability of the local elements and over-all buckling should tend to result in an optimum design for creep buckling. As an example, if the area of a column has to be changed because the allowable stress ( $\sigma'$ ) is lower than the optimum design stress ( $\sigma$ ), then

$$A' = A \frac{\sigma}{\sigma'} \quad (86a)$$

$$d' = d \left(\frac{\sigma}{\sigma'}\right)^{1/3} \quad (86b)$$

$$\text{and } t' = t \left(\frac{\sigma}{\sigma'}\right)^{2/3} \quad (86c)$$

increases the area properly by insisting that the  $\frac{d'}{b}$  and  $\frac{t'}{d'}$  ratios be equal so that the local and over-all modes remain equally stable. The primed terms refer to the new geometry while the unprimed terms refer to the minimum weight geometry disregarding the lower allowable stress. Similar equations can be derived for other types of cross sections.

The basic load equation can be employed to check on the design area. Errors in reading the graphs can result in slight errors in the detail geometry. Comparing the load that can be resisted by the designed details (e.g.,  $P = \sigma a_1 dt$ ) to the actual applied load can serve as a check upon the calculations. Small errors can be rectified by modifying the area as indicated in the preceding paragraph. Large errors would suggest redoing the calculations.

The detail design will result in odd size gages and dimensions which should be modified in an actual design to conform with available sizes. Wherever possible these modifications should be apportioned in such a manner as described previously to maintain the proper relationships between the thickness ratios and never to decrease these ratios below the ones prescribed by the minimum weight design.

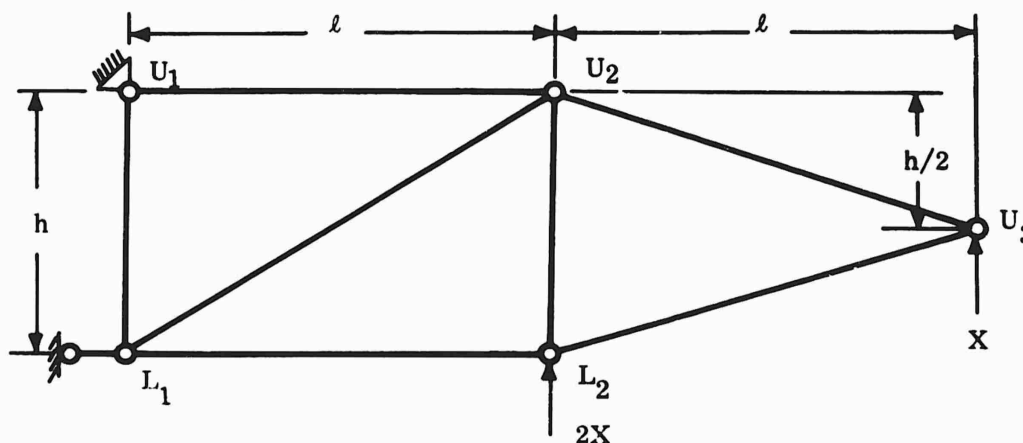
### SECTION III - ILLUSTRATIVE EXAMPLES

Two structures, representative of aerospace constructions, will be investigated in order to illustrate the nondimensional design technique presented in this report. The first is a heated (800° to 1000°F) beam truss with the design dependent on a relatively simple load-temperature-time history. The second is a portion of a wing with the covers heated to as high as 2000°F with two load-temperature-time histories representative of possible aerospace missions with relatively rapid or slow exits and reentries.

It is not intended that these examples cover all the design details or to represent exact material properties and final designs. They are presented to demonstrate the simplicity and ease of employing the nondimensional design technique in preliminary designs.

#### A. BEAM TRUSS

A beam truss is loaded as indicated below. The lengths of the beam truss members and their loads are presented in Table 3. The loads in the members are given in terms of limit loads which change with temperature and are applied for the times specified.



The design technique will be illustrated (using slide rule accuracy) for one type of cross section (wide flanged columns) and two possible materials, 6Al-4V Titanium and 17-7 PH (TH1050) Stainless Steel. The actual design would have to be investigated for other probable cross sections and materials. The material properties are determined from scant experimental data presented in References 10 to 13 and are shown in Figures 1b and 23. The data are for sheet material and are assumed to apply. A more sophisticated investigation would require a greater amount of experimental data with a statistical procedure to obtain the proper confidence level for the material properties.

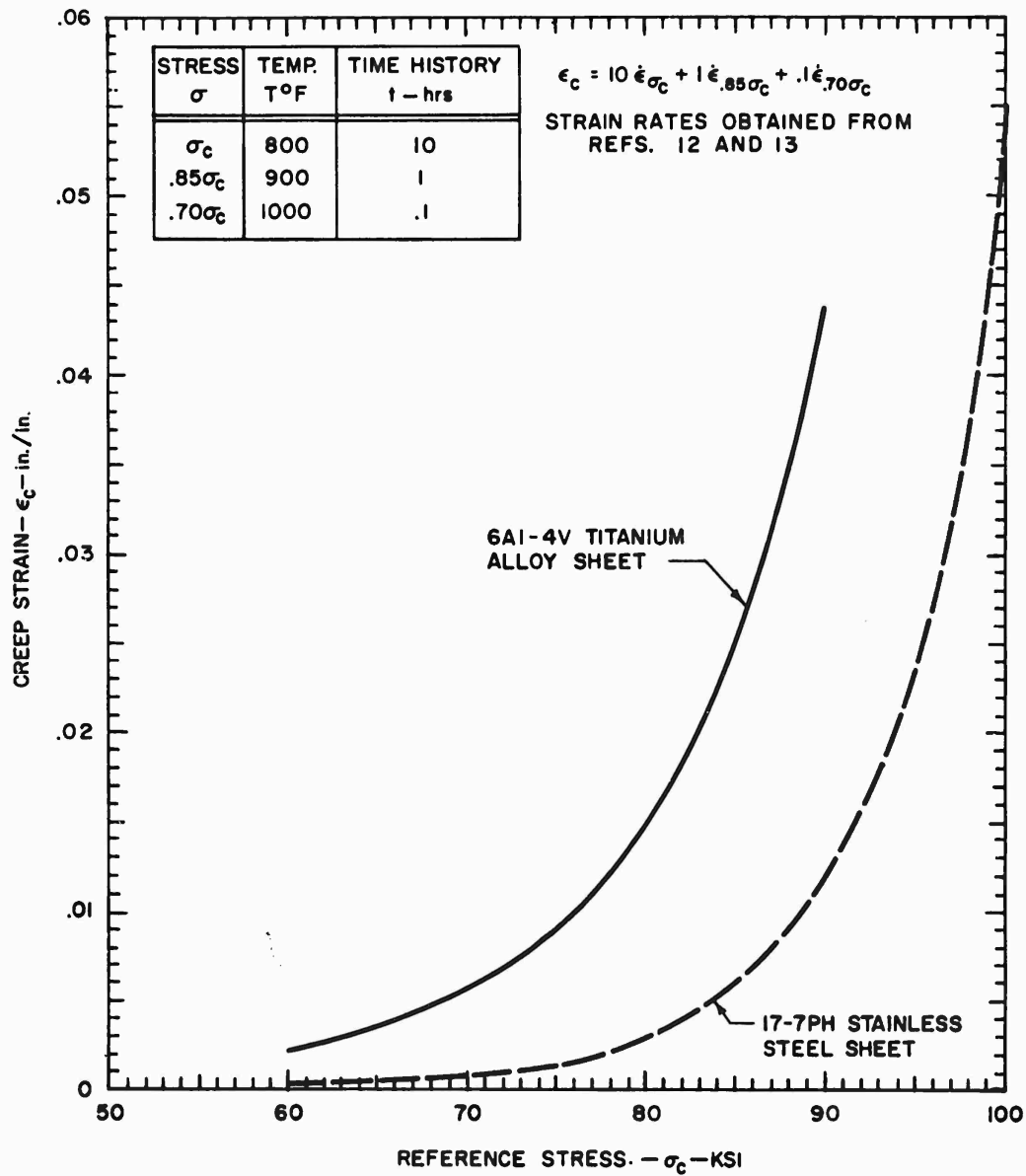


Figure 23. Creep Strain vs. Reference Stress

# 1. LOAD TEMPERATURE TIME HISTORY

**TABLE 3 - LENGTHS AND LOADS IN TRUSS MEMBERS**

Member	length b		load/X = P/X	
$U_1 - U_2$	$l$	30.0	$- 4 l/h$	- 12.0
$U_2 - U_3$	$(l^2 + (h/2)^2)^{1/2}$	30.41	$-(l^2 + (h/2)^2)^{1/2}/h$	- 3.041
$U_1 - L_1$	$h$	10.0	- 3.0	- 3.0
$U_2 - L_2$	$h$	10.0	- 2.5	- 2.5
$L_1 - U_2$	$(l^2 + h^2)^{1/2}$	31.62	$3(l^2 + h^2)^{1/2}/h$	9.486
$L_2 - U_3$	$(l^2 + (h/2)^2)^{1/2}$	30.41	$(l^2 + (h/2)^2)^{1/2}/h$	3.041
$L_1 - L_2$	$l$	30.0	$l/h$	3.0

Note:  $l = 30''$ ,  $h = 10''$

Limit Load X = 10,000 lb. at 800°F for 10 hours  
8,500 lb. at 900°F for 1 hour  
7,000 lb. at 1000°F for 0.1 hour

# 2. DESIGN STRESSES

The maximum stresses that the elements can attain without destroying the structural adequacy must be determined. This stress must be evaluated by considering all possible modes of failure. The structure may be inadequate because of instability or because of stresses which cause rupture or excessive deformations. The stresses should be sufficiently low so that the structure does not fail statically (short time strength), dynamically (fatigue), or through inelastic action (stress rupture, creep) when magnified by appropriate factors of safety. The technique of designing for instability has been presented previously. The upper limit that the stress can attain must be evaluated by considering the other modes of failure.

Allowable stresses are determined in Table 4 by considering short-time strength (with a factor of safety of 1.5) and long-time creep deformation (with a factor of safety of 1.1). The table is self explanatory. The factors of safety can be varied at the discretion of the designer to note their influence upon the final design. It should be noted that the designer should consider other modes of failure as well as other materials. The data presented are intended merely to indicate the design technique rather than to obtain an actual design.

### 3. DESIGN OF MEMBERS

#### a. Tension Members

The tension members would be designed simply by supplying sufficient area so that the allowable stress is not exceeded. The distribution of the area is not critical. The optimum material is the one in which the  $\sigma_a/\rho$  ratio is maximum. Note that the allowable stress at the reference temperature (800°F) is the minimum of the creep stress ( $\sigma_c$ ) and the lowest value in columns 5 and 12 of Table 4. This would preclude failure from short-time or long-time tensile stresses for the required lifetime of the structure.

$$\text{Since} \quad \left( \frac{\sigma_{am}}{\rho} \right)_{800 \text{ Tit.}} = \frac{65.5}{.160} = 410$$

$$\text{and} \quad \left( \frac{\sigma_{am}}{\rho} \right)_{800 \text{ St.}} = \frac{80.0}{.276} = 289$$

therefore the titanium is more efficient for the tensile members and  $\sigma_{am} = 65.5$  and  $\rho = .160$  are employed in the design. Knowing the allowable limit stress in tension, it is then possible to determine the area and weight of the tensile members of the beam truss. The calculations are shown in Table 5.

TABLE 4 - LIMIT ALLOWABLE AXIAL STRESSES

Material		17-7PH (TH 1050) Stainless Steel							6Al-4V Titanium						
1	2	3	4	5	6	7	8	9	10	11	12	13	14	15	16
Temp.	(1) r	Short-Time Strength F.S. = 1.5 <sup>(2)</sup>			Long-Time Creep Strength F.S. = 1.1 <sup>(3)</sup>			Allowable Limit Stress	Short-Time Strength F.S. = 1.5 <sup>(2)</sup>			Long-Time Creep Strength F.S. = 1.1 <sup>(3)</sup>			Allowable Limit Stress
		(4) $\sigma_u$	(4) $\frac{\sigma_u}{F.S.}$	(4) $\frac{\sigma_u}{F.S.} / r$	(6) $\sigma_a$	(7) $\sigma_c$	(7) $\sigma_a = \frac{r \sigma_c}{F.S.}$	(8) $\sigma_{am}$	(5) $\sigma_u$	(5) $\frac{\sigma_u}{F.S.}$	(5) $\frac{\sigma_u}{F.S.} / r$	(6) $\sigma_a$	(7) $\sigma_c$	(7) $\frac{r \sigma_c}{F.S.}$	(8) $\sigma_{am}$
800°	1.00	126	84.0	84.0	80.0	89	80.9	80.0	122	81.3	81.0	65.5	76	69.0	65.5
900°	.85	102	68.0	[80.0]	68.0		68.9	68.0	100	66.7	78.1	55.9		58.9	55.9
1000°	.70	92	61.3	88.0	56.0		56.7	56.0	69	46.0	[65.5]	46.0		48.5	46.0

(1) r = load ratio = load at temp./load at 800°F (reference temperature)

(2) F.S. = factor of safety = 1.5 for short-time strength

(3) F.S. = factor of safety = 1.1 for long-time creep strength for  $\epsilon_c = .01$

(4) Reference 11

(5) Reference 13

(6) Allowable stress at temp. so as not to exceed  $\sigma_u/F.S.$  at any other temperature

$$= r \left[ \text{min. value of } \left( \frac{\sigma_u}{F.S.} / r \right) \text{ i.e., cols. 5 and 12} \right]$$

(7) Reference stress at 800°F resulting in accumulated creep strain  $\epsilon_c = .01$  for the design environment (Figure 23). Strain rates from References 12 and 13

(8) Controlling allowable limit stress. Note that short time strength governs for both materials, however, an increase in the 1.1 factor of safety or a decrease in the allowable creep strain can make the creep criteria govern.

TABLE 5 - DESIGN OF TENSION MEMBERS

	Limit Load at 800°F	Tension Area	Weight/In.	Length of Member	Weight of Member
Member	P (Ref. Table 3)	$A = \frac{P}{\sigma_{am}}$ $\sigma_{am} = 65,500$ (Table 4)	$W = A\rho$ $\rho = .160$	b (Table 3)	Wb
$L_1 - U_2$	94,860	1.440	.230	31.62	7.28#
$L_2 - U_3$	30,410	.465	.074	30.41	2.26
$L_1 - L_2$	30,000	.457	.073	30.0	2.19

b. Compression Members

1) Geometry Factors

Assume that the wide flange cross section must buckle by bending about the X - X axis because of the lateral support supplied by covers which introduce the load into the truss. We obtain the following geometric parameters with the aid of Table 1.

area distribution,  $z = .083$

area ratio,  $\alpha_1 = 1.333$

inertia ratio,  $\alpha_3 = .167$

stability constant for flange,  $C_h = .388$

stability constant for web,  $C_t = 3.62$

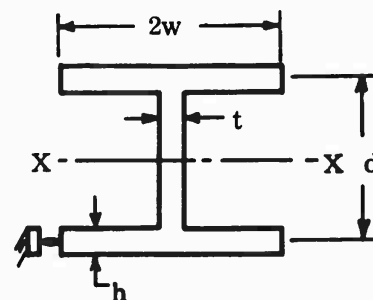
stability constant for column,  $C_c = \pi^2$

modified stability constant  
for column  $C_d = \frac{C_c \alpha_3}{\alpha_1} = .125\pi^2 = 1.23$

modified geometric constant  $K_G = \frac{C_d}{\alpha_1} C_t^{1/2} = \frac{.125}{1.333} \pi^2 \sqrt{3.62} = 1.75$

width ratio,  $\frac{w}{d} = (z)^{1/2} (C_h/C_t)^{1/4} = .165$

thickness ratio,  $\frac{h}{t} = (z)^{1/2} (C_t/C_h)^{1/4} = .503$





## 2) Material Factors

The material parameters are obtained from Figure 1b and are tabulated in Table 6 for the different materials and temperatures.

TABLE 6 - MATERIAL PARAMETERS

Material Temperature	6Al-4V Titanium			17-7 PH (TH1050) St. Steel		
	800	900	1000	800	900	1000
$\log \beta^*$	-5.6	-4.7	-4.2	-6.9	-5.2	-5.0
$E_A/10^{6*}$	10.2	8.9	7.6	24.6	23.0	21.0
$\sigma_o/10^{3*}$	5.0	5.2	5.25	9.0	8.8	8.2
$E_A/\sigma_o 10^2$	20.4	17.1	14.48	27.35	26.2	25.6
$E_A^{3/2}/\sigma_o^{5/2}$	18.4	13.5	10.5	15.9	15.2	15.8

\*Figure 1b

## 3) Load Indices

The load index for the various members and loading conditions can be readily calculated from the geometry and material parameters. The load index is calculated with the aid of Eq. (11a) which can be expressed as

$$\bar{P} = \frac{P}{b^2} \frac{E_A^{3/2}}{\sigma_o^{5/2}} K_G$$

Data from Tables 3 and 6 are then employed to obtain the ultimate load indices presented in Table 7A.

TABLE 7A - ULTIMATE LOAD INDICES  $\bar{P}_A$

Member	6Al-4V Titanium			17-7 PH (TH1050) St. Steel		
	800°	900°	1000°	800°	900°	1000°
$U_2 - U_1$	6440	3950	2580	5540	4570	3820
$U_2 - U_3$	1590	980	640	1370	1130	940
$U_1 - L_1$	14,500	8900	5810	12,470	10,300	8610
$U_2 - L_2$	12,080	7410	4850	10,390	8580	7170

## 4) Design Stresses In Compression

The critical stress ratio for these load indices is obtained from the nondimensional plot of Figure 6 and is Tabulated in Table 8A. The stresses and weights for these conditions are also calculated and tabulated. The maximum weight for each material governs the design for that material in order to ensure structural adequacy under all conditions. The smaller of these maximum weight values determines the material, the design weight, and stress. The results are tabulated in Table 8A which is self explanatory.

TABLE 8A - STRESSES AND WEIGHTS

Titanium	Member			
	$U_2 - U_1$	$U_2 - U_3$	$U_1 - L_1$	$U_2 - L_2$
$P_{800^\circ\text{F}}$	180,000	45,600	45,000	37,500
$\rho = .160$				
Min. Wt. $P\rho/\sigma_{au}$	0.293	0.075	0.073	0.061
$\sigma_{au} = 1.5 \sigma_{am} = 98,300^{(1)}$				
$800^\circ\text{F} \quad \sigma/\sigma_o \text{ (Fig. 6)}$	15.2	13.7	16.0	15.8
$\sigma_o = 5000 \quad \sigma_{cr} = (\sigma/\sigma_o)\sigma_o$	76,000	68,500	80,000	79,000
$A = rP/\sigma_{cr}$	2.37	0.67	0.56	0.47
$W = A\rho$	<span style="border: 1px solid black; padding: 2px;">0.379</span>	<span style="border: 1px solid black; padding: 2px;">0.197</span>	<span style="border: 1px solid black; padding: 2px;">0.090</span>	<span style="border: 1px solid black; padding: 2px;">0.076</span>
$900^\circ\text{F} \quad \sigma/\sigma_o \text{ (Fig. 6)}$	13.0	11.4	13.8	13.4
$\sigma_o = 5200 \quad \sigma_{cr} = (\sigma/\sigma_o)\sigma_o$	67,600	59,300	71,800	69,600
$A = rP/\sigma_{cr}$	2.26	0.66	0.53	0.46
$W = A\rho$	0.334	0.105	0.085	0.073
$1000^\circ\text{F} \quad \sigma/\sigma_o \text{ (Fig. 6)}$	11.5	10.2	12.3	12.1
$\sigma_o = 5250 \quad \sigma_{cr} = (\sigma/\sigma_o)\sigma_o$	60,400	53,600	64,600	63,500
$A = rP/\sigma_{cr}$	2.09	0.60	0.49	0.41
$W = A\rho$	0.334	0.095	0.078	0.066

(1) Allowable ultimate stress =  $1.5 \sigma_{am}$  (limit allowable stress from Table 4)

     Optimum design weight for both materials (minimax)

TABLE 8A - STRESSES AND WEIGHTS (Cont)

17-7PH St. Stl.	Member			
	$U_2 - U_1$	$U_2 - U_3$	$U_1 - L_1$	$U_2 - L_2$
Min. Wt. $\sigma_{au} = 120,000^{(1)}$	0.414	0.105	0.104	0.086
800°F $\sigma/\sigma_o$ (Fig. 6)	10.9	9.8	11.6	11.4
$\sigma_o = 9000$ $\sigma_{cr} = (\sigma/\sigma_o)\sigma_o$	98,100	88,200	104,400	102,600
$\rho = .276$ $A = rP/\sigma_{cr}$	1.83	0.52	0.43	0.37
$W = A\rho$	0.505	0.144	0.119	0.104
900°F $\sigma/\sigma_o$ (Fig. 6)	9.0	8.0	9.7	9.2
$\sigma_o = 8800$ $\sigma_{cr} = (\sigma/\sigma_o)\sigma_o$	79,200	70,400	85,400	81,000
$A = rP/\sigma_{cr}$	1.93	0.50	0.45	0.39
$W = A\rho$	0.533	0.138	0.124	0.108
1000°F $\sigma/\sigma_o$ (Fig. 6)	8.8	8.7	10.8	10.6
$\sigma_o = 8200$ $\sigma_{cr} = (\sigma/\sigma_o)\sigma_o$	72,200	71,300	88,600	86,900
$A = rP/\sigma_{cr}$	1.74	0.45	0.36	0.30
$W = A\rho$	0.480	0.124	0.099	0.083

(1) Allowable ultimate stress =  $1.5 \sigma_{am}$  (limit allowable stress from Table 4)

  Design weight for the 17-7 PH St. Stl. material (maximum)

## 5) Detail Design

Having determined the optimum axial stress, the member can be designed as shown in Table 9A.

It is interesting to note that although the steel has a higher modulus to density ratio it is not employed in the minimum weight designs of the compression members in the temperature ranges considered. This can be attributed to two causes. The optimum design stresses for the applied loads are well into the plastic range. Any effect of a high elastic moduli ratio is considerably reduced in this region and the allowable stress to density ratio tends to govern the selection of the material (as was the case with tension members). Secondly, it can be shown that the optimum material for a column is governed by a ratio of the density to the three fifths power of the stability modulus (i. e. ,  $W \propto \rho / (E_R)^{3/5}$ )

An analysis of this ratio in the elastic range of titanium and stainless steel would indicate that the steel is slightly less efficient at 800° F but that this is reversed at the higher temperatures. Thus the steel would tend to become more efficient at the higher temperatures when the applied loads are so small that the optimum design stress is in the elastic range.

To investigate this possibility, the structure was redesigned for load indices of 1% of the original load indices, presented in Table 7A. This is equivalent to increasing the length and depth of the truss by a factor of 10 (i. e. ,  $l = 10(30) = 300$ , and  $h = 10(15) = 150$ ) while the loads on the truss remain unchanged. It should be noted that increasing the loads on the truss by a hundred-fold would result in the original load indices and in cross sections in titanium which are ten times those indicated in Table 9A.

The design of the cross sections of the tension members would be identical to the original structure (Table 5) since the scaling factor does not change the magnitude of the loads in the members.

The design of the compression members presented in Tables 8B and 9B illustrates the conclusion stated above. The designs are lighter in titanium for the load condition 800° F (which still designs the members) but heavier for the load conditions at 900° F and 1000° F. The weight ratios are presented in Table 8C and are in excellent agreement with the  $\rho / (E_R)^{3/5}$  ratio.

TABLE 8B - STRESSES AND WEIGHTS

Material	Member			
	$U_2 - U_1$	$U_2 - U_3$	$U_1 - L_1$	$U_2 - L_2$
<b>Titanium</b> ( $\rho = .160$ )				
Min. Wt. <sup>(1)</sup>	0.293	0.075	0.073	0.061
800°F $\sigma/\sigma_o$ (Fig. 6 <sup>(2)</sup> )	5.29	3.02	7.32	6.81
$\sigma_o = 5000$ $\sigma_{cr} = \sigma_o (\sigma/\sigma_o)$	26,500	15,100	36,600	34,000
$A = rP/\sigma_{cr}$	6.80	3.02	1.23	1.10
$W = A\rho$	1.09	0.483	0.197	0.176
900°F $\sigma/\sigma_o$ (Fig. 6 <sup>(2)</sup> )	4.35	2.49	6.02	5.59
$\sigma_o = 5200$ $\sigma_{cr} = \sigma_o (\sigma/\sigma_o)$	22,600	12,950	31,300	29,100
$A = rP/\sigma_{cr}$	6.76	2.99	1.22	1.10
$W = A\rho$	1.08	0.479	0.195	0.175
1000°F $\sigma/\sigma_o$ (Fig. 6 <sup>(2)</sup> )	3.67	2.10	5.08	4.72
$\sigma_o = 5250$ $\sigma_{cr} = \sigma_o (\sigma/\sigma_o)$	19,300	11,000	26,700	24,800
$A = rP/\sigma_{cr}$	6.54	2.89	1.18	1.06
$W = A\rho$	1.05	0.463	0.189	0.169
<b>17-7PH St. Steel</b> ( $\rho = .276$ )				
Min. Wt. <sup>(1)</sup>	0.414	0.105	0.104	0.086
800°F $\sigma/\sigma_o$ (Fig. 6 <sup>(2)</sup> )	4.98	2.85	6.70	6.41
$\sigma_o = 9000$ $\sigma_{cr} = \sigma_o (\sigma/\sigma_o)$	44,800	25,600	60,300	57,700
$A = rP/\sigma_{cr}$	4.01	1.78	0.746	0.650
$W = A\rho$	1.11	0.491	0.206	0.180
900°F $\sigma/\sigma_o$ (Fig. 6 <sup>(2)</sup> )	4.61	2.64	6.39	5.93
$\sigma_o = 8800$ $\sigma_{cr} = \sigma_o (\sigma/\sigma_o)$	40,600	23,200	56,200	52,200
$A = rP/\sigma_{cr}$	3.77	1.67	0.681	0.610
$W = A\rho$	1.04	0.461	0.188	0.168
1000°F $\sigma/\sigma_o$ (Fig. 6 <sup>(2)</sup> )	4.29	2.45	5.94	5.52
$\sigma_o = 8200$ $\sigma_{cr} = \sigma_o (\sigma/\sigma_o)$	35,200	20,100	48,700	45,300
$A = rP/\sigma_{cr}$	3.58	1.59	0.646	0.580
$W = A\rho$	0.988	0.438	0.178	0.160

(1) Table 8A; (2)  $\bar{P}_B = 0.01 \bar{P}_A$ 



 Design weight for each material (maximum)  
 Optimum design weight for both materials (minimax)

TABLE 8C - RATIOS OF  $W_{\text{TITANIUM}}/W_{\text{ST. STEEL}}$

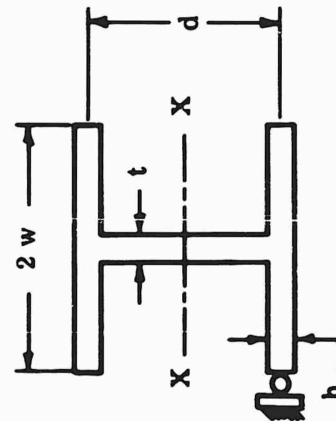
Temp.	Weight Ratios of Members				Theoretical Ratios
	$U_2 - U_1$	$U_2 - U_3$	$U_1 - L_1$	$U_2 - L_2$	$\frac{\rho_T}{\rho_S} \left( \frac{E_{RS}}{E_{RT}} \right)^{3/5}$
800 F	0.983	0.984	0.955*	0.982	0.983
900 F	1.04	1.04	1.04	1.04	1.025
1000 F	1.06	1.06	1.06	1.06	1.067

\* The minimum weight design stress for this member in 17-7PH Steel is slightly in the plastic range. This reduces the ratio below that of the theoretical value.

TABLE 9A - GEOMETRY OF OPTIMUM STRUCTURE (HIGH LOAD INDEX)

Member	Mat'l	$\sqrt{\frac{\sigma_o}{E A}}^*$	$\sigma/\sigma_o$	$\xi_c$	d	2w	$\xi_p$	t	h	A
			Table 8A	Fig. 4	$b \left[ \frac{\xi_c \sigma_o}{C_d E A} \right]^{\frac{1}{2}}$	.33d	Fig. 5	$d \left[ \frac{\xi_p \sigma_o}{C_t E A} \right]^{\frac{1}{2}}$	.503t	1.333dt Table 8A
$U_2 - U_1$	T1-800*	.0222	15.2	83	5.45"	1.80"	27.0	.327"	.164"	2.36
$U_2 - U_3$	T1-800*	.0222	13.7	28	3.20	1.06	17.0	.152	.077	.65
$U_1 - L_1$	T1-800*	.0222	16.0	160	2.47	.82	36.0	.173	.087	.57
$U_2 - L_2$	T1-800*	.0222	15.8	131	2.28	.75	34.0	.155	.078	.47

\* Material Parameters, Table 6



Cross Section of Compression Members

TABLE 9B - GEOMETRY OF OPTIMUM STRUCTURE (LOW LOAD INDEX)

Member	Mat'l	$\sqrt{\frac{\sigma_o}{E A}}$ *	$\log^* \beta$	$\sigma/\sigma_o$	$\xi_c$	d	2w	$\xi_p$	t	h	A
					Fig. 4	$b \left[ \frac{\xi_{co}}{C_d E A} \right]^{\frac{1}{2}}$	.33d	Fig. 5	$d \left[ \frac{\xi_{po}}{C_t E A} \right]^{\frac{1}{2}}$	.503t	1.333dt Table 8B
$U_2 - U_1$	Ti-800	.0222	-5.6	5.29	5.29	13.81	4.60	5.29	.371	.187	6.82
$U_2 - U_3$	Ti-800	.0222	-5.6	3.02	3.02	10.60	3.52	3.02	.215	.108	3.03
$U_1 - L_1$	Ti-800	.0222	-5.6	7.32	7.32	5.42	1.81	7.32	.171	.086	1.23
$U_2 - L_2$	Ti-800	.0222	-5.6	6.81	6.81	5.23	1.74	6.81	.159	.080	1.11

\* Material Parameters, Table 6



## B. WING PORTION

A design of a wing section is appropriate since aerospace vehicles still require wings for aerodynamic operations during exit and reentry into an atmosphere.

### 1. STRUCTURE

A typical type of wing construction for an aerospace vehicle is shown in Figure 24 in which great care has been exercised to minimize thermal stresses. Differential expansion between the covers is accommodated by expansion strips (Sec. A-A). The vertical airloads are carried by beam action in the corrugated covers to the corrugated spar webs by means of vertical strips. The shear loads due to torsion of the wing box are carried to the truss ribs by a single pin tie in each cover. The depth of the continuous spar caps and truss members are kept to a minimum to reduce any stresses due to thermal gradients. The spar webs are corrugated to permit differential expansions between the webs and the covers or spar caps.

Typical elements of each type of construction will be designed for two kinds of aerospace missions considering several feasible materials.

### 2. UNIT SOLUTIONS

An analysis of the structure shown in Figure 24 for a pressure of 1 psf on the bottom cover has been performed and the results are summarized below.

#### a. Bending Moment in Covers

$$M \text{ per psf} = 1.39 \text{ in. lb/in.}$$

#### b. Spar No. 1

The shear load (Q) acting upon the spar increases linearly while the moment (M) increases parabolically. Since the beam is of constant depth (assumed to be 22 inches), the load (P) in the spar caps also increases parabolically. The maximum values occur at the root and are noted as follows:

$$Q = 20.6 \text{ lb. per psf}$$

$$M = 1800 \text{ in. lb. per psf}$$

$$P = 81.9 \text{ lb. per psf}$$

#### c. Rib Truss

The loads in the truss members were computed for a cover load of 1 psf and are shown in the sketch on page 97.

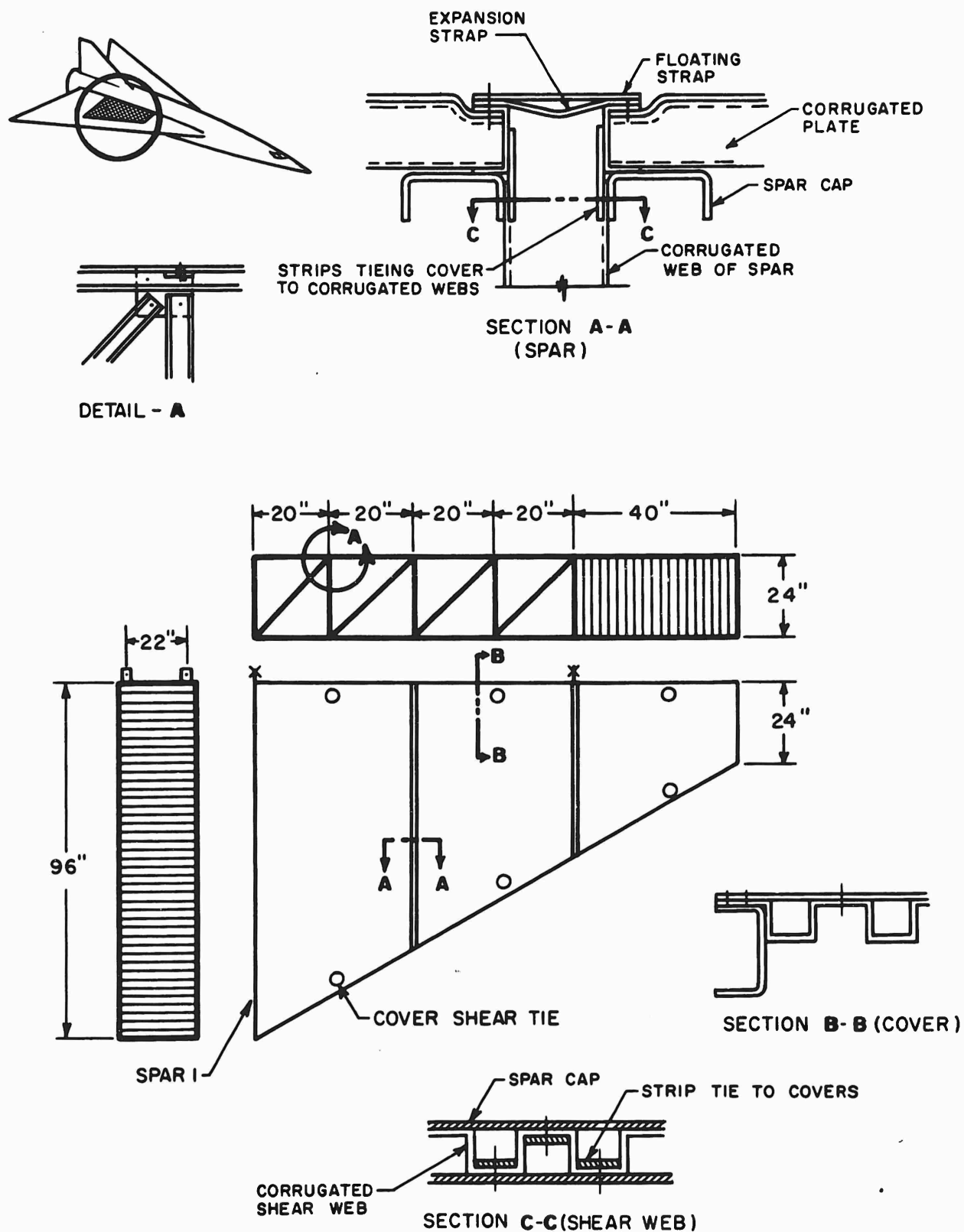
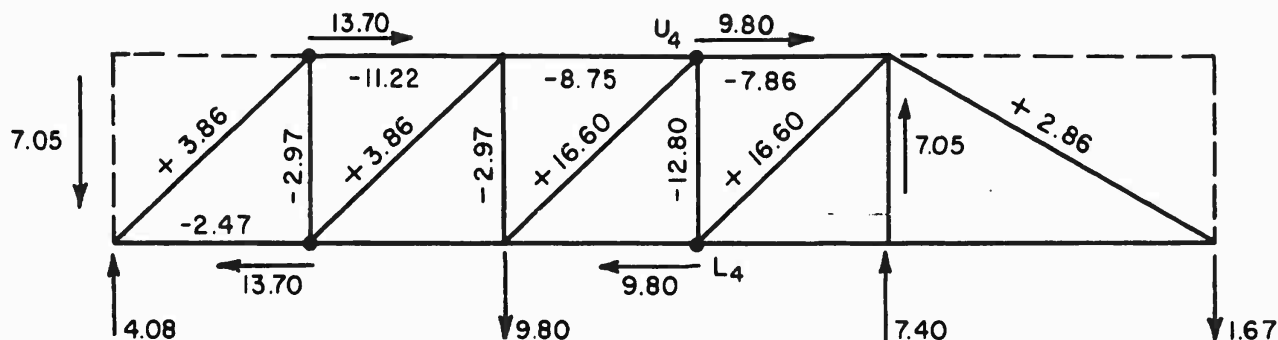


Figure 24. Wing Structure



In order to provide a reasonably representative spectrum of flight experiences upon which to base the design technique demonstration, two orbital mission profiles have been delineated. Each profile defines a possible history of exit from and reentry to the sensible atmosphere but is significantly different during both exit and reentry phases in respect to the speed-altitude-time relationship. Basically, the flight patterns assumed are compatible with the concept of a vehicle having aerodynamic lift and maneuver capabilities derived from highly swept wing surfaces. The exit profiles adopted show the differences in mechanical and heat loading experiences which can exist when the speed-altitude histories are such that in one case relatively high altitude is attained at relatively low speed (Mission 2) by the use of aerodynamic lift, whereas, in the other case (Mission 1) the speed-altitude history is characterized by significantly higher speed at any altitude. For the reentry phase, Mission 2 represents a global range, lift modulated, flight path requiring approximately a two hour time lapse, whereas Mission 1 is based upon a constant high angle of attack equilibrium glide flight path for which the time from reentry initiation is one hour.

The results of this study can then be represented on graphs which depict the pressure and temperature histories of each element. A conservative step history, in which the temperature and pressure is never less than the actual, is then employed to design the structure with a finite number of loading conditions. The time intervals are selected so as to be large in regions of temperature and load which will not significantly affect the design and to be small in regions of significant temperature or load. The technique is illustrated for Mission 1 in Figures 25a and 25b. The design loading conditions for Missions 1 and 2 are summarized in Tables 10A and 10B for the lower cover and the lower and upper cap materials. The temperature of the upper cap was estimated to be approximately 85 percent of the temperature of the lower cap.

The value of  $r$  represents the ratio of the load (or stress) in a given time interval to the load (or stress) in the interval which would determine the short-time strength. This is determined by examining the load and temperature intervals and the available materials (chosen so that they do not depreciate appreciably in the required thermal environment). The reference condition ( $r = 1$ ) for Mission 1 is characterized by a very high loading at a moderate temperature (exit). Relatively low loadings exist at the higher temperatures (reentry). The reference condition for Mission 2 is characterized by a relatively high load at a relatively high temperature during reentry.

#### 4. MATERIAL SELECTION

A survey of the temperature and the load ratios on the lower covers and caps indicated that the refractory materials (TZM molybdenum and FS-85 columbium) would be satisfactory but that the superalloys (René 41, etc.) would be unsatisfactory because of poor creep strength at the exposure temperatures. Preliminary calculations, employing Figure 3b, indicated that a René 41 lower cap designed for extremely low stresses would still creep excessively with each mission. Thus the design of the lower cap in René 41 would be much heavier than a design in TZM or FS-85.

The refractory alloys TZM and FS-85 did not indicate any significant tendency to creep even when the maximum stress became two-thirds of the ultimate stress at the designing temperature (Figure 26). The creep was calculated with the aid of Figures 2 and 3b by assuming a maximum stress; computing the stress, creep rate, and incremental creep strains for each time interval; and accumulating these creep strains to obtain the total creep strain.

TZM, FS-85 or René 41 can be employed in the upper caps even though the creep of the René 41 is not insignificant. A plot of the creep per mission (of an upper cap of René 41) as a ratio of the maximum stress to the ultimate stress is shown in Figure 27. The design of the upper spar cap in René 41 indicates that the minimum weight design for 100 missions is determined by the stability (F.S. = 1.5) of the cap while it can be determined by the creep allowable (F.S. = 1.1) for 200 missions.

The materials considered do not exhaust the possibilities; although they represent the extent of material data readily available to the author and serve to illustrate the design technique.

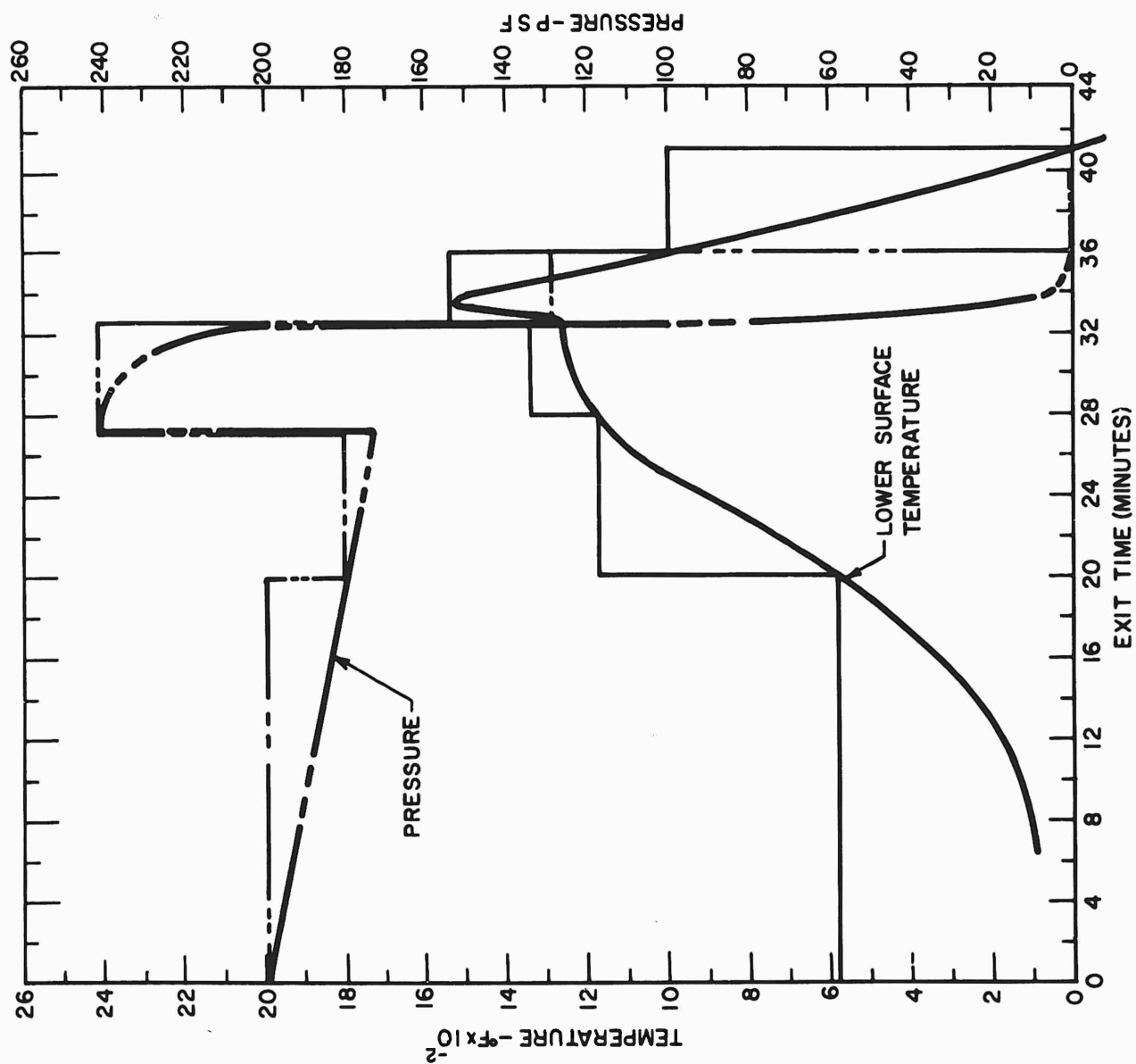


Figure 25a. Pressure - Temperature History - Mission 1 Exit

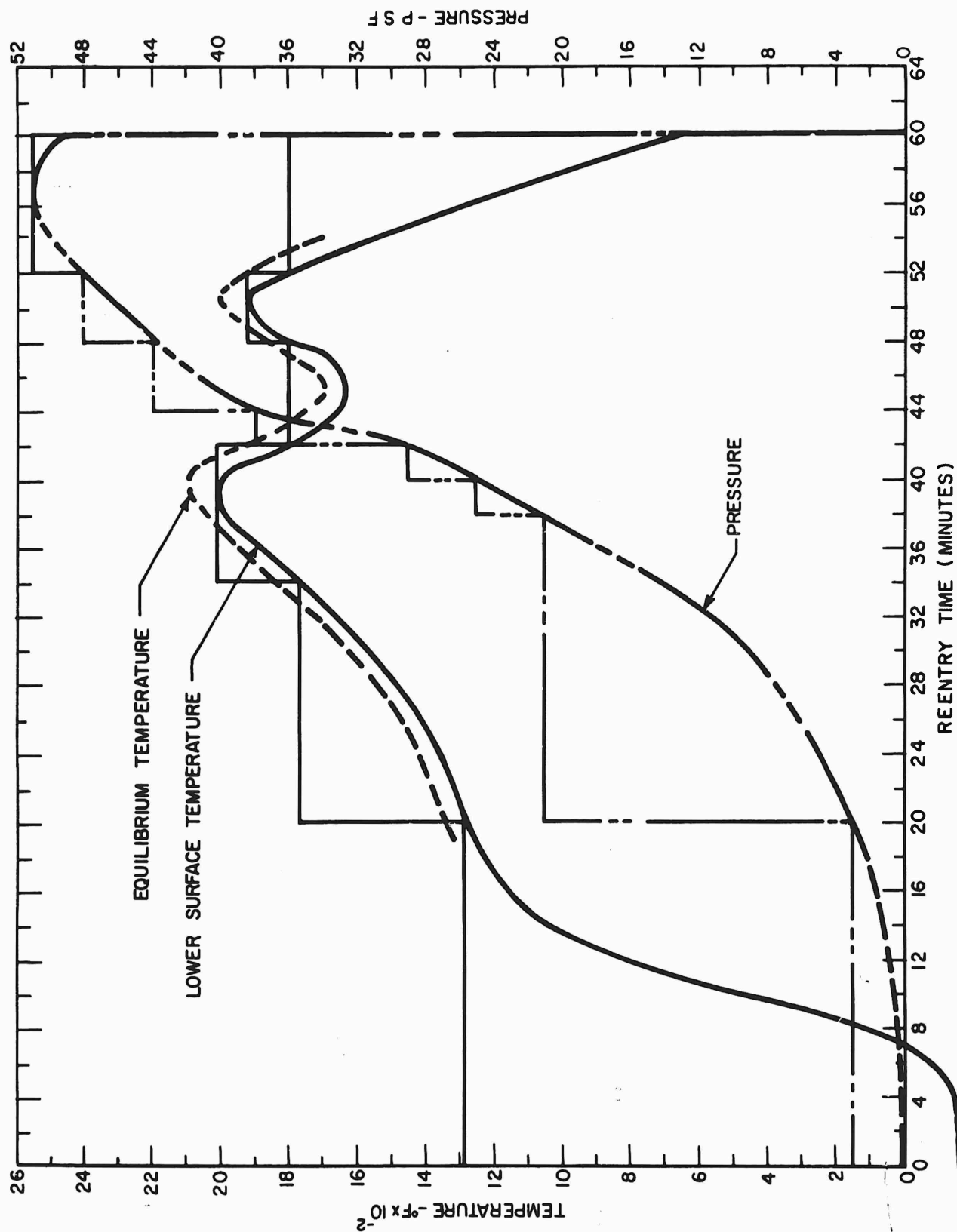


Figure 25b. Pressure - Temperature History - Mission 1 Reentry

TABLE 10A - TEMPERATURE-TIME HISTORY FOR MISSION 1

TIME INCREMENT	TEMPERATURE			PRESSURE	
Hrs.	Bottom Cover °F	Bottom Cap °F	Top Cap °F	q psf	r
<u>EXIT</u>					
.333	580	500	425	199	.826
.117	1175	1050	893	180	.747
.0167	1175	1050	893	241	1.000
.075	1340	1240	1054	241	1.000
.0583	1540	1320	1122	128	.531
.0833	1000	840	714	-	-
<u>REENTRY</u>					
.333	1295	1200	1020	3	.0124
.233	1760	1700	1445	21	.0871
.0667	2010	1890	1607	21	.0871
.0333	2010	1950	1658	25	.104
.0333	2010	1950	1658	29	.120
.0333	1800	1720	1462	38	.158
.0667	1800	1720	1462	44	.183
.0667	1920	1800	1530	48	.199
.133	1800	1700	1445	51	.212

TABLE 10B - TEMPERATURE-LOAD HISTORY FOR MISSION 2

TIME INCREMENT	TEMPERATURE			PRESSURE	
Hrs.	Bottom Cover °F	Bottom Cap °F	Top Cap °F	q psf	r
<u>EXIT</u>					
.067	400	400	340	100	1.053
.067	1270	960	816	100	1.053
.067	1770	1610	1369	95	1.000
.067	1770	1610	1369	76	.8
.067	1770	1610	1369	58	.611
.067	1770	1610	1369	40	.421
.133	1640	1610	1369	27	.284
.133	1560	1510	1284	-	-
.067	1470	1420	1207	-	-
.067	1100	1100	935	-	-
.088	400	400	340	-	-
<u>REENTRY</u>					
.167	115	115	98	-	-
.1	1160	750	638	2.7	.0284
.083	830	750	638	2.7	.0284
.183	925	830	706	2.7	.0284
.183	1055	1020	867	2.7	.0284
.183	1315	1230	1046	5.4	.0568
.183	1530	1450	1233	5.4	.0568
.183	1835	1670	1420	11.0	.116
.55	1965	1780	1513	43.0	.453
.183	1660	1530	1301	59.9	.631



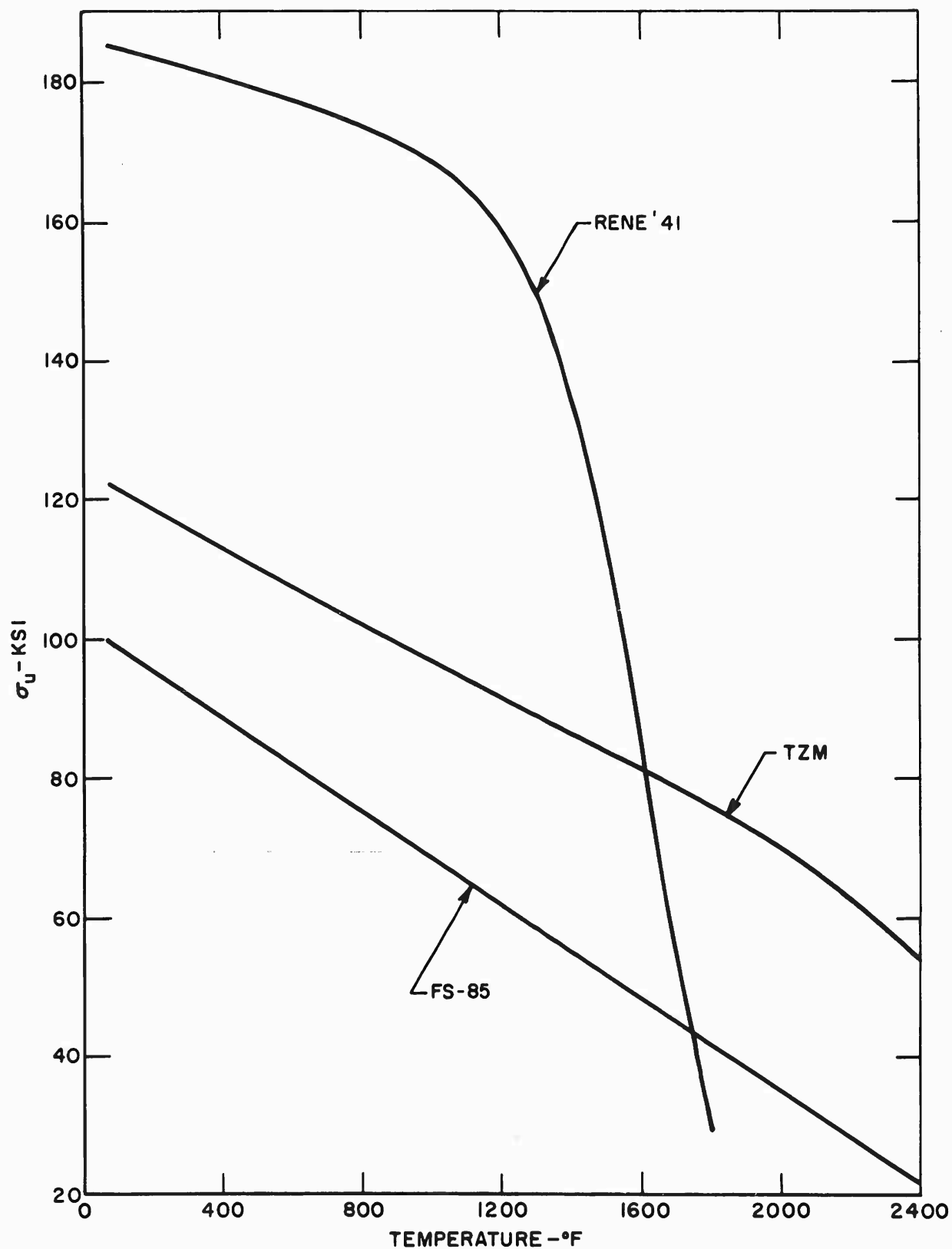


Figure 26. Ultimate Strength vs. Temperature

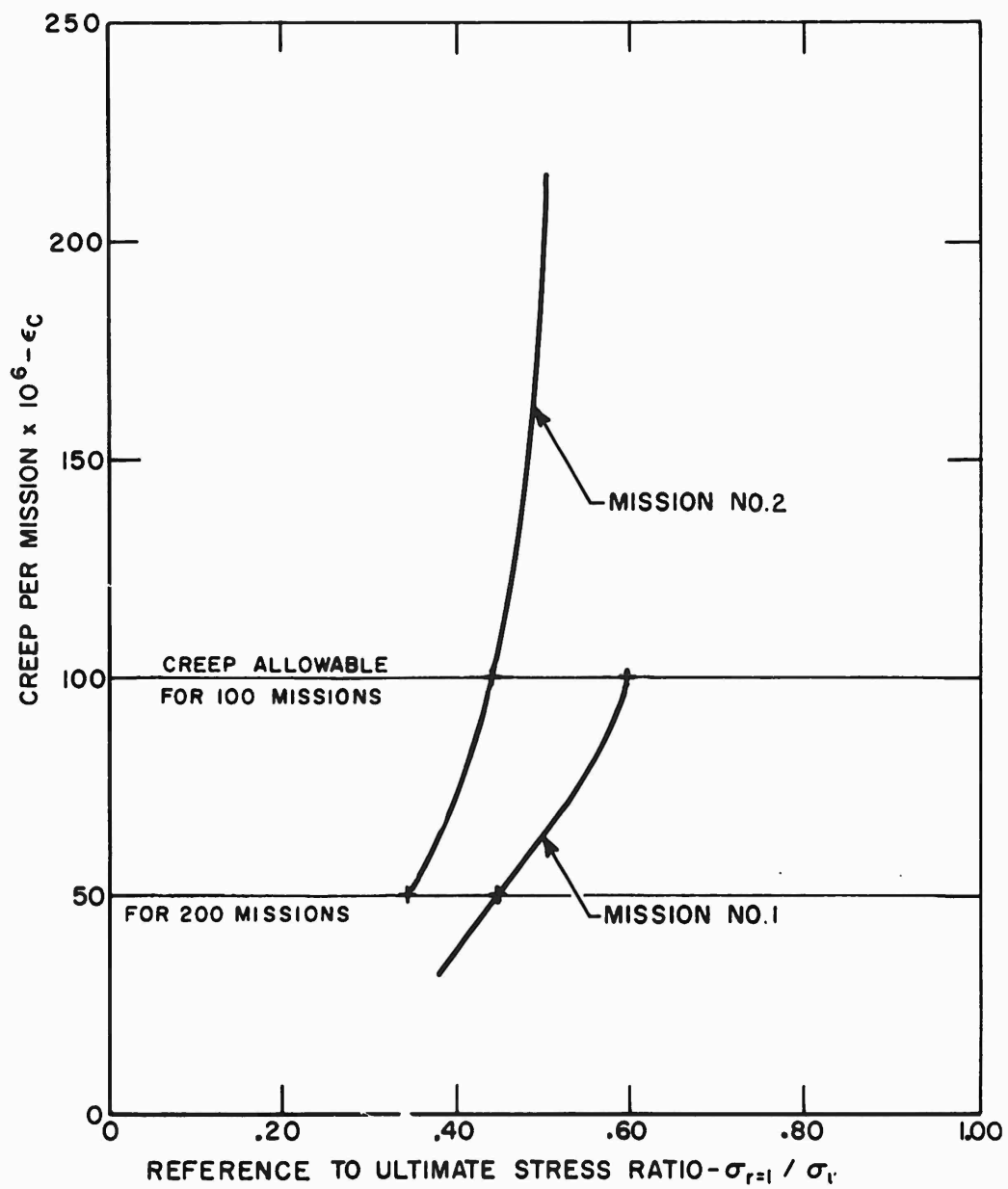


Figure 27. Creep of Upper Cap of Rene' 41

## 5. DESIGN OF STRUCTURAL COMPONENTS FOR MISSION 1

### a. Lower Cover

#### 1). Design Condition (Figure 24, Section B-B)

$$T = 1340^{\circ}\text{F}$$

$$M = 241 (1.39) = 336 \text{ in. lb/in. (Limit Load)}$$

$$= 504 \text{ in. lb/in. (Ultimate Load)}$$

#### 2). Material Data (Figures 1b and 26)

(1)	(2)	(3)	(4)	(5)	(6)	(7)	(8)	(9)
Mat'l	$\rho$	$E_A$ (Fig. 1b)	$\sigma_o$ (Fig. 1b)	$\log \beta$ (Fig. 1b)	$(\sigma/\sigma_o)_{opt}$ (Fig. 20)	$\sigma_{opt}$ (6) x (4)	$\sigma_u$ (Fig. 26)	$\sigma_c = \sigma_u / 4.55^*$
TZM	.369	39,000,000	7700	-3.1	7.5	57,800	89,000	19,600
FS-85	.380	19,000,000	3200	-6.1	13.5	43,200	57,000	12,500

$$* 4.55 = \frac{\alpha 6t}{\alpha 6c} = \frac{.82}{.18} \quad [\text{Ref. Eq. (A-8f)}]$$

#### 3). Design Configuration

As indicated in the Appendix, the single face corrugation with the face in compression ( $\theta = 90^{\circ}$ ,  $n = .815$ ,  $f = 4t$ ) is more efficient than a double faced corrugation, especially if the optimum stress is below the ultimate stress of the material. In addition, the double face corrugations will result in large deflections and in a thinner and smaller web which may become critical for the shear load which was not considered. The corrugation with no faces would usually be most efficient since  $\sigma_{opt}$  is generally greater than  $.37 \sigma_u$  (see Appendix) but cannot be employed since the cover must have a smooth exterior. It should be noted, however, that a single faced corrugation can resist only about 9 percent of the moment in the other direction [Eq. (A-10)].

The design of single face corrugations is simplified in the fact that the compressive stress is usually elastic which results in linear design equations ( $\xi_p = \sigma/\sigma_o$ ).

#### 4). Design

From Eq. (79a) and (79b) we have

$$d = \left[ \frac{\alpha_6 M}{\alpha_4 \sigma} \left( \frac{E_A C_t}{\xi_p \sigma_o} \right)^{1/2} \right]^{1/2} \sim \left( \frac{.18M}{.71} \frac{E_A^{1/2} C_t^{1/2}}{\sigma^{3/2}} \right)^{1/2} \quad (79a)$$

$$t = d \left( \frac{\xi_p \sigma_o}{C_t E_A} \right)^{1/2} \sim d \left( \frac{\sigma}{C_t E_A} \right)^{1/2} \quad (79b)$$

where

$$\left. \begin{array}{l} \alpha_6 = .18 \\ \alpha_4 = .710 \\ \alpha_1 = 6.225 \end{array} \right\} \text{(see Appendix )}$$

and

$$C_t = \frac{\pi^2 k}{12(1-\nu^2)} \text{ and is assumed equal to } \frac{\pi^2 24}{12(1-\nu^2)} \sim 21.72$$

The value of  $k = 24$  corresponds to a plate in pure bending. This is probably conservative for a plate in bending and tension (for which no stability constants could be found). Values of  $k$  for plates in bending and compression can be found in various texts (e.g., Table 36, Reference 1; Table 34, Reference 2; etc.).

Substituting in Eqs. (79a) and (79b) results in the following design for TZM:

$$d = 1.168$$

$$t = .00562$$

$$A = \alpha_1 t = .035$$

and

$$W = A\rho = .0129$$

The deflection of the beam can be obtained from the following equation:

$$\Delta = \frac{5}{48} \frac{\sigma}{E_A} \frac{l^2}{\alpha_6 d} = .398 \quad (\text{at ultimate load}) \quad (87a)$$

If the deflection is too large then the stress required to result in an acceptable deflection at ultimate load can be obtained by introducing Eq. (79a) into Eq. (87a) and by assuming that the compressive stress is elastic. Solving for the stress results in

$$\sigma = \left[ \frac{48 \Delta M^{1/2} E^{5/4} \alpha_6^{3/2}}{5 l^2 \alpha_4^{1/2}} \right]^{4/7} \quad (87b)$$

If the design has been completed and the deflection must be changed, then the following equations can be employed:

$$\sigma' = \sigma \left( \frac{\Delta'}{\Delta} \right)^{4/7} \quad (88a)$$

$$d' = d \left( \frac{\Delta'}{\Delta} \right)^{-3/7} \quad (88b)$$

$$t' = t \left( \frac{\Delta'}{\Delta} \right)^{2/7} \quad (88c)$$

$$A' = A \left( \frac{\Delta'}{\Delta} \right)^{2/7} \quad (88d)$$

and  $W' = W \left( \frac{\Delta'}{\Delta} \right)^{2/7} \quad (88e)$

where the primed terms refer to the desired deflection and geometry.

The design for FS-85 columbium utilizing Eqs. (79a) and (79b), results in

$$d = 1.361$$

$$t = .0075$$

$$A = .046$$

and  $W = .0175 > .0129$

Thus TZM is more efficient. This is to be expected since TZM has a higher modulus and allowable stress coupled with a lower density.

It is interesting to compare designs of the cover as a double face or single face corrugation in TZM. Utilizing the optimum stress of 57,800 psi corresponding to a  $\sigma/\sigma_0$  of 7.5, results in plastic stresses ( $\xi_p = 9.0 \neq 7.5$ ) and the following double face corrugation design:

$$d = .454 < 1.168$$

$$t = .0041 < .00562$$

$$A = 10.225 (.0041) = .042 > .035$$

and  $\Delta = 1.086 > .398$

Thus the double face corrugations weigh and deflect more than the single face. Space requirements or significant negative moments may, however, favor the double face corrugations.

b. Corrugated Spar Web (Figure 24, Section C-C)

1). Design Condition

$$T = 1240^{\circ}\text{F (Highest Temp. at Lower End)}$$

$$Q = 20.6 (241) = 4960\# \text{ limit}$$

$$= 7450\# \text{ ultimate}$$

2). Material Data (Figures 1b and 26)

Mat'l	$E_A$	$\sigma_o$	$\log \beta$	$\sigma_u$
TZM	40,300,000	7950	- 3.2	91,000
FS-85	19,400,000	3600	- 6.4	61,000

3). Design Configuration

A square corrugation ( $n = 1, \theta = 90^{\circ}$ ) was employed because of fabrication considerations. From Eqs. (46a through e) the following geometric constants are obtained:

$$a_{10} = 2$$

$$a_{40} = .333$$

$$a_{50} = .083$$

$$a_{80} = 1.000$$

$$a_{90} = .765$$

$$a_7 = f/t = 0$$

$$b = 22 \text{ in.}$$

and  $C_t = \frac{\pi^2}{12(1-\nu^2)} \quad (5.34) = 4.83 \quad (\text{Eq. 735 of Reference 2})$

#### 4). Design

From Eq. (44b) we have

$$\bar{P} = \frac{Q \sqrt{3}}{b^2 \sigma_o a_8 a_9 \sin^{-7/4} \theta} \left( \frac{E_A C_t \sqrt{3}}{\sigma_o} \right)^{7/8} = \frac{\tau \sqrt{3}}{\sigma_o} \xi_s^{7/8} = \frac{\sigma}{\sigma_o} \xi_s^{7/8}$$

Substituting the appropriate values for TZM molybdenum gives

$$\bar{P} = 49.3$$

which results in

$$\sigma / \sigma_o = 7.8 \quad (\text{Figure 11})$$

$$\text{and } \xi_s = 8.4 \quad (\text{Figure 12})$$

This indicates that the minimum weight design will result in a slightly plastic stress. As a check,

$$(8.4)^{7/8} (7.8) = 50 \text{ vs. } 49.3 = \bar{P} \quad (\text{slightly high but satisfactory})$$

$$\therefore \sigma = 7.8 (7950) = 62,000$$

From Eqs. (48a) we obtain

$$t = b a_9 \left( \frac{\xi_s \sigma_o}{E_A C_t \sqrt{3}} \right)^{7/8} = .0093$$

As a check,

$$\sigma t = 576 \text{ vs. } 582 = \frac{Q \sqrt{3}}{b}$$

$$d = t \left( \frac{E_A C_t \sqrt{3}}{\sigma_o \xi_s} \right)^{1/2} = .681$$

$$A = a_{10} t = .0186$$

$$W = A \rho = .00687$$

Similarly, for FS-85 columbium:

$$\bar{P} = 115 \quad (\text{Eq. 44b})$$

$$\sigma / \sigma_0 = 12.6 \quad (\text{Figure 11})$$

$$\xi_s = 12.6 \quad (\text{Figure 12})$$

∴ The design stress is elastic.

$$\text{As a check, } (12.6)^{15/8} = 115 \text{ vs } 115 = \bar{P}$$

The details of the design are

$$\sigma = 45,200$$

$$t = .0130 \quad (\text{Eq. 48a})$$

$$\text{As a check, } \sigma t = 586 \text{ vs. } 582 = \frac{Q \sqrt{3}}{b}$$

$$d = .770 \quad (\text{Eq. 48b})$$

$$A = .026$$

$$W = .00988 > .00687$$

∴ TZM is more efficient.

If the area had to be modified by the factor  $x = \sigma' / \sigma$ , then in order to maintain the thickness ratio relationship of Eq. (43)  $\left[ \frac{t}{b} = a_9 \left( \frac{t}{d} \right)^{7/4} \right]$ , we obtain

$$t' = x t \quad (89a)$$

$$d' = x^{-3/7} d \quad (89b)$$

$$A' = x A \quad (89c)$$

$$W' = x W \quad (89d)$$



c. Vertical Truss Member ( $U_4 - L_4$ , Fig. 24)

1). Design Conditions

$$T = 1240^\circ\text{F} \text{ (Highest Temperature at Lower End)}$$

$$P = 12.80 (241) = 3090\# \text{ Limit} \\ = 4630\# \text{ Ultimate}$$

2). Material Data

The material properties are the same as those tabulated in Paragraph b.2) above.

3). Design Configuration

A bent up channel ( $t = h$ ) was employed because of ease of procurement and fabrication. The column was assumed to be able to buckle only in the plane of the truss because of the out-of-plane support supplied by the spar. The ends were assumed to be pinned. From Table 1, and the given geometry and boundary conditions, we obtain

$$\begin{aligned} b &= 22 & C_t &= .362 \\ \alpha_1 &= 1.333 & C_c &= \pi^2 \\ \alpha_3 &= .167 & C_d &= C_c \left( \frac{\alpha_3}{\alpha_1} \right) = 1.23 \\ C_h &= .388 & w &= z(t/h)d = .167 d \end{aligned}$$

4). Design

From Eq. (11a) we obtain

$$\bar{P} = \frac{P}{b^2 \sigma_o} \left( \frac{E_A}{\sigma_o} \right)^{3/2} \left( \frac{\alpha_3}{\alpha_1} \right) C_c \sqrt{C_t} = 760$$

From Figures 4, 5 and 6 we obtain

$$\sigma / \sigma_o = 8.6 \text{ (Figure 6) and } \sigma = 68,500$$

$$\xi_p = 12.0 \text{ (Figure 5)}$$

$$\xi_c = 24.0 \text{ (Figure 4)}$$

As a check,  $\frac{\sigma}{\sigma_0} \xi_c \xi_p^{1/2} = 719 \text{ vs. } 760 = \bar{P}$

The value of  $\xi_c$  is difficult to read accurately in Figure 4 because  $\log \beta$  is not a negative integer. A better estimate of the value of  $\xi_c$  is obtained from  $\xi_c = \frac{\bar{P}}{\frac{\sigma}{\sigma_0} (\xi_p)^{1/2}}$

$= 25.4$ . A readjustment of  $\sigma/\sigma_0$  and  $\xi_p$  is not indicated because of the small change in  $\xi_c$ .

Employing Eqs. (3), (13d), (11c), and (7a) results in

$$d = 1.41 \quad (\text{Eq. 3})$$

$$w = .235 \quad (\text{Eq. 13d})$$

$$t = .0361 \quad (\text{Eq. 11c})$$

As a check,  $A = a_1 dt = (1.333) (1.41) (.0361) = .0679 \text{ vs. } .0676 = \frac{4630}{8.6(7950)} = P/\sigma$   
 $W = A\rho = .0025$

Similarly, for FS-85 columbium

$$\bar{P} = 1850 \quad (\text{Eq. 11a})$$

$$\sigma/\sigma_0 = 15.3 \quad (\text{Figure 6}) \text{ and } \sigma = 55,200$$

$$\xi_p = 18 \quad (\text{Figure 5})$$

$$\xi_c = 28 \quad (\text{Figure 4})$$

As a check,  $\frac{\sigma}{\sigma_0} \xi_c \xi_p^{1/2} = 1820 \text{ vs. } 1850 = \bar{P}$

$$\therefore d = 1.43 \quad (\text{Eq. 3})$$

$$w = .238 \quad (\text{Eq. 13d})$$

$$t = .0435 \quad (\text{Eq. 11c})$$

As a check,  $A = \alpha_1 dt = .0831$  vs.  $.0840 = \frac{4630}{55,200} = P/\sigma$

$W = A\rho = .00316 > .0025$

∴ TzM is more efficient.

d. Spar Cap (Figure 24, Section A-A; Note: Cap of Spar #1 is a single channel)

1). Design Condition

$T = 1054^\circ\text{F}$

$P_{\text{Root}} = (81.9)(241) = 19,650\# \text{ limit}$

$= 29,500\# \text{ ultimate}$

where the load P increases parabolically due to a uniform load on the beam.

2). Material Data (Figures 1b and 26)

Mat'l	$E_A$	$\sigma_o$	$\log \beta$	$\sigma_u$
TZM	42,500,000	8000	- 3.4	96,000
Rene' 41	24,500,000	5600	- 9.4	167,000

3). Design Configuration

A shallow bent-up channel was employed because of ease of procurement and fabrication and also to minimize thermal stresses due to thermal gradients. To illustrate the design technique it was decided to design the spar caps so they would not have any tendency to buckle in a plane parallel to the covers. The spar caps can deflect to a limited degree in this direction before introducing any significant loads in the corrugation webs and covers. Excessive lateral deflections would introduce loads which were not considered in the design of the corrugations. The spar cap cannot buckle in the plane of the web because of the planar stiffness of the web.

The geometry constants are

$b = 96 \text{ in.}$

$\alpha_1 = 1.333$

$\alpha_3 = .167$

$C_h = .388$

$$C_t = 3.62$$

$$C_c = 27.3$$

[Table 14 of Reference 1 for a fixed-free column of constant cross section with a parabolically increasing load.]

$$C_d = C_c \left( \frac{\alpha_3}{\alpha_1} \right) = 3.42$$

$$w = z (t/h) d = .167 d$$

For TZM,

$$\bar{P} = 755 \quad (\text{Eq. 11a})$$

$$\sigma/\sigma_o = 9.1 \quad (\text{Figure 6})$$

$$\xi_c = 23.5 \quad (\text{Figure 4})$$

$$\xi_p = 12.5 \quad (\text{Figure 5})$$

$$\text{As a check, } (\sigma/\sigma_o) \xi_c \xi_p^{1/2} = 757 \text{ vs. } 755 = \bar{P}$$

$$\sigma = (\sigma/\sigma_o) \sigma_o = 72800$$

$$d = 3.45 \quad (\text{Eq. 3})$$

$$t = .088 \quad (\text{Eq. 11c})$$

$$\text{As a check, } A = \alpha_1 dt = .405 \text{ vs. } .405 = \frac{29,500}{72,800} = P/\sigma$$

$$W = .1491$$

For René 41,

$$\bar{P} = 309 \quad (\text{Eq. 11a})$$

$$\frac{\sigma}{\sigma_o} = \xi_c = \xi_p = 14.6 \text{ elastic} \quad (\text{Figures 4, 5, and 6})$$

As a check,  $\frac{\sigma}{\sigma_0} \xi_c \xi_p^{1/2} = (14.6)^{5/2} = 809 \text{ vs. } 809 = P$

$$\sigma = 81,800$$

$$d = 3.00 \quad (\text{Eq. 3})$$

$$w = .50 \quad (\text{Eq. 13d})$$

$$t = .091 \quad (\text{Eq. 11c})$$

As a check  $A = a_1 dt = .364 \text{ vs. } .361 = \frac{29,500}{81,800} = P/\sigma$

$$W = A\rho = .1043 < .1491$$

∴ René 41 is more efficient for a single mission.

An analysis of the deterioration and creep data (Figures 3 and 27) of René 41 results in the following allowables:

	Number of Missions		
	1 (.0894 hr. at 1658°F)‡	100 (8.94 hrs. at 1658°F)‡	200 (17.88 hrs. at 1658°F)‡
Short-Time ‡ Strength - psi (F.S. = 1.5)	111,500	86,400	82,500
Creep Strength ( $\epsilon_c \leq .01$ ) - psi (F.S. = 1.1)	-	91,500**	<span style="border: 1px solid black;">67,600</span> **
Stability - psi (F.S. = 1.5)	<span style="border: 1px solid black;">81,800</span>	<span style="border: 1px solid black;">81,800</span> *	81,800 *

  Design condition

\* It is assumed that the deterioration does not cause the stability stress to become significantly plastic.

‡ The environmental history of each mission (Table 10A) is equivalent to .0894 hour at 1658°F. This is computed by converting each interval to an equivalent time at the reference temperature which would result in the same Larson-Miller Parameter. The deterioration is then obtained from Figure 3a.

\*\* (167,000/F.S.) ( $\sigma/\sigma_u$ ) of Figure 27.

If the spar cap is to be designed for 100 missions or less, then the design described above is the most efficient. For 200 missions, however, the area must be increased by the ratio

$$x = \frac{81,800}{67,600} = 1.21$$

For a column, the maintenance of thickness ratios is defined by Eqs. (86a, b, and c) and results in

$$d' = x^{1/3} d = 3.196 \quad (90a)$$

$$t' = x^{2/3} t = .103 \quad (90b)$$

$$A' = x A = 0.440 \quad (90c)$$

$$W' = x W = .1261 < .1491 \quad (90d)$$

∴ René 41 is still the more efficient material for 200 missions.

## 6. DESIGN OF STRUCTURAL COMPONENTS FOR MISSION 2

Mission 2 can be analyzed in a similar manner. It is obvious, however, that the TZM molybdenum will be more efficient than FS-85 for the lower structural elements (because the modulus and strength is higher and the density is lower than FS-85) while TZM and René 41 should be considered for the upper structural elements.

### a. Lower Cover in TZM

For T = 1770°F

$$M = (1.5) (95) (139) = 198 \text{ in. \#/in. ultimate}$$

$$E_A = 33,000,000 \quad (\text{Figure 1b})$$

$$\sigma_o = 6,700 \quad (\text{Figure 1b})$$

$$\log \beta = -3.0 \quad (\text{Figure 1b})$$

$$\sigma_u = 77,000 \quad (\text{Figure 26})$$

For a single face corrugation ( $\theta = 90^\circ$ ,  $n = .815$ , and  $f = 4t$ ), we obtain from the appropriate equations

$$\sigma_c = 77,000/4.55 = 16,900$$

$$d = .785 \quad (\text{Eq. 79a})$$

$$t = .00378 \quad (\text{Eq. 79b})$$

$$\Delta = .606 \quad (\text{Eq. 87a})$$

If we wish to restrict our deflection at ultimate load to a maximum of .4 inch, we modify our design by the use of Eqs. (88).

$$\therefore \sigma' = \left( \frac{.4}{.606} \right)^{4/7} 16,900 = 13,350$$

$$d' = (.661)^{-3/7} .785 = .938$$

$$t' = (.661)^{2/7} .00378 = .00366$$

b. Corrugation Web in TZM

$$\text{For } T = 1610^\circ\text{F}$$

$$Q = (1.5) (95) (20.6) = 2940\# \text{ ultimate}$$

$$E_A = 35,000,000 \quad (\text{Figure 1b})$$

$$\sigma_o = 7200 \quad (\text{Figure 1b})$$

$$\log \beta = -3.0 \quad (\text{Figure 1b})$$

$$\sigma_u = 81,000 \quad (\text{Figure 26})$$

we obtain for a corrugated web ( $\theta = 90^\circ$ ,  $n = 1.0$ ).

$$\bar{P} = 20.7 \quad (\text{Eq. 44b})$$

$$\frac{\sigma}{\sigma_o} = \xi_s = 5.05 \quad (\text{Figures 11 and 12})$$

As a check,  $\frac{\sigma}{\sigma_o} \xi_s^{7/8} = (5.05)^{15/8} = 20.7 \text{ vs } 20.7 = \bar{P}$

$$t = b a_9 \left[ \frac{\xi_s \sigma_o}{E_A C_t \sqrt{3}} \right]^{7/8} = .0064 \quad (\text{Eq. 48a})$$

As a check,  $\sigma t = 232 \text{ vs. } 231 = \frac{Q\sqrt{3}}{b}$

$$d = t \left( \frac{E_A C_t \sqrt{3}}{\sigma_o \xi_s} \right)^{1/2} = .570 \quad (\text{Eq. 48b})$$

c. Vertical Truss Member  $U_4 - L_4$  in TZM

For  $T = 1610^\circ\text{F}$

$$P = (1.5) (95) (12.80) = 1825\# \text{ ultimate}$$

and the same material properties reported in b above, we obtained for a bent-up channel

$$\bar{P} = 311 \quad (\text{Eq. 11a})$$

$$\frac{\sigma}{\sigma_o} = 7.5 \quad (\text{Figure 6})$$

$$\sigma = 54,000$$

$$\xi_c = 14 \quad (\text{Figure 4})$$

$$\xi_p = 9.3 \quad (\text{Figure 5})$$

As a check,  $(\sigma/\sigma_o) \xi_c \xi_p^{1/2} = 319 \text{ vs. } 311 = \bar{P}$

with resulting detail geometry

$$d = b \left( \frac{\xi_c \sigma_o}{C_d E_A} \right)^{1/2} = 1.06 \quad (\text{Eq. 3})$$



$$t = d \left( \frac{\xi_p \sigma_o}{C_t E_A} \right)^{1/2} = .0243 \quad (\text{Eq. 11c})$$

As a check,  $A = \alpha_1 t d = .0344$  vs.  $.0336 = \frac{1825}{54,000} = P/\sigma$

modifying the value of  $\xi_c$  results in a better agreement:

$$\xi_c' = \left( \frac{311}{319} \right) 14 = 13.6$$

$$d' = 1.045 \quad (\text{Eq. 3})$$

$$t' = .0239 \quad (\text{Eq. 11c})$$

and  $A' = \alpha_1 d' t' = .0334$  vs.  $.0336 = P/\sigma$

d. Spar Cap

For  $T = 1370^\circ\text{F}$

$$P = (1.5) (81.9) (95) = 11,680\# \text{ ultimate}$$

and the following material properties (Figures 1b and 26).

Mat'l	$E_A$	$\sigma_o$	$\log \beta$	$\sigma_u$
TZM	39,000,000	7600	- 3.1	87,000
Rene' 41	20,500,000	6500	- 6.5	140,000

For TZM

$$\bar{P} = 286 \quad (\text{Eq. 11a})$$

$$\frac{\sigma}{\sigma_o} = 7.5 \quad (\text{Figure 6})$$

$$\xi_c = 13.0 \quad (\text{Figure 4})$$

$$\xi_p = 9.0 \quad (\text{Figure 5})$$

As a check,  $(\sigma/\sigma_o) \xi_c \xi_p^{1/2} = 292 \text{ vs. } 286 = \bar{P}$

$$\sigma = 57,000$$

$$d = 2.62 \quad (\text{Eq. 3})$$

$$t = .0576 \quad (\text{Eq. 11c})$$

As a check,  $A = \alpha_1 dt = .202 \text{ vs. } .205 = \frac{11,680}{57,000} = P/\sigma$

$$W = A\rho = .0755$$

For René 41

$$\bar{P} = 169 \quad (\text{Eq. 11a})$$

$$\frac{\sigma}{\sigma_o} = \xi_c = \xi_p = 7.8 \quad (\text{Figures 4, 5, and 6})$$

As a check,  $(\sigma/\sigma_o) \xi_c \xi_p^{1/2} = (7.8)^{5/2} = 169 \text{ vs } 169 = \bar{P}$

$$\sigma = 50,600$$

$$d = 2.58 \quad (\text{Eq. 3})$$

$$t = .0674 \quad (\text{Eq. 11c})$$

As a check,  $A = \alpha_1 dt = .232 \text{ vs. } .231 = \frac{11,680}{50,600} = P/\sigma$

$$W = A\rho = .0668 < .0755 \quad (\text{René 41 more efficient for one mission}).$$

An analysis of the deterioration and creep data (Figures 3 and 27) of René 41 results in the following allowables.

	Number of Missions		
	1 (.571 hr. at 1513°F) ‡	100 (57.1 hrs. at 1513°F) ‡	200 (114.2 hrs. at 1513°F) ‡
Short-Time ‡ Strength - psi (F.S. = 1.5)	93,500	83,500	80,500
Creep Strength ( $\epsilon_c \leq .01$ ) - psi (F.S. = 1.1)	-	56,000 $\Delta$	43,200* $\Delta$
Stability	50,600	50,600*	50,600

□ Design Condition

‡ The environmental history of each mission (Table 10B) is equivalent to .571 hour at 1513°F. This is computed by converting each interval to an equivalent time at the reference temperature which would result in the same Larson-Miller Parameter. The deterioration is then obtained from Figure 3a.

\* For 100 missions or less, René 41 is more efficient. For 200 missions the TZM becomes more efficient since  $.0668 \left( \frac{50,600}{43,200} \right) = .0784 > .0755$ .

$\Delta$  (140,000/F.S.) ( $\sigma/\sigma_u$ ) of Figure 27.

## REFERENCES

1. Timoshenko, S., Theory of Elastic Stability, McGraw-Hill Book Co., Inc., 1936.
2. Bleich, F., Buckling Strength of Metal Structures, McGraw-Hill Book Co., Inc., 1952.
3. Stowell, E.Z., "A Unified Theory of Plastic Buckling of Columns and Plates," NACA Report 898, 1948.
4. Gerard, G. and Becker, H., "Buckling of Flat Plates," NACA TN 3781, July 1957.
5. Gerard, G. and Becker, H., "Buckling of Curved Plates and Shells," NACA TN 3783, August 1957.
6. Shanley, F.R., "Weight-Strength Analysis of Aircraft Structures," McGraw-Hill Book Co., Inc., 1952.
7. Switzky, H., Forray, M.J., and Newman, M., "Thermo-Structural Analysis Manual." WADD TR 60-517, Vol. I.
8. March, H.W. and Smith, C.B., "Buckling Loads of Flat Sandwich Panels in Compression. Various Type of Edge Conditions," Forest Products Laboratories Report No. 1525, March 1945.
9. Gerard, G., "Critical Shear Stress of Plates Above the Proportional Limit," Jour. Applied Mechanics, Vol. 15, No. 1, March 1948, pp. 7-12.
10. Anonymous - MIL-HDBK-5.
11. Favor, R.J., Deel, O.L., and Achback, W.P., "Design Information on 17-7PH Stainless Steel for Aircraft and Missiles," DMIC Report 137, September 1960.
12. Salvaggi, J., "Intermittent Stressing and Heating Tests on Aircraft Structural Metals," WADC TR 53-24, Part 4, May 1957.
13. Price, H.L. and Heimerl, G.J., "Tensile and Compressive Creep on 6Al-4V Titanium Alloy and Methods for Estimating the Minimum Creep Rate," NASA TN D-805, April 1961.
14. Lemcoe, M.M., and Trevino, A. Jr., "Determination of the Effects of Elevated Temperature on Material Properties of Several High Temperature Alloys," ASD TR 61-529, October 1961.

15. Shaver, C., "Investigation of the Mechanical Properties of René 41," Republic Aviation Corporation ESRMR 137, April 1962.
16. Brownfield, C.D. and Apodaca, R.D., "Effects of Severe Thermal and Stress Histories on Material Strength - Rate Process Theory Approach," ASD TR 61-194, August 1961.
17. Barr, R.Q. and Semchyshen, M., "Stress-Strain Curves for Wrought Molybdenum and Three Molybdenum-Base Alloys," Climax Molybdenum Company, December 1959.
18. "Technical Notes," Climax Molybdenum Company, February 1959.
19. "Data Sheets," Fansteel Metallurgical Corporation, FS-85.
20. Anderson, M.S., "Local Instability of the Elements of a Truss-Core Sandwich Plate," NACA TN 4292, July 1958.
21. Switzky, H., "The Design of Stable Structures," Republic Aviation Corporation Report No. ESAM-30, October 1958.
22. Epstein, A. and Hamilton, A.F., "Exit, Space and Reentry Structural Design Criteria," ASD TDR 62-641, July 1962.

## APPENDIX

## APPENDIX

### A. OPTIMUM GEOMETRY FOR CORRUGATIONS

The solution for the minimum weight design requires expressing the geometric properties of the cross section in terms of the web thickness and depth. Section II C2 defined the geometric properties of the cross section in terms of the corrugation angle ( $\theta$ ) and the flat ratio ( $n$ ) as well as the face thickness ( $f$ ), the web thickness ( $t$ ), and depth ( $d$ ). The determination of the variables  $n$  and  $\theta$  are often dictated by fabrication requirements (available dies, necessary bend radii and joining flats). In these cases it is a relatively simple matter to compute the geometric properties in terms of the web thickness and depth [eqs. (26), (31), (32), (46), (47) and (51)] by utilizing the requirement that the faces buckle simultaneously with the web. If the selection of  $\theta$  and/or  $n$  is left to the discretion of the designer, he has to employ additional relationships to determine the optimum area distribution. Panels in compression and shear are considered separately from corrugations in bending.

### B. CORRUGATED PANELS IN COMPRESSION OR SHEAR

For corrugations in compression or shear the value of  $n$  is usually made as small as possible consistent with fabrication requirements, even though the design equations would indicate that a large  $n$  is more efficient. This is done primarily to satisfy the assumptions that the flats are more stable than the webs and that the structure is sufficiently stiff in transverse shear to permit ignoring the shear energy of distortion. The applicability of the design equations is based upon the hypothesis that the corrugations can act in a manner similar to the sandwich core, but with a relatively large shear stiffness. Thus the corrugations must have an adequate axial stiffness to force nodes in the faces and a shear stiffness which will ensure that the value of

$$\left[ \text{approximately } 2 (1 + \nu) K \alpha_{42} \frac{P_{\text{crm}}/P_{\text{crs}} \text{ of Eq. (59)}}{\left( \frac{n \sin \theta + \cos \theta}{\sin \theta} \right) \left( \frac{d}{b} \right)^2} \right] \text{ for double faced}$$

corrugations] would be insignificant. Since the axial and shear stiffnesses of the corrugations decrease with increasing  $n$  and decreasing  $\theta$ , it is questionable whether the design equations presented in this report are satisfactory for large  $n$  or small  $\theta$ . Additional studies are recommended to derive more general minimum weight design procedures which will not limit the range of variations in the geometric parameters.

Assuming that  $n$  should be made as small as possible, it is still necessary to establish the value of  $\theta$  which will minimize the weight for given values of  $n$ . The technique employed is to express the weight of the corrugated structures with one, two, or no faces as a function of  $n$ ,  $\theta$ , and the stability parameter ( $\xi$ ). If the weight is to be a minimum, then the function must be stationary. The stability parameter, or the equivalent stability ratio ( $d/b$ ), should be stationary in order to maximize the

design stress (which minimizes the weight). If  $n$  is given, then the variation of the weight is proportional to the partial derivative of the weight function with respect to  $\theta$  times the variation in  $\theta$ , i. e.,

$$\delta W = \frac{\partial W}{\partial \theta} \delta \theta \quad (A-1)$$

Thus the weight of the structure would be a minimum when the variation of the weight with respect to the angle became stationary. In the cases investigated, the weight is directly proportional to a power of the thickness ratio and some complex function of  $n$  and  $\theta$ . Plotting this function for given values of  $n$  and variable  $\theta$  would indicate the value of  $\theta$  which will minimize the weight. The results of such an investigation are summarized in Figures A-1a and b and A-2a and b which present the optimum fabrication angle ( $\theta$ ) as a function of the flat ratio  $n$  for corrugation panels with one, two, or no faces in edge compression or shear and with relative edge fixity values of  $\sqrt{C_t/C_f} = 1$  or 1.14. The value of  $\sqrt{C_t/C_f} = 1.14$  was obtained from Figure 5a of Reference 20, for the value of  $(t_f/b_f)/(t_c/b_c) = 1/[2 \cos \theta (t_c/t_f)] \sim 1.14$  which indicated an equal stability of the corrugation and faces where the end fixities were calculated from the moment distribution at the junctions.

The technique for obtaining the weight function is indicated for a double faced corrugation in compression and summarized for the shear load and for the other types of configurations in compression or shear.

The weight per inch of structure is

$$W = Ab\rho = a_1 tb\rho \quad (A-2a)$$

Dividing by  $b^2\rho$  results in a nondimensional equation

$$\frac{W}{b^2\rho} = a_1 \left(\frac{t}{b}\right) = a_1 \left(\frac{t}{d}\right) \left(\frac{d}{b}\right) \quad (A-2b)$$

Equation (27c) can be manipulated to express  $t/d$  as a function of  $(d/b)$ , i. e.,

$$\frac{t}{d} = \left\{ \frac{K \left[ \left( \frac{a_4}{a_5} \right)^{1/2} + a_5 \right]}{a_1 \sin^2 \theta} \right\}^{1/2} \left( \frac{d}{b} \right)$$



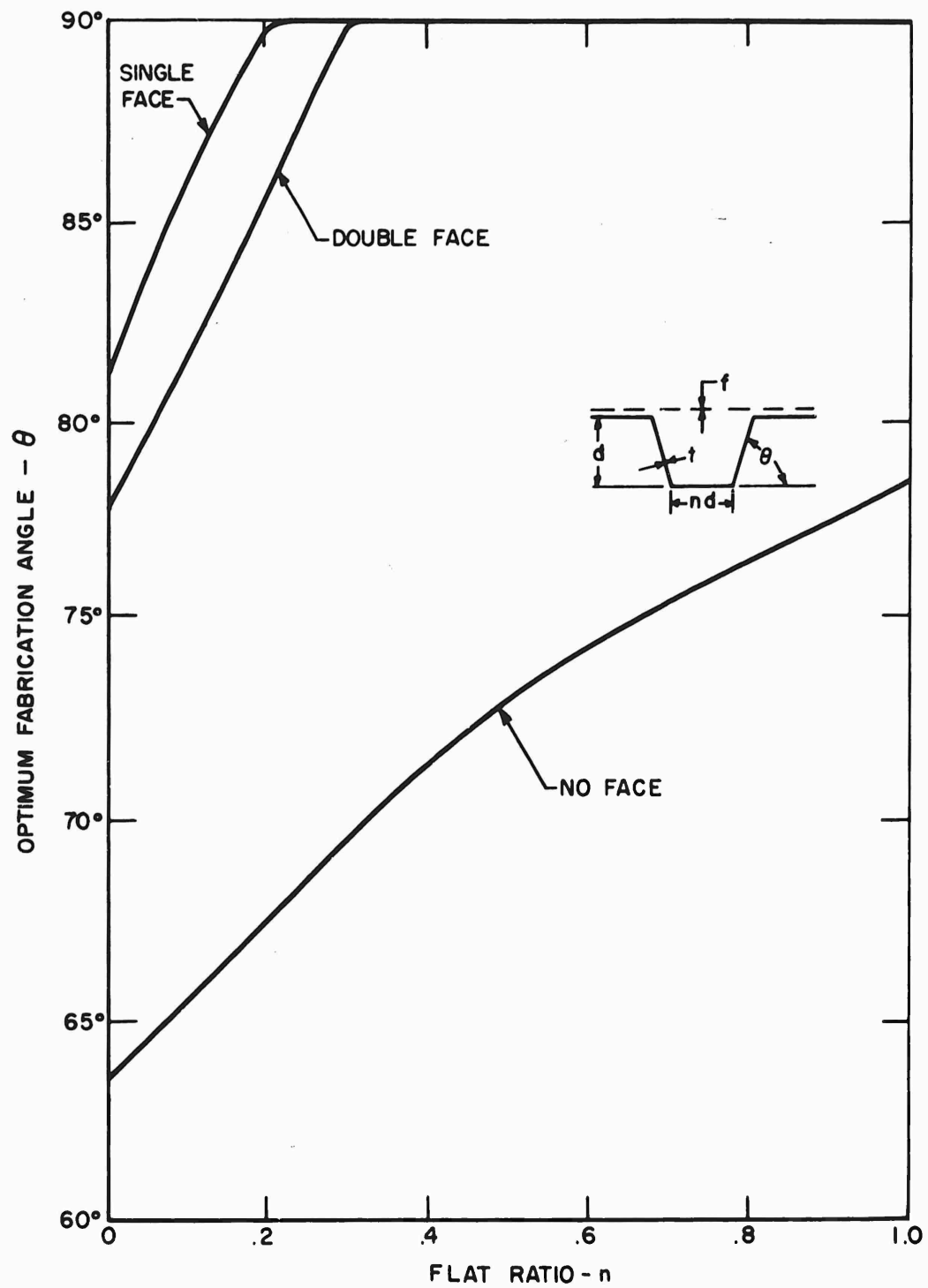


Figure A-1a. Optimum Fabrication Angle for Corrugation Panels in Compression ( $\sqrt{C_t/C_f} = 1$ )

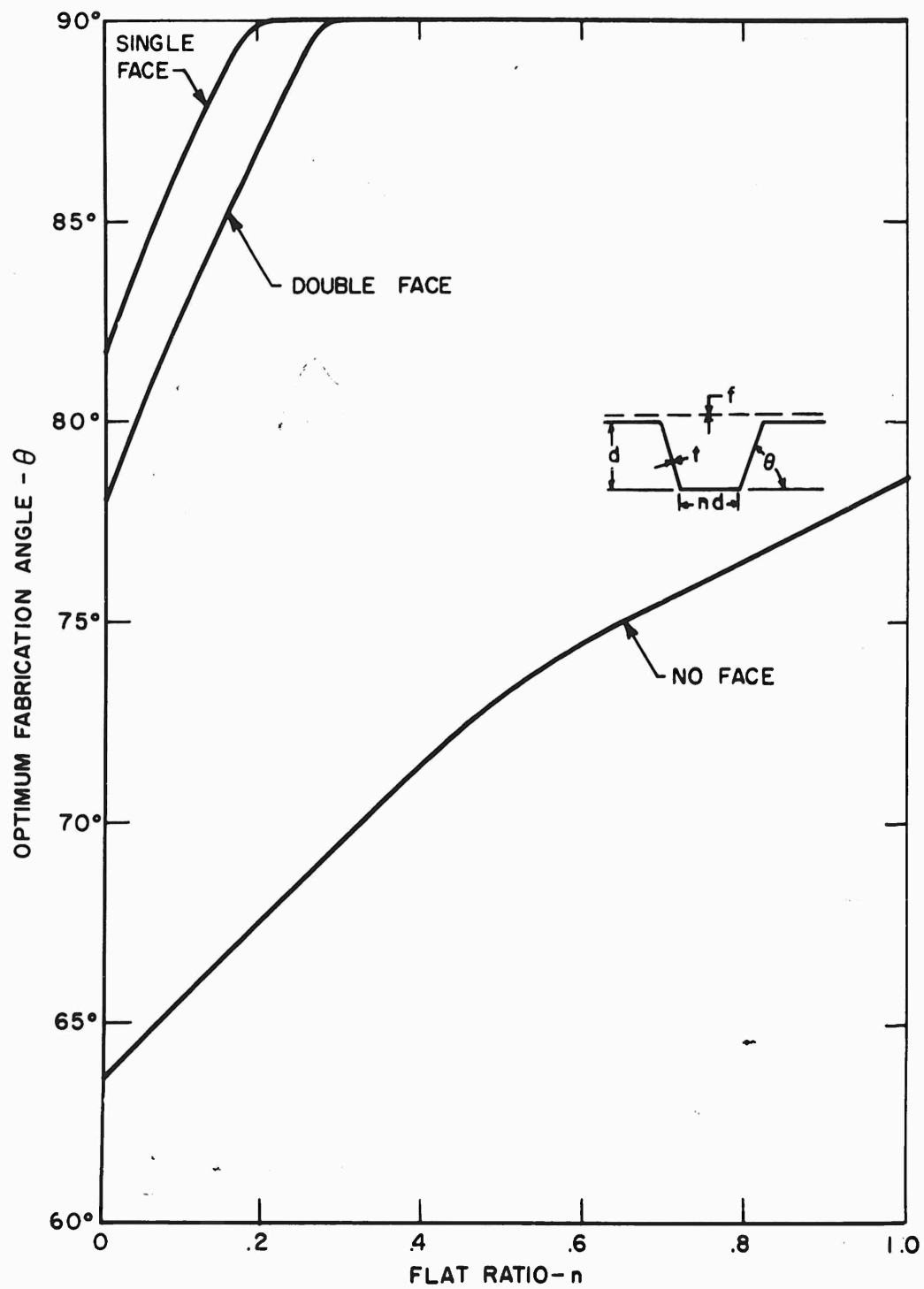


Figure A-1b. Optimum Fabrication Angle for Corrugation Panels in Compression ( $\sqrt{C_t/C_f} = 1.14$ )

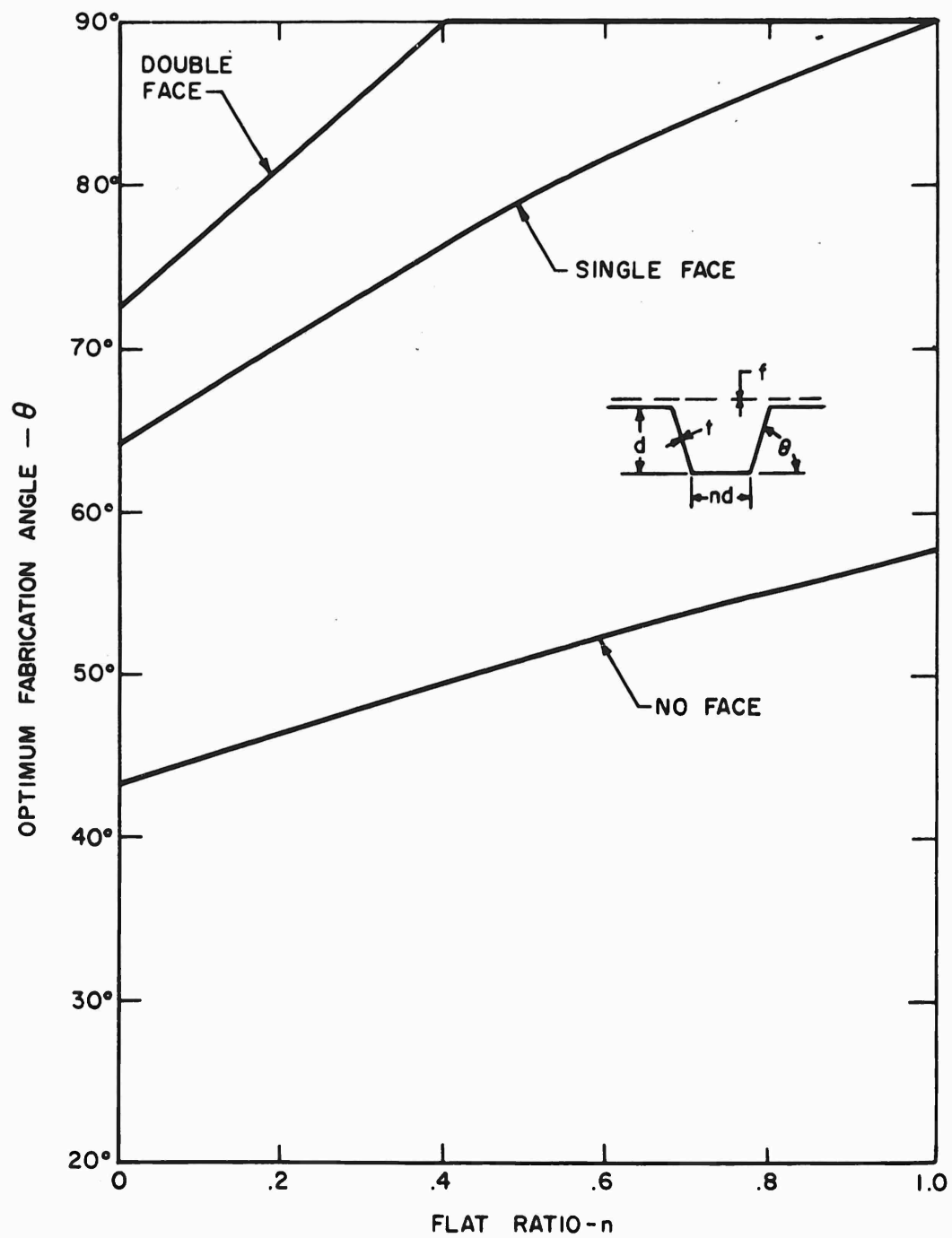


Figure A-2a. Optimum Fabrication Angle for Corrugation Panels in Shear ( $\sqrt{C_t/C_f} = 1$ )

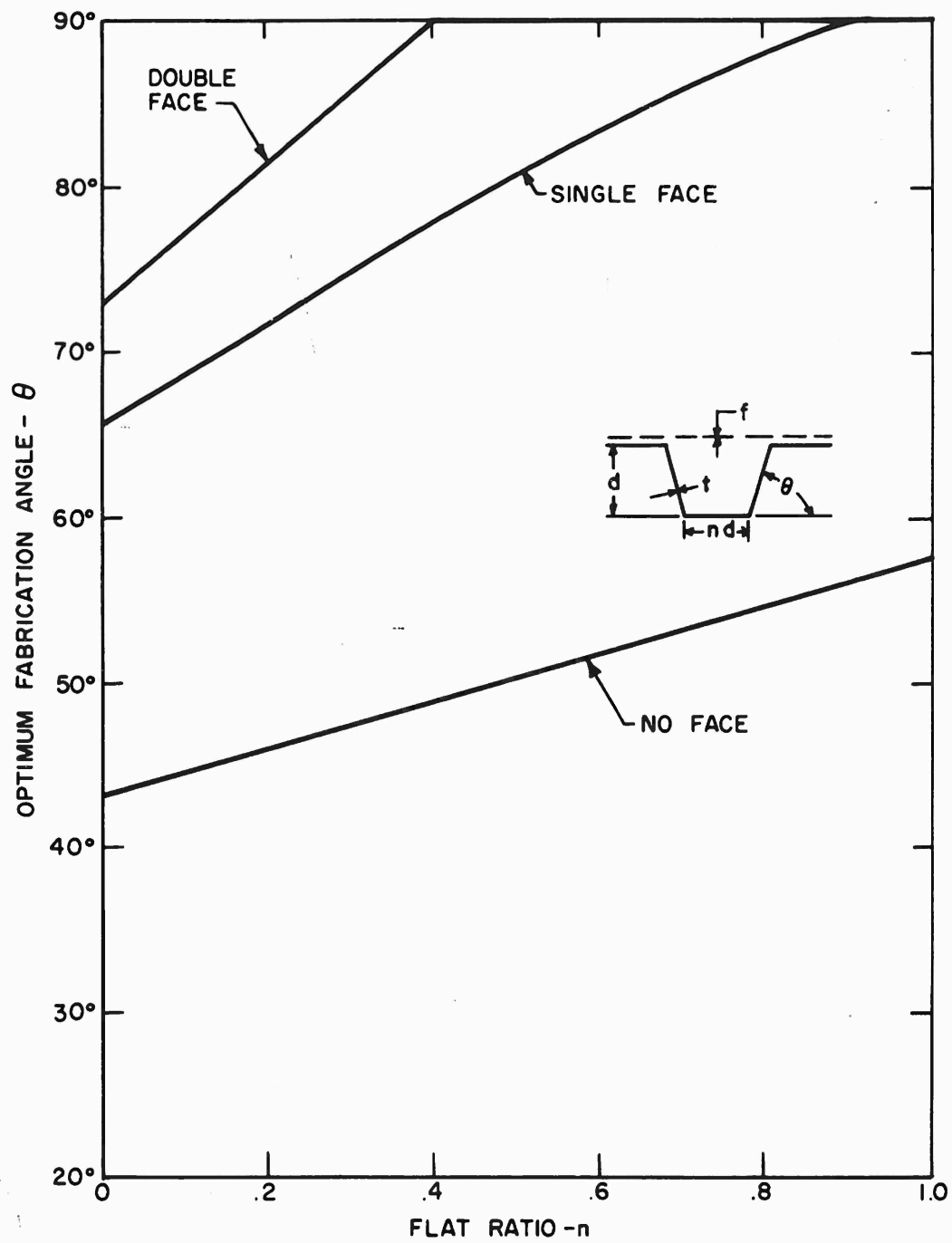


Figure A-2b. Optimum Fabrication Angle for Corrugation Panels in Shear ( $\sqrt{C_t/C_f} = 1.14$ )

Substituting Eq. (A-2c) into Eq. (A-2b) results in

$$\frac{W}{b^2 \rho} = \left[ \frac{a_1 K (\sqrt{a_4 a_5} + a_5)}{\sin^2 \theta} \right]^{1/2} \left( \frac{d}{b} \right)^2 \quad (\text{A-2d})$$

Thus a plot of  $\left[ \frac{a_1 (\sqrt{a_4 a_5} + a_5)}{\sin^2 \theta} \right]^{1/2} = \frac{W}{b^2 \rho K^{1/2} (d/b)^2}$  as a function of  $\theta$  for given values of  $n$  will indicate the value of  $\theta$  which would minimize  $W$ .

Similarly, for single-face or no-face corrugations in compression, we obtain, with the aid of Eq. (34),

$$\frac{W}{b^2 \rho} = \frac{K}{C_t} \left( \frac{\sqrt{a_4 a_5}}{\sin^2 \theta} \right) \left( \frac{d}{b} \right)^3 \quad (\text{A-3a})$$

$$\text{and} \quad \frac{W}{b^2 \rho (K/C_t) (d/b)^3} = \frac{\sqrt{a_4 a_5}}{\sin^2 \theta} \quad (\text{A-3b})$$

For single-face or no-face corrugations in shear we obtain, with the aid of Eq. (43),

$$\frac{W}{b^2 \rho} = \frac{a_1}{(a_9)^{4/3}} \left( \frac{d}{b} \right)^{7/3} \quad (\text{A-4a})$$

and

$$\frac{W}{b^2 \rho (d/b)^{7/3}} = \frac{a_1}{(a_9)^{4/3}} \quad (\text{A-4b})$$

Similarly, for double-face corrugations in shear we obtain with the aid of Eq. (50),

$$\frac{W}{b^2 \rho} = \frac{a_1}{a_9} \left( \frac{d}{b} \right)^2 \quad (\text{A-5a})$$

and

$$\frac{W}{b^2 \rho (d/b)^2} = \frac{a_1}{a_9} \quad (\text{A-5b})$$

### C. CORRUGATED BEAMS

In order to maximize the section modulus ( $I/c$ ), it is desirable to place as much material as possible at the extreme fibers. This is done most efficiently with a corrugation angle of  $\theta = 90^\circ$ . A smaller angle may be more efficient, however, for corrugations with no faces. The smaller angle reduces the flat and web area per unit length, which is desirable for lightly loaded structures. This reduced area is obtained at the expense of reducing the transverse shear area (which was ignored in the design). Corrugations with faces tend to be most efficient at the maximum angle of  $90^\circ$  since smaller angles require thicker faces with larger areas. Additional studies in this area of investigation are recommended.

To increase the section modulus, the depth and flat ratio should be made as large as possible consistent with the requirements of stability. The optimum value of  $n$  can be determined by making the elements equally stable. It should be noted that the design criteria for beams assumed that the effects of transverse shear stresses were negligible. This was done because it would be difficult to assess the effect of the transverse shear stresses since they are not a fixed ratio of the bending stresses.

For corrugations with no faces, the value of  $n$  is obtained by equating the stability of the flat to the stability of the web.

$$C_h \left( \frac{t}{nd} \right)^2 = C_t \left( \frac{t}{d} \right)^2 \quad (A-6a)$$

and

$$n = \left( C_h / C_t \right)^{1/2} \quad (A-6b)$$

If  $C_h / C_t = 3.62/21.72 = 1/6$ , then

$$n = 0.408 \quad (A-6c)$$

For corrugation with one or two faces, the values of  $(f/t)$  and  $n$  are obtained by equating the stability of the flat to the stability of the face and the web.

Assuming that the joining of the flat to the face results in a node, we obtain for equal stability of flat and face

$$C_f \left( \frac{f}{2nd} \right)^2 = C_h \left( \frac{t}{nd/2} \right)^2 \quad (A-7a)$$

$$\therefore \frac{f}{t} = 4 \left( C_h / C_f \right)^{1/2} \quad (A-7b)$$

= 4 if the end fixities of the face and flat panels are assumed equal ( $C_f = C_h$ ).

Multiple attachments of face to corrugation flat or beads in the face can increase the stability of the face and is equivalent to increasing the value of  $C_f$ .

Equal stability of flat and web results in

$$C_h \left( \frac{t}{nd/2} \right)^2 = C_t \left( \frac{t}{d} \right)^2$$

$$n = 2 \left( C_h / C_t \right)^{1/2}$$

$$= 0.815, \text{ if } C_h / C_t = 1/6$$

Stiffening of the web (e.g., beads) or flat (e.g., multiple attachments) will increase the values of  $C_t$  or  $C_h$ .

The above values of  $n$  and  $f/t$  result in the following geometric properties for corrugation beams:

For no faces, Eq. (32) with  $n = 0.408$  becomes

$$\alpha_{10} = 3.40 \quad (\text{A-8a})$$

$$\alpha_{40} = 0.452 \quad (\text{A-8b})$$

$$\alpha_{60} = 0.50 \quad (\text{A-8c})$$

For one face, Eq. (31) with  $n = 0.815$  and  $f/t = 4$  becomes

$$\alpha_{11} = 6.225 \quad (\text{A-8d})$$

$$\alpha_{41} = 0.710 \quad (\text{A-8e})$$

$$\alpha_{61} = 0.82 \text{ (tension) or } 0.18 \text{ (compression)} \quad (\text{A-8f})$$

For two faces, Eq. (26) with  $n = 0.815$  and  $f/t = 4$  becomes

$$\alpha_{12} = 10.225 \quad (\text{A-8g})$$

$$\alpha_{42} = 2.352 \quad (\text{A-8h})$$

$$\alpha_{62} = 0.50 \quad (\text{A-8i})$$

Manipulation of Eq. (74a), (79a), and (79b) and (79d) results in the following expression for the weight of the corrugation in terms of the geometric and material factors, the applied moment, and the design stress:

$$\frac{W}{b\rho} = \alpha_1 \left( \frac{a_6}{a_4} \right)^{1/2} \left( \frac{M}{\sigma} \sqrt{\frac{\xi_p \sigma_o}{C_t E_A}} \right)^{1/2} \quad (A-9a)$$

If the corrugations are designed for the same compressive stress, then the one-face corrugation in compression would be the most efficient since

$$\alpha_1 \left( \frac{a_6}{a_4} \right)^{1/2} = 3.15 \text{ (one face)} < 3.58 \text{ (no face)} < 4.70 \text{ (two faces)} \quad (A-9b)$$

In general, however, the design compressive stress for the no-face and two-face corrugations is usually higher than that employed for the one-face corrugation ( $\sigma_{0c} =$

$\sigma_{2c} \geq \sigma_{1t} \left( \frac{a_{61c}}{a_{61t}} \right) = \sigma_{1t}/4.55$ ), and the relative efficiencies are not as great.

The no-face corrugation can become more efficient for an elastic design compressive stress of

$$\left( \frac{a_{10} \sqrt{a_{60}/a_{40}}}{a_{11} \sqrt{a_{61}/a_{41}}} \right)^4 \frac{a_{61c}}{a_{61t}} \geq .37$$

times the allowable tensile stress. The double-face corrugation approaches but never attains the efficiency of the single-face corrugation as the optimum compressive stress approaches the allowable tensile stress. The higher tensile stress plus the plasticity of the material results in a heavier double corrugation.

The single-face corrugation has, however, a serious shortcoming. The maximum moment that can be resisted with the face in tension (M-) is significantly lower than the moment with the face in compression (M+). This is because of the higher compressive stress caused by the larger extreme fiber distance, and because of the lower stability of the web caused by the larger region of compressive stresses, i.e.,

$$\frac{M-}{M+} = \frac{a_{6+}}{a_{6-}} \frac{C_{t+}}{C_{t-}} = \frac{0.18}{0.82} \frac{(0.905)(9.5)}{(0.905)(24)} = 0.087 \quad (A-10)$$

Thus, one-face corrugations are usually more efficient (lighter and stiffer) than two-face corrugations provided that the negative moment is relatively small and the depth is not limited.



<p>Aeronautical Systems Division, Flight Dynamics Lab, Wright-Patterson AFB, Ohio Rpt No. ASD-TTR-62-763. THE MINIMUM WEIGHT DESIGN OF STRUCTURES OPERATING IN AN ARO-SPACE ENVIRONMENT. Final report, Oct. 1962. 134 p., incl., illus., tables, 22 refs. Unclassified Report</p>	<ol style="list-style-type: none"> <li>1. Stresses</li> <li>2. Mathematical analysis</li> <li>3. Space vehicle structure</li> <li>I. AFSC Project 1467.</li> <li>Task 146701</li> <li>II. Contract</li> <li>AF 33(657)-7872</li> <li>Republic Aviation Corp., Farmingdale, N. Y.</li> <li>IV. Switzky, H.</li> <li>V. R4C 442-1 (ARD-823-2)</li> <li>VI. In ASTIA collection</li> </ol>	<p>A nondimensional design technique is developed to obtain the minimum weight of structural components (columns, plates, and beams) subjected to an aerospace environment. Design curves are developed and presented for various structural configurations in terms of the applied loads and geometric and material parameters which can be readily evaluated. The design technique can be employed to obtain, in a relatively</p> <p style="text-align: right;">( over )</p>
<p>Aeronautical Systems Division, Flight Dynamics Lab, Wright-Patterson AFB, Ohio Rpt No. ASD-TTR-62-763. THE MINIMUM WEIGHT DESIGN OF STRUCTURES OPERATING IN AN ARO-SPACE ENVIRONMENT. Final report, Oct. 1962. 134 p., incl., illus., tables, 22 refs. Unclassified Report</p>	<ol style="list-style-type: none"> <li>1. Stresses</li> <li>2. Mathematical analysis</li> <li>3. Space vehicle structure</li> <li>I. AFSC Project 1467.</li> <li>Task 146701</li> <li>II. Contract</li> <li>AF 33(657)-7872</li> <li>Republic Aviation Corp., Farmingdale, N. Y.</li> <li>IV. Switzky, H.</li> <li>V. R4C 442-1 (ARD-823-2)</li> <li>VI. In ASTIA collection</li> </ol>	<p>A nondimensional design technique is developed to obtain the minimum weight of structural components (columns, plates, and beams) subjected to an aerospace environment. Design curves are developed and presented for various structural configurations in terms of the applied loads and geometric and material parameters which can be readily evaluated. The design technique can be employed to obtain, in a relatively</p> <p style="text-align: right;">( over )</p>
<p>simple and rapid manner, preliminary estimates of the structural design weight as well as a good approximation to the final design. The design procedure for minimum weight is illustrated for a truss-like spar and a wing section which are typical of aerospace structures.</p>	<p>simple and rapid manner, preliminary estimates of the structural design weight as well as a good approximation to the final design. The design procedure for minimum weight is illustrated for a truss-like spar and a wing section which are typical of aerospace structures.</p>	<p>simple and rapid manner, preliminary estimates of the structural design weight as well as a good approximation to the final design. The design procedure for minimum weight is illustrated for a truss-like spar and a wing section which are typical of aerospace structures.</p>

Aeronautical Systems Division, Flight Dynamics Lab, Wright-Patterson AFB, Ohio Rpt No. ASD-TTR-62-763. THE MINIMUM WEIGHT DESIGN OF STRUCTURES OPERATING IN AN AERO-SPACE ENVIRONMENT. Final report, Oct. 1962. 134 p., incl., illus., tables, 22 refs. Unclassified Report

A nondimensional design technique is developed to obtain the minimum weight of structural components (columns, plates, and beams) subjected to an aerospace environment. Design curves are developed and presented for various structural configurations in terms of the applied loads and geometric and material parameters which can be readily evaluated. The design technique can be employed to obtain, in a relatively

( over )

simple and rapid manner, preliminary estimates of the structural design weight as well as a good approximation to the final design. The design procedure for minimum weight is illustrated for a truss-like spar and a wing section which are typical of aerospace structures.

1. Stresses
2. Mathematical analysis
3. Space vehicle structure
- I. AFSC Project 1467. Task 146701
- II. Contract
- III. AF 33(657)-7872 Republic Aviation Corp., Farmingdale, N. Y.
- IV. Switzky, H.
- V. RAC 442-1 (ARD-823-2)
- VI. In ASTIA collection

Aeronautical Systems Division, Flight Dynamics Lab, Wright-Patterson AFB, Ohio Rpt No. ASD-TTR-62-763. THE MINIMUM WEIGHT DESIGN OF STRUCTURES OPERATING IN AN AERO-SPACE ENVIRONMENT. Final report, Oct. 1962. 134 p., incl., illus., tables, 22 refs. Unclassified Report

A nondimensional design technique is developed to obtain the minimum weight of structural components (columns, plates, and beams) subjected to an aerospace environment. Design curves are developed and presented for various structural configurations in terms of the applied loads and geometric and material parameters which can be readily evaluated. The design technique can be employed to obtain, in a relatively

( over )

simple and rapid manner, preliminary estimates of the structural design weight as well as a good approximation to the final design. The design procedure for minimum weight is illustrated for a truss-like spar and a wing section which are typical of aerospace structures.

1. Stresses
2. Mathematical analysis
3. Space vehicle structure
- I. AFSC Project 1467. Task 146701
- II. Contract
- III. AF 33(657)-7872 Republic Aviation Corp., Farmingdale, N. Y.
- IV. Switzky, H.
- V. RAC 442-1 (ARD-823-2)
- VI. In ASTIA collection

<p>Aeronautical Systems Division, Flight Dynamics Lab, Wright-Patterson AFB, Ohio Rpt No. ASD-TTR-62-763. THE MINIMUM WEIGHT DESIGN OF STRUCTURES OPERATING IN AN AEROSPACE ENVIRONMENT. Final report, Oct. 1962. 134 p., incl., illus., tables, 22 refs. Unclassified Report</p> <p>A nondimensional design technique is developed to obtain the minimum weight of structural components (columns, plates, and beams) subjected to an aerospace environment. Design curves are developed and presented for various structural configurations in terms of the applied loads and geometric and material parameters which can be readily evaluated. The design technique can be employed to obtain, in a relatively</p> <p>( over )</p>	<ol style="list-style-type: none"> <li>1. Stresses</li> <li>2. Mathematical analysis</li> <li>3. Space vehicle structure</li> </ol> <ol style="list-style-type: none"> <li>I. AFSC Project 1467.</li> <li>II. Task 146701</li> <li>III. AF 33(657)-7872</li> <li>IV. Republic Aviation Corp., Farmingdale, N. Y.</li> <li>V. Switzky, H. RAC 442-1 (AFD-823-2)</li> <li>VI. In ASTIA collection</li> </ol>	<ol style="list-style-type: none"> <li>1. Stresses</li> <li>2. Mathematical analysis</li> <li>3. Space vehicle structure</li> </ol> <ol style="list-style-type: none"> <li>I. AFSC Project 1467.</li> <li>II. Task 146701</li> <li>III. AF 33(657)-7872</li> <li>IV. Republic Aviation Corp., Farmingdale, N. Y.</li> <li>V. Switzky, H. RAC 442-1 (AFD-823-2)</li> <li>VI. In ASTIA collection</li> </ol>
<p>simple and rapid manner, preliminary estimates of the structural design weight as well as a good approximation to the final design. The design procedure for minimum weight is illustrated for a truss-like spar and a wing section which are typical of aerospace structures.</p>		<p>simple and rapid manner, preliminary estimates of the structural design weight as well as a good approximation to the final design. The design procedure for minimum weight is illustrated for a truss-like spar and a wing section which are typical of aerospace structures.</p>

Aeronautical Systems Division, Flight Dynamics Lab, Wright-Patterson AFB, Ohio  
Rpt No. ASD-TR-62-763. THE MINIMUM WEIGHT DESIGN OF STRUCTURES OPERATING IN AN AEROSPACE ENVIRONMENT. Final report, Oct. 1962, 134 p., incl., illus., tables, 22 refs.  
Unclassified Report

A nondimensional design technique is developed to obtain the minimum weight of structural components (columns, plates, and beams) subjected to an aerospace environment. Design curves are developed and presented for various structural configurations in terms of the applied loads and geometric and material parameters which can be readily evaluated. The design technique can be employed to obtain, in a relatively

( over )

simple and rapid manner, preliminary estimates of the structural design weight as well as a good approximation to the final design. The design procedure for minimum weight is illustrated for a truss-like spar and a wing section which are typical of aerospace structures.

1. Stresses
2. Mathematical analysis
3. Space vehicle structure
- I. AFSC Project 1467.
- II. Task 146701
- III. Contract
- IV. AF 33(657)-7872
- V. Republic Aviation Corp., Farmingdale, N. Y.
- VI. Switzky, H.
- VII. RAC 442-1 (ASD-823-2)
- VIII. In ASTIA collection

Aeronautical Systems Division, Flight Dynamics Lab, Wright-Patterson AFB, Ohio  
Rpt No. ASD-TR-62-763. THE MINIMUM WEIGHT DESIGN OF STRUCTURES OPERATING IN AN AEROSPACE ENVIRONMENT. Final report, Oct. 1962, 134 p., incl., illus., tables, 22 refs.  
Unclassified Report

A nondimensional design technique is developed to obtain the minimum weight of structural components (columns, plates, and beams) subjected to an aerospace environment. Design curves are developed and presented for various structural configurations in terms of the applied loads and geometric and material parameters which can be readily evaluated. The design technique can be employed to obtain, in a relatively

( over )

simple and rapid manner, preliminary estimates of the structural design weight as well as a good approximation to the final design. The design procedure for minimum weight is illustrated for a truss-like spar and a wing section which are typical of aerospace structures.

1. Stresses
2. Mathematical analysis
3. Space vehicle structure
- I. AFSC Project 1467.
- II. Task 146701
- III. Contract
- IV. AF 33(657)-7872
- V. Republic Aviation Corp., Farmingdale, N. Y.
- VI. Switzky, H.
- VII. RAC 442-1 (ASD-823-2)
- VIII. In ASTIA collection